

IONIC CONDUCTIVITY STUDY ON
CARBOXYMETHYLCELLULOSE BLENDED
WITH POLYVINYL ALCOHOL
INCORPORATED WITH AMMONIUM
BROMIDE BASED SOLID BIOPOLYMER
ELECTROLYTES AS APPLICATION IN
ELECTROCHEMICAL DEVICE.



UMP

NORFATIAH BINTI MAZUKI

اونيورسيٲي ملايسيا قهغ

UNIVERSITI MALAYSIA PAHANG

MASTER OF SCIENCE

UNIVERSITI MALAYSIA PAHANG

UNIVERSITI MALAYSIA PAHANG

DECLARATION OF THESIS AND COPYRIGHT

Author's Full Name : NORFATIHAH BINTI MAZUKI

Date of Birth : 05/05/1995

Title : IONIC CONDUCTIVITY STUDY ON
CARBOXYMETHYLCELLULOSE BLENDED WITH
POLYVINYL ALCOHOL INCORPORATED WITH
AMMONIUM BROMIDE BASED SOLID BIOPOLYMER
ELECTROLYTES AS APPLICATION IN
ELECTROCHEMICAL DEVICE

Academic Session : SEM 2 2019/2020

I declare that this thesis is classified as:

- CONFIDENTIAL (Contains confidential information under the Official Secret Act 1997)*
- RESTRICTED (Contains restricted information as specified by the organization where research was done)*
- OPEN ACCESS I agree that my thesis to be published as online open access (Full Text)

I acknowledge that Universiti Malaysia Pahang reserves the following rights:

1. The Thesis is the Property of Universiti Malaysia Pahang
2. The Library of Universiti Malaysia Pahang has the right to make copies of the thesis for the purpose of research only.
3. The Library has the right to make copies of the thesis for academic exchange.

Certified by:

(Student's Signature)

950505-11-5364

New IC/Passport Number

Date:

(Supervisor's Signature)

Name of Supervisor

Date:

NOTE : * If the thesis is CONFIDENTIAL or RESTRICTED, please attach a thesis declaration letter.

THESIS DECLARATION LETTER (OPTIONAL)

Librarian,
Perpustakaan Universiti Malaysia Pahang,
Universiti Malaysia Pahang,
Lebuhraya Tun Razak,
26300, Gambang, Kuantan.

Dear Sir,

CLASSIFICATION OF THESIS AS RESTRICTED

Please be informed that the following thesis is classified as RESTRICTED for a period of three (3) years from the date of this letter. The reasons for this classification are as listed below.

Author's Name	NORFATIAH BINTI MAZUKI
Thesis Title	IONIC CONDUCTIVITY STUDY ON CARBOXYMETHYLCELLULOSE BLENDED WITH POLYVINYL ALCOHOL INCORPORATED WITH AMMONIUM BROMIDE BASED SOLID BIOPOLYMER ELECTROLYTES AS APPLICATION IN ELECTROCHEMICAL DEVICE.
Reasons	<ul style="list-style-type: none">(i) The thesis includes material that was obtained under the promise of confidentiality(ii) The thesis details methods/procedures which could affect the competitiveness of a line of research if made available online(iii) The student intends to publish the thesis as a monograph or series of articles and electronic publication could compromise opportunities for publication

Thank you.

Yours faithfully,

UNIVERSITI MALAYSIA PAHANG

(Supervisor's Signature)

Date:

Stamp:

Note: This letter should be written by the supervisor, addressed to the Librarian, *Perpustakaan Universiti Malaysia Pahang* with its copy attached to the thesis.

SUPERVISOR'S DECLARATION

I hereby declare that I have checked this thesis and in my opinion, this thesis is adequate in terms of scope and quality for the award of the degree of Master of Science.

(Supervisor's Signature)

Full Name : DR AHMAD SALIHIN BIN SAMSUDIN

Position : SENIOR LECTURER

Date :

اونيورسيتي مليسيا قهغ

UNIVERSITI MALAYSIA PAHANG



STUDENT'S DECLARATION

I hereby declare that the work in this thesis is based on my original work except for quotations and citations which have been duly acknowledged. I also declare that it has not been previously or concurrently submitted for any other degree at Universiti Malaysia Pahang or any other institutions.

(Student's Signature)

Full Name : NORFATIAH BINTI MAZUKI

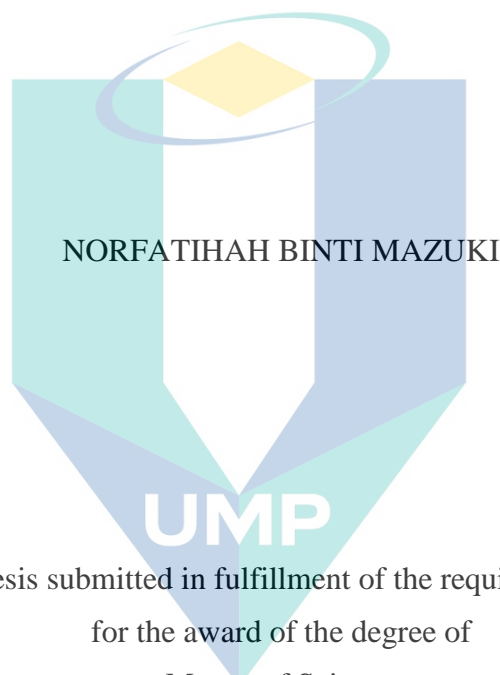
ID Number : MSM18003

Date :

اونيورسيتي ملايسيا قهغ

UNIVERSITI MALAYSIA PAHANG

IONIC CONDUCTIVITY STUDY ON CARBOXYMETHYLCELLULOSE
BLENDED WITH POLYVINYL ALCOHOL INCORPORATED WITH
AMMONIUM BROMIDE BASED SOLID BIOPOLYMER ELECTROLYTES AS
APPLICATION IN ELECTROCHEMICAL DEVICE.



Thesis submitted in fulfillment of the requirements
for the award of the degree of
Master of Science

اونيورسيتي ملايسيا قهغ

UNIVERSITI MALAYSIA PAHANG

Faculty of Industrial Science and Technology

UNIVERSITI MALAYSIA PAHANG

SEPTEMBER 2020

ACKNOWLEDGEMENTS



In the name of Allah S.W.T., the Beneficent, the Merciful and salutations to the prophet, Muhammad S.A.W. First and foremost, Alhamdulillah, Alhamdulillah, Alhamdulillah, thanks to Allah for the gratitude of the forehead who bestowed His grace that have given me strengths, patience, courage, maturity and time to complete my research and thus successfully in finishing my thesis writing. I would like to extend my deepest praise to Prophet MUHAMMAD S.A.W. for his advices and guideline as a muslim, which always useful while accomplishing this thesis.

Next, I would like to state deepest gratitude to my lovely supervisor Dr Ahmad Salihin Bin Samsudin for full support, advice, guidance me in my study and research. Without timely perception and patience from him, my research cannot work efficiently. His strict supervised yet still shows his good side to his student makes me want to be like him someday. I am not shy to admit that Dr Ahmad Salihin is my idol in academic. There were a lot of his kindness that always keeps me to motivate and work hard to do this research.

Further, I also would like to sent my special thanks to my family for their never-ending support and encouragement to me for do this research briefly. I am indebted to my both beloved parents, **Mazuki Bin Mohamed** and **Haslina Binti Mohd Nor** for non-stop praying my master journey would be well and successful. They also inspire me to not give up in this beautiful journey. Special thanks also goes to my lovely siblings, Mohd Afendi, Mohd Afiq, Mohd Alif and Mohd Azrul for always made my day when I am not in good mood during this journey.

Moreover, my greatest thanks to my twin from different mother, my partner in crime, my best friend ever, Fatin Farisha Alia Binti Azmi for never tired of treating my weird and always support my decision, encourage me during my down running the research. There no word can describe how lucky I am to be friend with her since our first meet at first year degree. Next, my sincere trillion thanks to my beloved teammates, Ionic Materials Team (IoMaT) familys, Mrs. Saadiyah, Mrs. Muhitil Jalilah, Ms. Khalidah and Mr. Faizrin for all kindness, happiness, joyful and support which make me feel very grateful to be part of IoMT family. They are like my second family after my blood family. Also, not forget my PG FAN friends including Aiman, Amir, Abang Am and especially kak Farha and Nina who also play important part in release my stress when I feel fed up with unsuccess work and also other my postgraduate friend, Kak Molla and Kak Hanis for giving me a place to stay and accompany me doing my research at laboratory. Furthermore, I also would like to thanks to Ms. Nadiah Hamidon a.k.a. cik nad who suddenly popped up helping me in last preparation for my master study.

Not forget also my appreciation to Universiti Malaysia Pahang (UMP) for financial support through Research Scheme (MRS) and staffs of Faculty of Industrial Sciences & Technology Laboratory, UMP for helping and providing us the research facilities. Last but not least, thank you to those who contribute to the successful of this research either directly or indirectly. Without all of them that I have mentioned from up to bottom, these impossible task at the beginning cannot be turn to possible task. Thank you again and again from my deepest heart. May Allah repays all your kindness for making my master journey one of the best memories ever.

ABSTRAK

Dalam kerja ini, campuran polimer karbonatoksiletel selulosa (CMC) – polyvinyl alcohol (PVA) berdasarkan elektrolit biopolimer pepejal (SBEs) yang bergabung dengan pelbagai kandungan ammonium bromide (NH_4Br) telah dilaporkan. Filem elektrolit terdiri daripada CMC-PVA yang bertindak sebagai polimer utama dan NH_4Br sebagai penyumbang proton telah berjaya disediakan melalui teknik tebaran tuangan. Interaksi antara polimer utama dan dopan ionik telah diuji dan disahkan melalui analisis spektroskopi inframerah jelmaan fourier (FTIR) di mana terdapat anjakan dan perubahan puncak intensiti dikenalpasti. Analisis belauan sinar X telah membuktikan sampel menjadi lebih amorfus apabila 20 wt.% NH_4Br diperkenalkan kedalam sistem. Sifat-sifat terma elektrolit biopolimer pepejal (SBEs) telah dikaji menggunakan analisis termogravimetri (TGA) dan kalorimetri pengimbasan pembezaan (DSC). Ia dapat diperhatikan dalam TGA bahawa suhu penguraian (T_d) telah meningkat dengan tambahan NH_4Br yang menunjukkan peningkatan dalam kestabilan haba elektrolit biopolimer. Sementara itu, analisis DSC telah mendedahkan suhu peralihan kaca (T_g) menurun dengan peningkatan kandungan NH_4Br dan ini telah mencadangkan kerja ini mempunyai kestabilan haba yg bagus. Berdasarkan analisis impedans, sistem SBEs telah menunjukkan peningkatan kekonduksian ionik apabila 20 wt.% NH_4Br diperkenalkan kedalam sistem dimana nilai optimum kekonduksian ionik telah dicapai pada $3.21 \times 10 \pm 0.005 \times 10^{-4} \text{ S cm}^{-1}$. Kajian ke atas kekonduksian berlainan suhu untuk semua sampel SBEs ditemui mengikut hukum Arrhenius dimana nilai regresi menghampiri uniti ($R^2 \sim 1$). Peningkatan NH_4Br telah menyebabkan tenaga pengaktifan sistem CMC-PVA- NH_4Br menurun dan didapati berkadar songsang dengan trend kekonduksian ionik. Kajian dielektrik SBEs telah dijalankan dengan menggunakan ketelusan dielektrik dan spektrum modulus elektrik yang mematuhi teori tidak Debye. Ciri-ciri pengangkutan SBEs ini telah disiasat menggunakan teknik kesepadanan impedansi. Teknik ini mendedahkan kekonduksian ionik CMC-PVA- NH_4Br berdasarkan elektrolit biopolimer dipengaruhi terutamanya oleh pekali resapan ionik dan pengangkutan ionik. Kaedah polarisasi *dc* telah digunakan untuk menentukan nombor pemindahan kationik untuk sampel dengan kekonduksian ionik tertinggi. Elektrod tiada penyekatan berbalik telah digunakan dalam kerja ini untuk mencari nombor pemindahan proton (H^+) dan didapati nilai t_{H^+} adalah 0.31. Ini menunjukkan bahawa spesies pengaliran kebanyakannya disebabkan oleh konduksi kationik. Dalam kajian ini, sampel dengan nilai kekonduksian tertinggi, 20 wt. % NH_4Br digunakan dalam fabrikasi peranti kapasitor keluaran dua lapisan elektrik (EDLC). Berdasarkan teknik voltammetri sapuan linear (LSV), tetingkap potensi elektrokimia untuk elektrolit biopolimer yang paling tinggi kekonduksian menunjukkan voltan operasi sehingga 1.55 V. Kapasitans khusus (C_{sp}) CMC-PVA-20 wt. % NH_4Br elektrolit biopolimer dikira dari voltammetri berkitar (CV) dan hasilnya menunjukkan persetujuan yang baik dengan C_{sp} yang diperolehi dari Galvanostatic Charge-Discharge (GCD). Nilai purata ketumpatan kuasa dan ketumpatan tenaga diperhatikan masing-masing pada $\sim 31.36 \text{ W kg}^{-1}$ and $\sim 1.19 \text{ Wh kg}^{-1}$. Tinjauan kerja pada sistem CMC-PVA- NH_4Br berdasarkan biopolimer elektrolit dianggap mempunyai potensi untuk digunakan dalam peranti penyimpanan tenaga.

ABSTRACT

In the present work, a polymer blend carboxymethyl cellulose (CMC)-polyvinyl alcohol (PVA) based solid biopolymer electrolytes (SBEs) incorporated with various amount of ammonium bromide (NH_4Br) is reported. The electrolyte films comprised of CMC-PVA which act as host polymer and NH_4Br as the proton provider were successfully prepared via the casting technique. The interactions between host polymer and ionic dopant were tested and confirmed via Fourier Transform Infrared Spectroscopy (FTIR) analysis where shifting and changes in intensity of the peaks were observed. The X-ray Diffraction analysis proved that the sample became amorphous when up to 20 wt. % NH_4Br was introduced into the system. The thermal properties of the SBEs were studied using Differential Scanning Calorimetry (DSC) and Thermo Gravimetric Analysis (TGA). It was observed in the TGA that the decomposition temperature (T_d) increased with the addition of NH_4Br which indicates the improvement in thermal stability of biopolymer electrolytes. Meanwhile, the DCS analysis revealed that the glass transition temperature (T_g) also decreased as the NH_4Br content increased and this suggests that the present sample has good thermal stability. Based on impedance analysis, the SBEs of the present work showed an improvement in ionic conductivity when 20 wt. % of NH_4Br was introduced into the system where the optimum room temperature ionic conductivity of $3.21 \pm 0.005 \times 10^{-4} \text{ S cm}^{-1}$ was achieved. The temperature dependence for all of the SBEs were discovered to obey the Arrhenius behavior with the value of the regression approaching unity ($R^2 \sim 1$). The increment of NH_4Br caused the activation energy of the CMC-PVA- NH_4Br system to decrease in an inversely proportional way to the ionic conductivity trend. The dielectric behavior of the SBEs were determined using electrical modulus spectra and dielectric permittivity which revealed a non-Debye behavior. The transport properties of the present SBEs were investigated via Impedance fitting analysis approach. These methods revealed that the ionic conductivity of the CMC-PVA- NH_4Br based biopolymer electrolyte is primarily influenced by the ions diffusion coefficient and ionic mobility. The cationic transference number for the sample with the highest ionic conductivity was determined using the *dc* polarization method. Non-blocking reversible electrodes were used to identify the proton (H^+) transference number (t_{H^+}) which was observed to be 0.31. This indicates that cationic conduction was the predominant source of the conducting species. Consequently, the sample with highest conductivity (20 wt. % NH_4Br) was used to fabricate an electrical double layer capacitor (EDLC) device. Based on the Linear Sweep Voltammetry (LSV) technique, the electrochemical potential window of the most conducting biopolymer electrolyte showed an operating voltage up to 1.55 V. The specific capacitance (C_{sp}) of the CMC-PVA-20 wt. % NH_4Br biopolymer electrolyte was calculated from Cyclic Voltammetry (CV) curve and the results showed good agreement with the C_{sp} obtained from Galvanostatic Charge-Discharge (GCD). The average value of power density and energy density was observed to be at $\sim 31.36 \text{ W kg}^{-1}$ and $\sim 1.19 \text{ Wh kg}^{-1}$, respectively. Thus, these findings suggest that the biopolymer electrolyte-based CMC-PVA- NH_4Br system has a good potential for applications in energy storage devices.

TABLE OF CONTENT

DECLARATION	
TITLE PAGE	
ACKNOWLEDGEMENTS	ii
ABSTRAK	iii
ABSTRACT	iv
TABLE OF CONTENT	v
LIST OF TABLES	ix
LIST OF FIGURES	x
LIST OF SYMBOLS	xiii
LIST OF ABBREVIATIONS	xv
CHAPTER 1 INTRODUCTION	1
1.1 Background of Research	1
1.2 Problem Statement	4
1.3 Significance of the Research	5
1.4 Objectives	6
1.5 Thesis Outline	6
CHAPTER 2 LITERATURE REVIEW	8
2.1 Introduction	8
2.2 Polymer Electrolytes	8
2.2.1 Classification of Polymer Electrolytes	10
2.2.2 Classification of Polymer Host	14
2.3 Techniques to Enhance Ionic Conduction Properties	18
2.3.1 Polymer Blend	18

2.3.2	Addition of ionic dopants	20
2.4	Polymer Electrolytes in electrochemical device application	22

CHAPTER 3 METHODOLOGY **26**

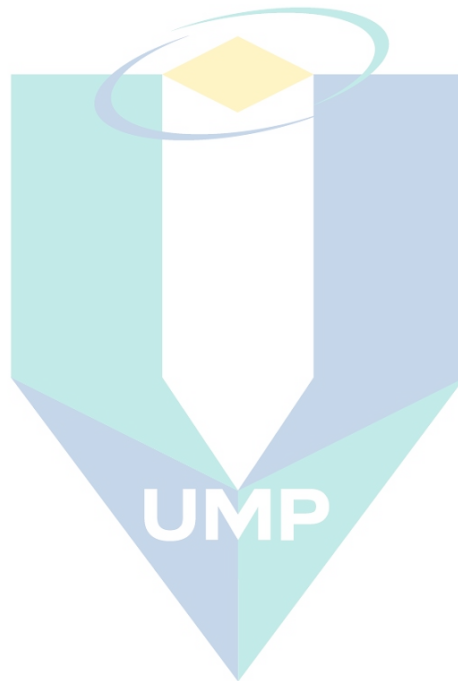
3.1	Introduction	26
3.2	Preparation of Solid Biopolymer Electrolytes	28
3.3	Characterization of SBEs system	29
3.3.1	Fourier Transform Infrared Spectroscopy (FTIR)	29
3.3.2	X-ray Diffraction (XRD)	30
3.3.3	Thermogravimetric Analysis (TGA)	31
3.3.4	Differential Scanning Calorimetry (DSC)	32
3.3.5	Electrical Impedance Spectroscopy (EIS)	32
3.3.6	Transference Number Measurement (TNM)	35
3.3.7	Linear Sweep Voltammetry (LSV)	36
3.4	Preparation of Electrodes	37
3.5	Preparation of Electrical Double Layer Capacitor (EDLC)	37
3.6	Electrical Double Layer Capacitor Characterization	38
3.6.1	Cyclic Voltammetry (CV)	38
3.6.1	Galvanostatic Charge-Discharge (GCD)	39

CHAPTER 4 RESULTS AND DISCUSSION **41**

4.1	Introduction	41
4.2	Appearance of Blend Biopolymer Electrolyte	41
4.3	Fourier Transform Infrared Spectroscopy (FTIR) Analysis	42
4.3.1	IR spectra of CMC-PVA blend	42
4.3.2	IR spectra of Ammonium Bromide (NH ₄ Br)	45

4.3.3	IR spectra of CMC-PVA doped NH ₄ Br SBEs	46
4.4	X-ray Diffraction Analysis	53
4.4.1	XRD spectra of CMC-PVA and NH ₄ Br	53
4.4.2	XRD spectra of CMC-PVA doped NH ₄ Br	54
4.5	Thermal Stability Analysis	57
4.5.1	TGA spectra of CMC-PVA and CMC-PVA doped NH ₄ Br	57
4.5.2	DSC spectra of CMC-PVA and CMC-PVA doped NH ₄ Br	61
4.6	Summary of structural and thermal analysis	64
4.7	Impedance Spectroscopy Analysis of CMC-PVA doped NH ₄ Br	65
4.7.1	Nyquist Plot of CMC-PVA+NH ₄ Br	65
4.7.2	Ionic Conductivity Analysis of CMC-PVA+NH ₄ Br	71
4.7.3	Temperature Dependence Analysis of CMC-PVA+NH ₄ Br	74
4.7.4	Dielectric Analysis of CMC-PVA+NH ₄ Br	77
4.7.5	Modulus Analysis of CMC-PVA+NH ₄ Br	84
4.8	Transport Properties Analysis of CMC-PVA+NH ₄ Br	90
4.9	Proton (H ⁺) Transference Measurement Analysis	93
4.10	Linear Sweep Voltammetry (LSV) Analysis	95
4.9	Electrochemical Properties of Electrical Double Layer Capacitor (EDLC)	97
4.9.1	Cyclic Voltammetry (CV) Analysis	97
4.9.2	Galvanostatic Charge-Discharge (GCD) Analysis	100
CHAPTER 5 CONCLUSION		108
5.1	Introduction	108
5.2	Conclusion	108
5.3	Recommendations	110

REFERENCES	111
APPENDIX A	139
APPENDIX B	143
LISTS OF JOURNAL PUBLICATION AND CONFERENCE PROCEEDING	145
BIODATA OF THE AUTHOR	146



اونيورسيتي مليسيا قهغ

UNIVERSITI MALAYSIA PAHANG

LIST OF TABLES

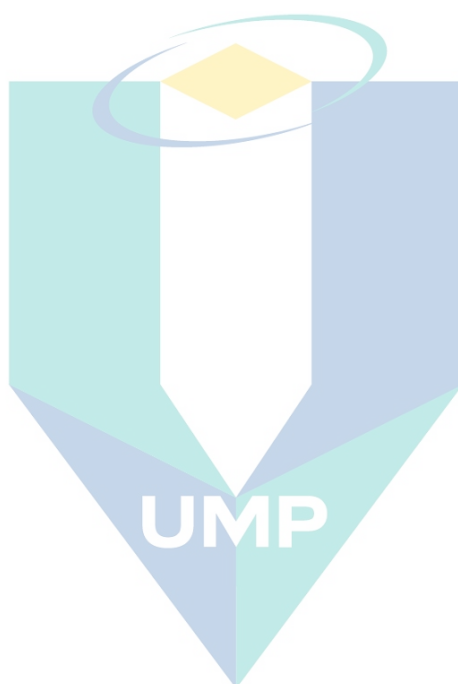
Table 2.1	Previous study on gel-based polymer electrolytes.	12
Table 2.2	List of previous studies on composite and ceramic based polymer electrolytes	13
Table 2.3	List of previous studies on solid polymer electrolytes.	14
Table 2.4	Previous studies on synthetic polymers as a single host polymer.	15
Table 2.5	Natural polymers as the host polymer.	16
Table 2.6	Previous research on polymer blending based electrolytes.	20
Table 2.7	Some examples of charge carriers used in polymer complexes electrolytes.	21
Table 2.8	List of biopolymer electrolytes used in electrochemical devices	25
Table 3.1	Designations of CMC-PVA-NH ₄ Br based SBEs system.	28
Table 4.1	List of functional groups for pure CMC from previous works.	44
Table 4.2	List of functional group of pure PVA from previous works.	44
Table 4.3	List of functional groups for CMC-PVA polymer blend.	45
Table 4.4	List of functional groups for pure NH ₄ Br.	46
Table 4.5	Crystallite sizes of all SBEs system.	56
Table 4.6	Maximum decomposition temperature and total weight loss of various content CMC-PVA SBEs system.	61
Table 4.7	The parameter for CMC-PVA-NH ₄ Br	70
Table 4.8	Previous studies of single polymer and polymer blend-salt complexes electrolytes	73
Table 4.9	Regression value of CMC-PVA-NH ₄ Br.	76
Table 4.10	List of specific capacitances obtained from CV curve.	99
Table 4.11	Previous work on EDLC based polymer electrolytes.	105

LIST OF FIGURES

Figure 1.1	Schematic diagram of the basic mechanisms of electrochemical devices (a) battery, (b) supercapacitor, (c) solar cell and (d) fuel cell.	2
Figure 2.1	Classification and category of polymer electrolyte.	9
Figure 2.2	Structure of carboxymethyl cellulose (CMC)	17
Figure 2.3	Schematic diagram of CMC-PVA polymer blend via hydrogen bonding.	19
Figure 2.4	Schematic diagram of mechanism in EDLC.	23
Figure 2.5	Comparison plot for electrochemical devices.	24
Figure 3.1	General overview of experimental work of this research.	27
Figure 3.2	Process for making a solid biopolymer electrolyte films sample.	29
Figure 3.3	A simplified schematic of X-ray diffraction.	31
Figure 3.4	General Nyquist plot	34
Figure 3.5	Ionic transference number experimental arrangement via <i>dc</i> polarization technique.	35
Figure 3.6	Schematic diagram of linear sweep voltammetry circuit.	36
Figure 3.7	Schematic diagram of linear sweep voltammetry.	36
Figure 3.8	Arrangement of EDLC in the present research.	37
Figure 3.9	Schematic diagram of cyclic voltammetry plots of EDLC coin cell	38
Figure 3.10	Schematic diagram of galvanostatic charge-discharged plots of EDLC coin cell.	40
Figure 4.1	Solid biopolymer electrolyte film.	42
Figure 4.2	FTIR spectra of CMC-PVA solid biopolymer electrolyte.	43
Figure 4.3	FTIR spectra of pure ammonium bromide.	45
Figure 4.4	IR spectra of CMC-PVA doped with various amounts of NH_4Br at 4000 to 700 cm^{-1} .	46
Figure 4.5	IR spectra of CMC-PVA- NH_4Br at region 1200 to 900 cm^{-1} .	47
Figure 4.6	IR spectra of CMC-PVA- NH_4Br at region 1500 to 1200 cm^{-1} .	48
Figure 4.7	IR spectra of CMC-PVA- NH_4Br at region 1800 to 1400 cm^{-1} .	49
Figure 4.8	IR spectra of CMC-PVA- NH_4Br at the regions of 4000 to 2700 cm^{-1}	51
Figure 4.9	Schematic diagram of interaction between CMC-PVA and NH_4Br .	52
Figure 4.10	XRD patterns for pure CMC-PVA polymer blend and NH_4Br .	53
Figure 4.11	XRD patterns of biopolymer electrolytes for all NH_4Br content.	55
Figure 4.12	TGA curve of CMC-PVA polymer blend.	58
Figure 4.13	TGA curve of biopolymer electrolytes at various amount of NH_4Br	60

Figure 4.14	DSC spectra of CMC-PVA	62
Figure 4.15	DSC Thermograms at selected amounts of NH_4Br .	63
Figure 4.16	Nyquist plot for CMC-PVA- NH_4Br based SBEs system, (a) CMC-PVA polymer blend, (b) AB5, (c) AB10 and (d) AB15.	66
Figure 4.17	Nyquist plot for (a) AB20, (b) AB25, (c) AB30 and (d) AB35.	68
Figure 4.18	Ionic conductivity of solid biopolymer electrolytes system.	72
Figure 4.19	(a) Temperature dependence plot of CMC-PVA polymer blend and (b) log ionic conductivity versus $1000/T$ plot for different NH_4Br content.	74
Figure 4.20	The activation energy plot of biopolymer electrolytes system.	77
Figure 4.21	Frequency dependence on dielectric constant for CMC-PVA- NH_4Br systems.	78
Figure 4.22	Dielectric constant, ϵ_r patterns for SBEs system at various temperature.	80
Figure 4.23	Frequency dependence on dielectric loss for CMC-PVA- NH_4Br systems.	82
Figure 4.24	Dielectric loss, ϵ_i patterns for sample SBEs system at various temperature.	84
Figure 4.25	Real modulus versus frequency for biopolymer electrolytes containing different NH_4Br content.	85
Figure 4.26	Real modulus, M_r patterns for CMC-PVA- NH_4Br SBEs system at various temperature.	87
Figure 4.27	Imaginary modulus versus frequency for biopolymer electrolytes containing different NH_4Br content	87
Figure 4.28	Imaginary modulus, M_i patterns for CMC-PVA- NH_4Br SBEs system at various temperature.	89
Figure 4.29	Mobility of charge carriers, μ and diffusion coefficient, D versus varied amount of NH_4Br .	91
Figure 4.30	Number of ions, η versus varied amount of NH_4Br .	92
Figure 4.31	Current relaxation curve during dc polarization	94
Figure 4.32	Nyquist plot for CMC-PVA+20 wt. % NH_4Br biopolymer electrode using non-blocking MnO_2 electrode.	94
Figure 4.33	LSV response of SBE system of highest ionic conductivity.	96
Figure 4.34	Cyclic Voltammetry of the highest conducting SBE at (a) 20 to 50 mV s^{-1} and (b) 2 to 10 mV s^{-1} scan rate.	98
Figure 4.35	(a) GCD plot for varied current density and (b) specific capacitance and ESR versus current density of highest conducting sample.	101
Figure 4.36	Charge-discharge performances of EDLCs at selected cycles.	102
Figure 4.37	Coulombic efficiency as a function of the charge-discharge cycles at a constant current density of 0.1 mA cm^{-2} .	103

Figure 4.38	Specific capacitance and ESR performance for 20 wt. % NH_4Br electrolytes at 0.1 mA cm^{-2} .	104
Figure 4.39	Power density and energy density versus number of cycles of cell EDLC.	107
Figure 4.40	Comparable studies of energy density and power density from previous research	107
Scheme 4.1	Model of the equivalent circuit	67
Scheme 4.2	The equivalent circuit of SBE system for Nyquist plots consists of tilted spike.	69



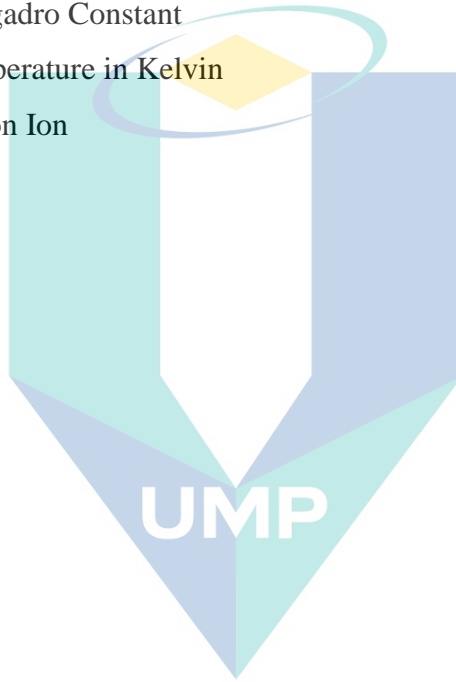
اونيورسيتي ملايسيا قهغ

UNIVERSITI MALAYSIA PAHANG

LIST OF SYMBOLS

ml	Mililiter
°C	Degree Celcius
g	Grams
°	Degree
σ	Ionic Conductivity
%	Percentage
π	Pi
θ	Theta
A	Area
cm	Centimetre
cm^{-1}	Per Centimetre
cm^2	Square Centimetre
f	Frequency
Hz	Hertz
MHz	Mega Hertz
Z_i	Imaginary Parts of Modulus
Z_r	Real Parts of Modulus
R_b	Bulk Resistance
E_a	Activation Energy
eV	Electron Voltage
T_d	Temperature Decomposition
T_g	Glass Transition Temperature
~	Approximately
a.u	Arbitrary Unit
η	Number of Ions
D	Diffusion Coefficient
μ	Ionic Mobility
t_{ion}	Ionic Transference Number
I	Normalized polarization current
t	Time
t_H^+	Cation Transference Number

V	Voltage
M_r	Real Modulus
M_i	Imaginary Modulus
ϵ_r	Dielectric Constant
ϵ_i	Dielectric Loss
ϵ_o	Free Space Permittivity
K_b	Boltzman Constant
e	Electric Charge Constant
N_A	Avogadro Constant
T	Temperature in Kelvin
H^+	Proton Ion



اونيورسيتي ملايسيا قهغ

UNIVERSITI MALAYSIA PAHANG

LIST OF ABBREVIATIONS

CMC	Carboxymethyl Cellulose
CV	Cyclic Voltammetry
DSC	Differential Scanning Calorimetry
EDLC	Electrical Double Layer Capacitor
EIS	Electrical Impedance Spectroscopy
FTIR	Fourier Transform Infrared Spectroscopy
GCD	Galvanostatic Charge Discharge
GPE	Gel Polymer Electrolyte
ILPE	Ionic Liquid Polymer Electrolyte
LSV	Linear Sweep Voltammetry
NH ₄ Br	Ammonium Bromide
NH ₄ Cl	Ammonium Chloride
NH ₄ NO ₃	Ammonium Nitrate
PEs	Polymer Electrolytes
PVA	Polyvinyl Alcohol
SBEs	Solid Biopolymer Electrolytes
TGA	Thermogravimetric Analysis
TNM	Transference Number Measurement
XRD	X-ray Diffraction
PVDF-HFP	Poly(vinylidene fluoride-co-hexafluoropropylene)
PMMA	Poly(methyl methacrylate)
PNIPAM	Poly(N-isopropylacrylamide)
PEO	Poly-ethylene oxide
PAN	Polyacrylonitrile
P(AN-MAH)	Poly(acrylonitrile-maleic anhydride)

اونیورسیتی مالیزیاء
UNIVERSITI MALAYSIA PAHANG

CHAPTER 1

INTRODUCTION

1.1 Background of Research

Economic development became dependent on energy with the introduction and widespread adoption of electricity, fossil fuels and refined chemical fuels. Since it cannot be stored as electrical energy, electricity has to be transmitted in a closed circuit. Therefore, one of the earliest methods for storing energy is electrochemical discharges which was first discovered by the French physicists Hippolyte Fizeau in 1819 to 1896 and Leon Foucault in 1819 to 1868 (Wüthrich et al., 2009). Electrochemical discharges are well known and referred to as the effects of a cathode and anode, depending on which electrode has taken place in the phenomena (Greatbatch & Holmes, 1991; Chilikov & Protopchikov, 2008; Holbrook et al., 2000). There are three major components in the fabrication of electrochemical discharge, involving the cathode, anode and electrolytes. When a chemical medium allows an electrical charge to flow between the cathode and anode, it is known as an electrolyte. Powering a device will cause chemical reactions to occur at the electrodes, thus creating an energy flow to the device.

Currently, solid waste, especially electronic waste has become a global issue due to its hazardous effects on the environment. Used batteries are one of the examples of electronic waste that are nonbiodegradable. Furthermore, the use of commercial batteries containing liquid electrolyte can lead to physical and chemical instability and it is prone to leak because of the corrosive properties of the electrolyte material (Fonseca et al., 2006; Mobarak et al., 2012; Samsudin et al., 2014; Na et al., 2018). Several enhancements were done to solve this problem but they did not make much difference. Thus, in order to save the Earth and humans from further destruction, actions must be taken such as by producing green technology as one of the steps towards developing a safer future.

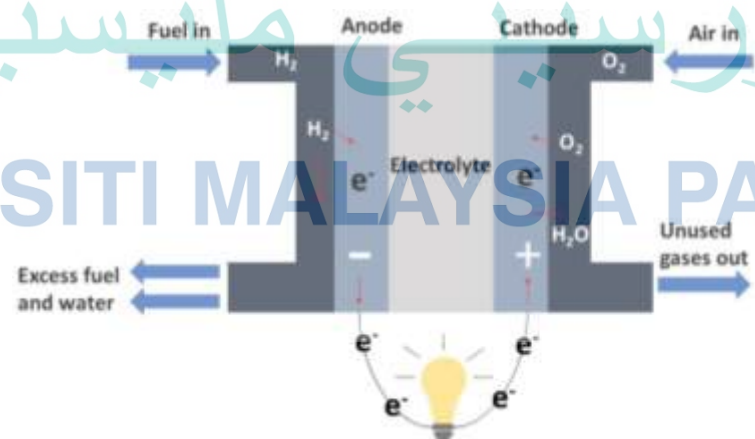
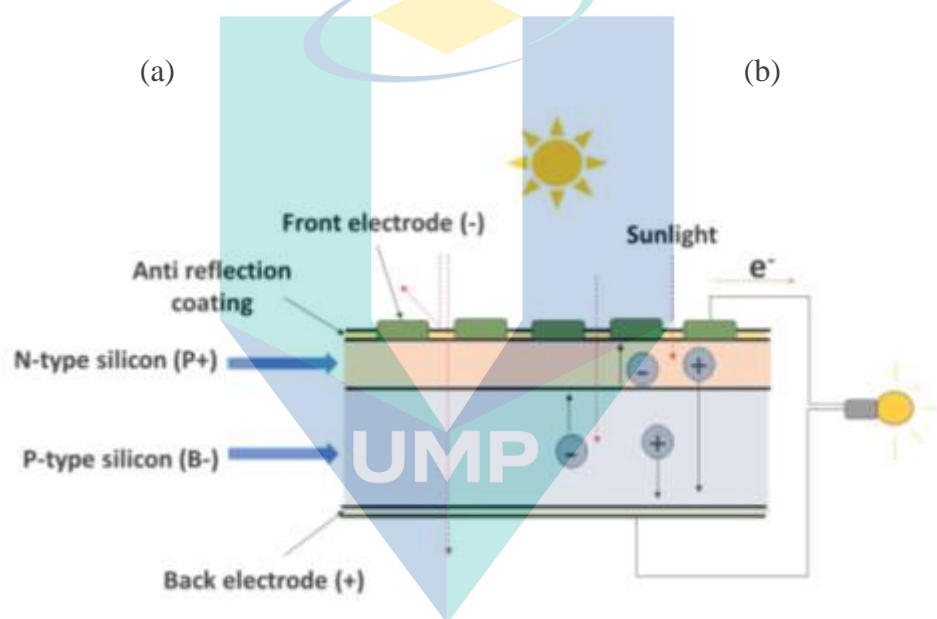
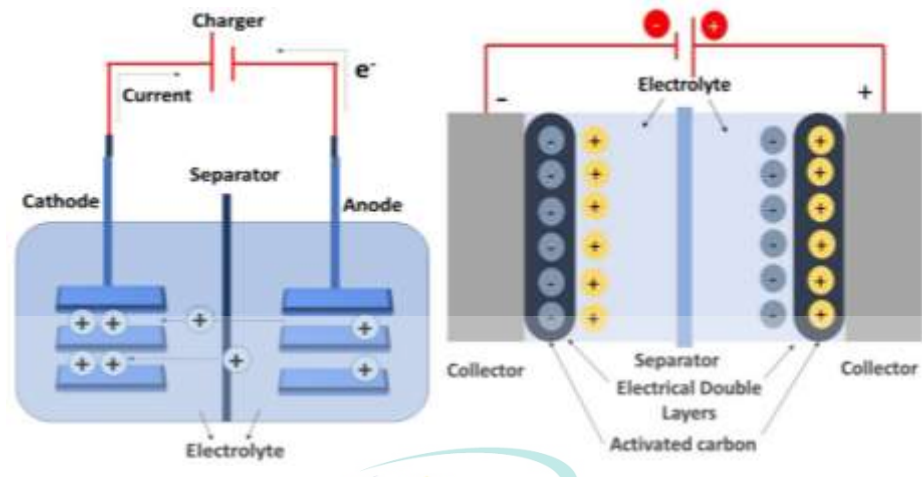


Figure 1.1 Schematic diagram of the basic mechanisms of electrochemical devices (a) battery, (b) supercapacitor, (c) solar cell and (d) fuel cell.

In an important discovery, Wright and co-workers discovered ionic conduction in polyethylene-based electrolytes (Wright, 1975). Since then, polymer electrolytes (PEs) have become dominant among materials scientists because of their possible use in electrochemical devices such as in solar cells, fuel cells, supercapacitors and batteries (Rajendran et al., 2003; Nik Aziz et al., 2010). The schematic diagrams of the basic components in electrochemical devices are illustrated in Figure 1.1. A good performance of electrochemical devices can be obtained from the excellent properties shown by polymer electrolytes such as having excellent thermal, mechanical and electrochemical stabilities as well as high ionic conductivity. The ionic conductivity is the main objective in this present work and can be given by the following relation:

$$\sigma = n\mu e \quad 1.1$$

where n = number of ions

μ = mobility of charge carrier

e = elementary charge.

According to Equation 1.1, the values of n and μ are the important parameters to focus on in order to control the ionic conductivity behaviour and to elucidate the mechanisms of ion transport and how these ions can affect the performance of electrochemical devices.

PEs are being targeted to be widely used in electrochemical devices because of their excellent properties including having high ionic conductivity, wide electrochemical windows, no leakage, easy handling, high energy density, no solvent, transparency, lightweight, and elasticity compared to the currently and widely used liquid electrolytes (Aziz et al., 2010; Alexandre et al., 2019). Most of the polymers used as PEs are polyvinyl alcohol (PVA) (Wang et al., 2017), polyvinylidene fluoride (PVdF) (Liu et al., 2017), poly methyl methacrylate (PMMA) (Kuppu et al., 2018), polyvinyl chloride (PVC) (Reddeppa et al., 2014) and poly (ethylene-co-methyl acrylate) (PEMA) (Kumar et al., 2018).

These synthetic polymers have attracted attention to be used in the preparation of PEs as host polymers but are unfortunately derived from petroleum resources. Thus,

biopolymers made from natural material have attracted the attention of researchers due to their various advantages over petroleum-derived polymers, including being biodegradable, low-cost and environmentally friendly. Many alternatives have been developed to preserve the environment and one of them is by using bio-derived or biopolymer materials which may eventually be a potential substitute for commercially available polymers.

1.2 Problem Statement

Solid waste management is a major worldwide issue. Without urgent action, the United Nations has projected the global waste to increase by 70 percent on current levels by 2050. Increasing amounts of discarded batteries in solid waste is a further cause for concern and can harm the environment and human health. Ahmad and Isa (2015a) reported this is because the electrolytes in commercial batteries are made from non-biodegradable and hazardous materials. Consumer demands for high quality and low-cost products have pushed manufacturers to improve and apply new materials which can minimize the fabrication cost. Furthermore, consumers also demand for electrochemical devices to have long lasting cycles of charge-discharge, higher energy power and most importantly, to be environmentally friendly. All of these demands are mostly assigned to liquid-based electrolytes.

Since ionic conduction was discovered in polyethylene that allows it to function as a polymer electrolyte by Wright (1975), it has attracted numerous attention worldwide as a potential replacement for liquid electrolytes by many researchers worldwide. The advantages of the polymer electrolytes include higher ionic conductivity properties and electrochemical stability towards electrodes. Although the development of polymer-based electrolytes is highly successful, the use of petroleum-derived synthetic polymers in the preparation of PEs is expensive and non-biodegradable, which are harmful to the environment and causes depletion of non-renewable resources. In addition, the use of single type polymers in the preparation of electrolytes has been widely explored but some limitations were discovered. These include the unfavourable instability of the polymer electrolytes in the application of electrochemical devices due to their low ionic conductivity, lower miscibility, higher crystallinity and also some of polymers require

appropriate solvents to dissolve as well as low mechanical properties (Mohamad et al., 2003; Ramlli & Isa, 2015).

One of the alternative approaches is via polymer blending which is considered to have high potential due to their properties such as good mechanical strength, good miscibility of two polymers, and providing more vacant sites that would lead to the enhancement of the ionic conductivity of polymer electrolytes. Owing to increasing awareness as well as to reduce pollution, researchers have shifted to greener natural materials, one of which are bio-polymers. Researchers are actively investigating the use of bio-polymers to replace conventional materials and also synthetic polymer electrolyte systems in electrochemical devices. Currently, various electrolytes based on bio-materials have been discovered, including cellulose derivatives, chitosan, alginate, algae, and starch.

Therefore, the present study focused on developing biopolymer electrolytes by blending two different polymers, namely carboxymethylcellulose (CMC) and polyvinyl alcohol (PVA) by doping with ammonium bromide (NH_4Br) where it is believed to the outcome will have enhanced conduction properties and contribute towards the preservation of the environment.

1.3 Significance of the Research

The many serious environmental and safety issues are something that cannot be ignored anymore, especially involving the problem of energy storage and the need to develop new alternatives to save the future. Most of the commercial batteries possess electrolytes with high ionic conductivity values but are made from hazardous and costly materials that are harmful to the environment and humans. To overcome these problems, alternative conducting solid biopolymer electrolyte (SBE) from environmentally friendly materials are being developed. Furthermore, waste from natural materials can be reduced and re-used to develop new technologies that benefits the nation and satisfy consumer needs. SBEs can naturally degrade in landfills and would not harm the environment compared to the existing plastic. The findings of this study will redound to the society as solid biopolymer plays an important role in science and technology today.

Carboxymethyl cellulose (CMC) is a material which is biodegradable, inexpensive to prepare, non-toxic and semi-crystalline as well as can provide an excellent ability of film-forming. Meanwhile, partial or complete hydrolysis of polyvinyl acetate is used to prepare polyvinyl alcohol (PVA) which is a well-known water-soluble polymer. PVA is also degradable and non-toxic while having high flexibility and tensile strength. With these properties, CMC and PVA are being explored as a potential host polymer in SBEs. By blending these two polymers, it is expected that the ionic conductivity can be improved via hydrogen bonding. In addition, the blending technique is also expected to enhance the thermal stability and miscibility of the electrolyte system. Furthermore, ammonium bromide (NH_4Br) was used as ionic dopant to enhance the ion conduction properties. Previous studies have also found that NH_4Br functions as a good proton donor to the polymer matrix. The feasibility of the CMC-PVA- NH_4Br SBE as an electrical double layer capacitor (EDLC) cell was also investigated in this thesis.

1.4 Objectives

1. To prepare CMC blended with PVA and incorporated with NH_4Br as solid biopolymer electrolytes.
2. To optimize the structural, thermal and ionic conduction properties of CMC-PVA- NH_4Br solid biopolymer electrolytes system.
3. To evaluate the electrochemical performance of prepared solid biopolymer electrolytes system as an electrical double layer capacitor (EDLC) device.

1.5 Thesis Outline

In Chapter 1, the background of the research and problem statements from previous researches that give significance to this work and to improve the earlier study were discussed. The research objectives and scope of the study was also discussed which gives a general explanation about the methodology of the research.

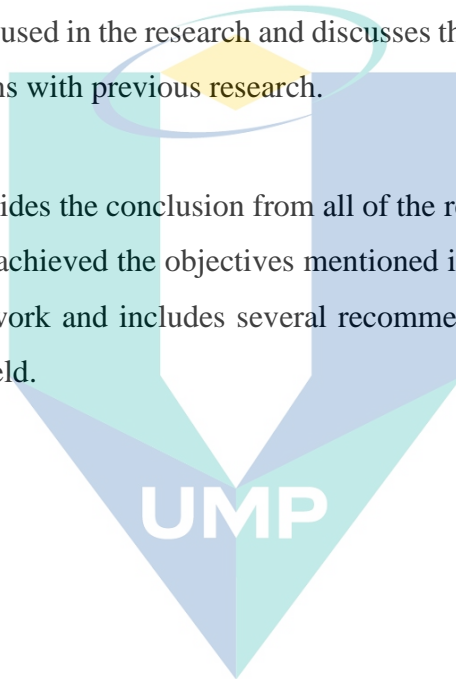
Chapter 2 contains the literature review which included information on electrolytes, type of polymer electrolytes, blending and dopant methods and utilization

of solid biopolymer electrolytes in electrical double layer capacitors (EDLC) that were used in past studies.

Chapter 3 describes the methodology used which includes preparation of the sample, the equipment and materials that were used for the research. It also contains the precautions during the research so that the samples are not damaged.

Chapter 4 explains about the result obtained from the characterization experiments that were used in the research and discusses the results in detail based on the theory and comparisons with previous research.

Chapter 5 provides the conclusion from all of the research findings and discusses whether this research achieved the objectives mentioned in Chapter 1. This chapter also concludes the entire work and includes several recommendations for improvements in future works in this field.



اونيورسيتي ملايسيا قهغ

UNIVERSITI MALAYSIA PAHANG

CHAPTER 2

LITERATURE REVIEW

2.1 Introduction

This chapter discusses in detail on information related to solid biopolymer electrolytes together with its specific applications. The development of new SBEs in the present work is based on previous studies on potential materials and methods to be applied as biopolymer electrolytes. These include a brief history of biopolymer electrolytes, techniques to enhance ionic conduction properties and biopolymer electrolytes in electrochemical devices applications.

2.2 Polymer Electrolytes

An electrolyte is a substance that can conduct electricity when dissolved in a solvent or water. Free ions in electrolytes function as an electrically conductive medium which interact at the cathode and anode (Aziz et al., 2010). Electrolytes are also known as the medium that are responsible for ionic transport, especially for H⁺ ion transport in SBEs and thus controls the power density. Ionic conductivity is one of the most important properties for electrolytes. To avoid a short circuit, electrolytes should have negligible ionic conductivity. Electrolytes are also the main component in electrochemical devices such as solar cells, batteries, supercapacitors and fuel cells (Park et al., 2006; Chen et al., 2008). Majid et al. (2005) stated that ionic dopants are needed to be added into solvents in order to form an electrolyte. In a solution, chemical dissociation occurs through the force exerted on the solute molecule to separate and hold its component atoms apart in ionic form.

The study of polymer electrolyte (PE) begun in the early 1970s by Fenton (1973). According to Ramesh and Wen (2010), various electrolytes-based solid state materials were investigated by researchers such as ceramics, crystalline, glass and finally polymer electrolytes. Multiple disciplines are involved in the research on PEs. These include the

field of organic and inorganic chemistry, electrochemistry and polymer science (Samsudin et al., 2012). Recent technological developments of novel PE materials such as those based on hybrid composite polymers, amorphous polymers and crystalline polymers have increased the attractiveness of their use in electrochemical devices which could revolutionize the industry (Vashishta et al., 1979; Samsudin et al., 2012). PE is a membrane which is made from salts dissolved in a polymer matrix with a high molecular weight (Ramesh & Lu, 2012). PEs can be broadly classified according to their sources and origins or according to their composition and physical state (Figure 2.1).

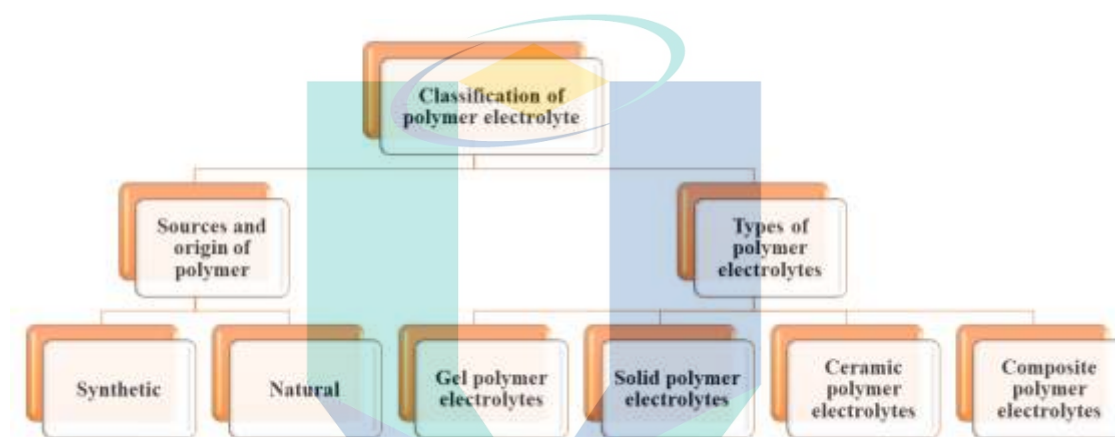


Figure 2.1 Classification and category of polymer electrolyte.

Recently, the depletion of natural resources and the increasing interest in recycling have directed attention among researchers to biomaterials, with a focus on renewable raw materials. This is because of increasing global environmental awareness on solid waste, especially electric waste. Batteries are one example of increasing solid waste that can harm the environment and living organisms due to the dangerous and non-biodegradable chemicals used in them (Ahmad & Isa, 2015a). PE systems possess good ionic conduction properties and are extensively used in electrochemical devices such as solid-state batteries and rechargeable batteries. A major example of its use is in lithium-ion batteries which possess many desirable properties that led to its ubiquitous use in portable electronic devices (Choudhary & Sengwa, 2013). However, the lithium-ion batteries are exposed to high risk as they use liquid electrolytes with organic solvents. Like the use of any technology, batteries based on lithium-ion have their own disadvantages such as low protection, shipping restrictions and high cost. Thus, researchers are looking into alternative and environmentally friendlier materials to be

used in batteries. They are potentially safer to the environment since they use natural materials and consequently have gained due attention among both academia and industry due to their high ionic conductivity electrodes and electrolytes having good contact with each other. These materials can also provide several advantages over liquid or gel-based electrolytes by not having self-discharge and leakage problems in batteries (Ning et al., 2009; Rani et al., 2014).

2.2.1 Classification of Polymer Electrolytes

PEs can be classified into five categories based on their physical state and appearance. These are ceramic polymer electrolytes, liquid polymer electrolytes (LPEs), gel polymer electrolytes (GPEs), solid polymer electrolytes (SPEs) and composite polymer electrolytes (CPE). The electrolytic properties have been improved using different approaches in order to achieve a better polymer, resulting in different types of PEs.

2.2.1.1 Gel Polymer Electrolytes

The GPE systems have been studied over the last few decades because of their good elasticity and high mechanical strength which are able to keep ionic conductivity after being constructed as an integrated flexible supercapacitor (Wang et al., 2015). GPEs are also commonly referred to as a plasticized-based polymer electrolyte due to their indeterminate physical state of being either liquid or solid or both at the same time. As stated by Appetecchi et al. (1994), GPEs also known as ionic gels, gained attention in 1975 due to work done by Feuillade and Perche (1975). In gels, there is a solid skeleton of polymer or long-chain molecules cross-linked intermolecularly or intramolecularly, which entrap an uninterrupted liquid phase (Sudhakar et al., 2010). Thus, GPEs possess the ability to diffuse like a liquid and the high cohesive properties of solids. This combines the organic liquid electrolytes' high ionic conductivity and the SPEs' dimensional stability (Samsudin, 2014).

The past decade has seen the rapid development of GPEs in many industrial applications, especially in energy storage devices. There were many reports in the literature on the use of GPE as the host polymer including poly(N-isopropylacrylamide) (PNIPAM), poly(vinylidene fluoride-co-hexafluoropropylene) (PVDF-HFP),

poly(methyl methacrylate) (PMMA) (Aishova et al., 2018), poly-ethylene oxide (PEO) (Siyal et al., 2019), polyacrylonitrile (PAN) (Wang et al., 2019) and poly(acrylonitrile-maleic anhydride) (P(AN-MAH)) (Huang et al., 2019). Most of the research on GPEs were on solid state GPEs for application to flexible supercapacitors (Yong et al., 2019). Due to the GPEs having enhanced ionic conductivity, low reactivity, low volatility, good mechanical and chemical properties, they promise good electrochemical performance (Ramesh & Wen, 2010; Ramesh et al., 2011). In addition, at room temperature, GPEs can exhibit high ionic conductivity of $\sim 10^{-3}$ to 10^{-2} S cm⁻¹ (Zhu et al., 2018).

However, despite these excellent advantages of GPEs, there are several shortcomings which can affect their utility in wider practical applications. Based on findings by Zhang et al. (2011) and Kim et al. (2008), the authors claimed that the impregnation with liquid or aqueous electrolytes solution contributed to poor mechanical strength. A sufficient mechanical strength is needed in polymer electrolytes in order to withstand the stress between the electrodes (Kim et al., 2003). Other than that, the presence of the water phase in the GPEs limits their temperature range of stable performance, thus possibly leading to explosions due to uncontrolled pressure build up (Armand et al., 2011; Quartarone et al., 2011).

Furthermore, liquid electrolytes have also gained attention among researchers around the world and are ubiquitously used in electrochemical devices, primarily in the form of Li-ion batteries. Fundamental studies designed to support the mechanism of ion conduction and the interaction between ion-ion and ion-polymer showed that liquid electrolyte behaviour depends on the transition glass temperature, molecular structure and its dynamics. Studies to improve Li-ion batteries have been ongoing for over three decades but has not been successful in commercialization due to many problems. These problems include corrosive solvent leakages, electrolytic degradation of electrolyte, long-term instability due to the liquid electrolyte evaporating, low charging efficiency, high self-discharge rate as well as poor safety due to the organic solvent used being highly flammable (Ramesh et al., 2011; Zhang, 2013). Table 2.1 lists previous studies on gel-based polymer electrolytes.

Table 2.1 Previous study on gel-based polymer electrolytes.

Materials	Ionic Conductivity (S cm ⁻¹)	References
PAN-EC-PC	10 ⁻³	(Mitra et al., 2001)
DADMATFSI-LiTFSI	1.00 x 10 ⁻³	(Hu et al., 2018)
PVA-Mg(Tf) ₂ -EMITf	2.10 x 10 ⁻⁴	(Wang et al., 2017)

2.2.1.2 Composite and Ceramic Polymer Electrolytes

Recently, composite polymer electrolytes have received enormous attention because it can provide lithium polymer batteries with enhanced compatibilities of electrode/electrolyte and are safer to use (Croce et al., 2001; Stephan et al., 2006). CPEs were prepared by dispersing fine organic or inorganic ceramic particles into the polymer electrolytes which have been proved to be one of the effective ways of improving key electrochemical structural parameters of PEs for rechargeable Li batteries (Osińska et al., 2015). CPEs are also known as nanocomposite polymer electrolytes due to the nanometre grain sized fillers in them. The incorporation of ceramic fillers with the host polymer can enhance the electrical and mechanical properties of CPEs (Sun et al., 2007; Nordström et al., 2010; Das et al., 2011). Fillers such as titania (TiO₂), manganese oxide (MgO), silica (SiO₂), alumina (Al₂O₃), zirconia (ZrO₂) and carbon nanotubes can be used to prepare PEs (Shin et al., 2004; Osińska et al., 2009; Liu et al., 2010; Johan et al., 2012; Lim et al., 2014b).

Previous studies have proven that adding ceramic fillers in contact with the lithium electrode can enhance the interfacial properties and ionic conductivity by increasing the amorphousness of the polymer chain through hindered recrystallization (Appetecchi et al., 2000). In ceramic compounds, ionic conduction occurs through defects in the ionic points that require energy and a rise in temperature to increase the process (Fergus, 2010). At this point, ceramic polymer electrolytes have become one of the candidates that are suited for high temperature applications. Table 2.2 tabulates previous studies on composite and ceramic based polymer electrolytes.

Table 2.2 List of previous studies on composite and ceramic based polymer electrolytes

Materials	Ionic Conductivity (S cm ⁻¹)	References
PEO-HCF ₃ SO ₃	8.14 x 10 ⁻³	(R. Kumar et al., 2017)
PVP-PVA-KNO ₃	1.29 x 10 ⁻³	(Rao et al., 2018)
PMMA-LiClO ₄ - DMP-CeO ₂	0.536 x 10 ⁻⁴	(Rajendran et al., 2002)
PEO ₈ -LiTFSI- TBPHP-LLZTO	9.39 x 10 ⁻⁴	(Xie et al., 2019)
LTAPO	8.36 x 10 ⁻⁴	(Lee et al., 2016)

2.2.1.3 Solid Polymer Electrolytes (SPEs)

In comparison to liquid and gel polymer electrolytes, research on solid polymer electrolytes (SPE) have shown it to have many desirable properties such as being easy to manufacture, high flexibility, low self-discharge, no leakage problems and good compatibility with electrodes (Yahya et al., 2006).

Many of the new polymers being researched for various applications are biodegradable. Three major areas of polymer applications include medical, agricultural and consumer goods packaging (Sudhakar et al., 2018). These applications have attracted interest in biopolymers as well. The use of portable electronic devices like mobile phones, power banks and laptops recently has been increasing. Subsequently, polymer research has gained interest among researchers to provide new insights in power sources. Besides that, SPEs also have unique properties namely, high ionic conductivity, high energy density due to the ease of manufacturing large surface area films, good electrode-electrolytes contact and their compatibility with various types of doping salts that make them attractive for potential application in energy storage devices (Wright, 1975; Rani et al., 2014; Ramlli et al., Wiers, 2015).

In recent decades, rapid technological advances have revolutionised human society but at the same time caused major environmental problems through plastic and electronic wastes (Wang et al., 2017). SPEs have the disadvantage of low mechanical strength but the use of high mechanical strength polymers as the SPE matrix could

neutralize this disadvantage. The crystallinity of polymers are near zero or are transparent (Rajantharan, 2011). Thus, many researchers chose to develop polymer electrolytes based on plant material such as cellulose derivatives because of their semi-crystalline nature (Kuutti et al., 2011; Nawaz et al., 2012). Table 2.3 lists previous work done using solids as polymer electrolytes.

Table 2.3 List of previous studies on solid polymer electrolytes.

Materials	Ionic Conductivity (S cm ⁻¹)	References
PVA-NH ₄ Br	10 ⁻⁴	(Hema et al., 2007)
PVA-PAN-NH ₄ SCN	2.4 x 10 ⁻³	(Sivadevi et al., 2015)
PVA-PVP-NH ₄ NO ₃	1.41 x 10 ⁻³	(Rajeswari et al., 2014)
I-Carrageenan-Mg(NO ₃) ₂	6.1 x 10 ⁻⁴	(Priya et al., 2018)
PVA-NaI	10 ⁻³	(Badr et al., 2010)

2.2.2 Classification of Polymer Host

Polymer host as an electrolyte has been classified into two types according to their sources and origins such as natural and synthetic polymers.

2.2.2.1 Synthetic polymer materials

Synthetic polymers are man-made polymers that are also referred to as plastics due to their wide use in industry such as the famous nylon and polyethylene. Many objects in our daily lives use synthetic polymers including for packing, wrapping and building materials. An example of synthetic polymer is nylon which is usually used in fabrics and textiles and polyvinyl chloride which is used in pipes. Other than that, synthetic polymers have also gained attention in the preparation of polymer electrolytes. The synthetic polymers that are widely used in research include polyethylene oxide (PEO) (Siyal et al., 2019), polyvinyl chloride (PVC) (Deraman et al., 2012), polymethyl methacrylate (PMMA) (Kuppu et al., 2018), polyvinylidene fluoride (PVdF) (Kumar et al., 2018) and polyvinyl alcohol (PVA) (Wang et al., 2017).

Moreover, synthetic polymers have good charge storage capacity in addition to its good optical and electrical properties that are dopant-dependent (Sivadevi et al., 2015). A survey of the literature revealed that the previous studies on ionic conductivity of synthetic polymers showed good values (Genova et al., 2015). However, these materials are gradually being depleted even though they have large amount of reserves and are non-renewable. Furthermore, almost all synthetic polymers are non-biodegradable and can harm the environment and humans. Nonetheless, polyvinyl alcohol (PVA) is a potential candidate to be used in polymer electrolyte films since it has hydrophilic properties. The hydrolysis of polyvinyl acetate produces the water-soluble crystalline PVA which is also biodegradable (Razzak et al., 2001).

Since its discovery, PVA has found many uses in the food, industrial, medical and commercial sectors (DeMerlis et al., 2003). Due to its similarity to natural polymers, hydrophilic properties, compatible structure, and biodegradability, PVA is commonly blended with other hydrophilic polymers, including biopolymers in industrial applications that confers films with enhanced mechanical properties (Gaaz et al., 2015). PVA is completely dissolved by boiling in water at $\sim 100^\circ\text{C}$ for 30 min (Albdiry et al., 2013).

The various grades of PVA are according to the structure of the crystal particles, molecular weight and distribution of the elements' dimensions. Moreover, Sivadevi et al. (2015) stated that PVA possesses a very high dielectric strength up to $>1,000\text{ kV mm}^{-1}$, thus has high potential to be used in electrochemical applications. Saadiah et al. (2019) also stated that PVA is a non-toxic material with high tensile strength and flexibility. The literature has shown the use of synthetic polymers as a single polymer can exhibit high ionic conductivity when doped with an ionic dopant as shown in Table 2.4.

Table 2.4 Previous studies on synthetic polymers as a single host polymer.

Sample	Ionic Conductivity (S cm^{-1})	References
PVA – KOH	8.5×10^{-4}	(Mokhtar et al., 2016)
PVA – NH_4NO_3	7.5×10^{-3}	(Hema et al., 2009)
PVA – NH_4SCN	2.58×10^{-3}	(Abdelgawad et al., 2014)
PVA- NH_4Br	5.70×10^{-4}	(Hema et al., 2007)
PEO- LiCF_3SO_3	4.6×10^{-5}	(Walker et al., 1993)
PVP- NH_4SCN	1.7×10^{-4}	(Ramya et al., 2007)
PVP- NH_4Cl	2.51×10^{-5}	(Vijaya et al., 2013)
PVC- $\text{NH}_4\text{CF}_3\text{SO}_3$	2.50×10^{-7}	(Deraman et al., 2014)

2.2.2.2 Bio-material polymer materials

The explosive growth of pollution nowadays has affected many organisms and raised concern among scientists on deficiencies in food, resources and energy as well as global environmental pollution. The discovery of ionic conduction using biodegradable polymers in 1975 by Wright and co-workers helped to develop technologies toward a sustainable future. Bio-materials are obtained from natural resources. Examples of natural polymers that are widely used in research include starch (Azlan et al., 2011), chitosan (Aziz et al., 2019), alginate (Rasali et al., 2018) and cellulose materials such as carboxymethyl cellulose (CMC) (El-Gamal et al., 2017), methyl cellulose (MC) (Nik Aziz et al., 2010) and hydroxyethyl cellulose (HEC) (Sit et al., 2012).

The most abundant natural polymer on Earth in terms of biomass is cellulose. Cellulose is an environmentally friendly polymer due to it being cheap, biodegradable, biocompatible and renewable (Moon et al., 2011; Zeng et al., 2011; Gale et al., 2016). Moreover, cellulose derivatives have become widely used in electrolytes among researchers due to their excellent properties which include biodegradable materials, high specific strength, low density and ability to form films (Debeaufort et al., 1994; Yue et al., 2003; Samir et al., 2005; Sit et al., 2012; Samad et al., 2013). Table 2.5 lists previous studies using natural polymers as the single polymer.

Table 2.5 Natural polymers as the host polymer.

Sample	Ionic Conductivity (S cm ⁻¹)	References
CMC – CH ₃ COONH ₄	5.77 x 10 ⁻⁴	(Rani et al., 2014)
CMC – NH ₄ Cl	1.43 x 10 ⁻³	(Ahmad et al., 2016)
CMC – NH ₄ NO ₃	7.71 x 10 ⁻³	(Kamarudin et al., 2013)
Chitosan-Tm(CF ₃ SO ₃) ₃	10 ⁻⁷	(Alves et al., 2017)
Starch-NH ₄ NO ₃	2.15 x 10 ⁻⁶	(Azlan et al., 2011)
HEC-NH ₄ Br	3.61 x 10 ⁻⁴	(Sit et al., 2012)
MC-NH ₄ F	6.40 x 10 ⁻⁷	(Nik Aziz et al., 2010)

According to Singh et al. (2013), CMC is synthesized from diverse plant biomasses, and in terms of dry weight, is comprised of 15 – 35 % lignin, 25 – 40 % hemicellulose and 40 – 50 % cellulose. Many types of agricultural waste can be used as sources of cellulose such as cashew tree gum, sugar beet pulp, sago waste, orange peel, papaya peel, cavendish banana pseudo stem and Mimosa pigra peels as reported by many researchers (Koh, 2013). CMC is water soluble due to the presence of hydrophilic carboxyl groups on the hydrophobic polysaccharide backbone as illustrated in Figure 2.2 (Chai et al., 2011). Cellulose materials have the distinctive property of heterogeneity because of its fibre structure.

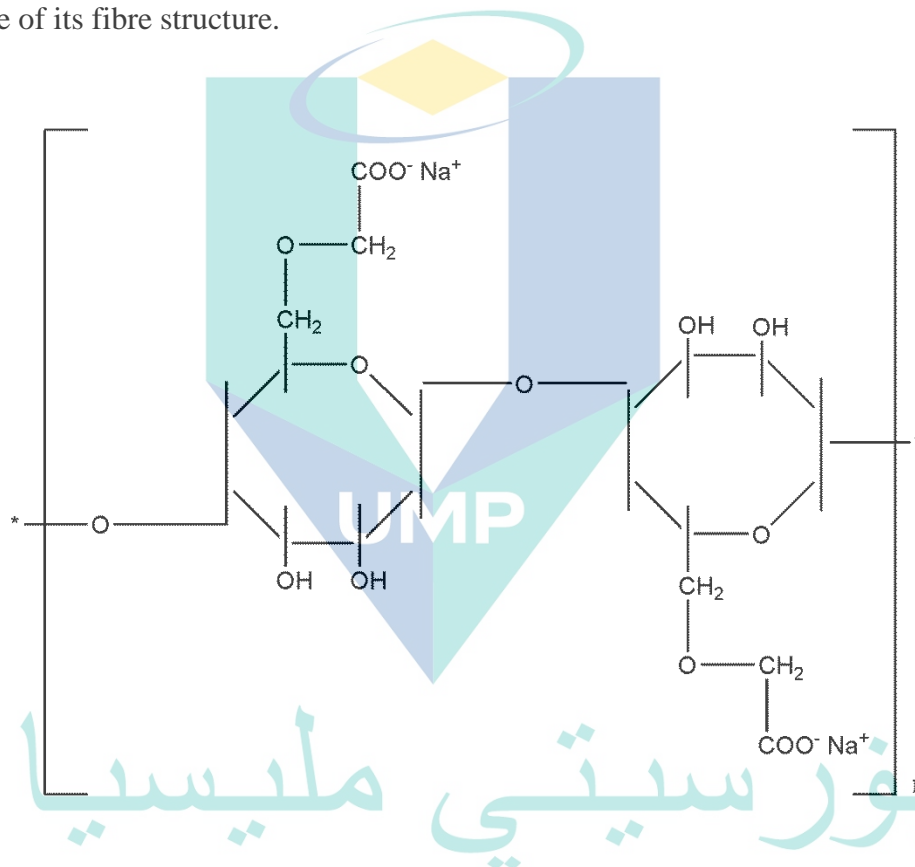


Figure 2.2 Structure of carboxymethyl cellulose (CMC)

Source: Rani et al., (2014)

As previously mentioned, CMC is a cheaply produced, semi-crystalline, non-toxic biodegradable material, as well as exhibiting an excellent film-forming ability. However, CMC also has some drawbacks which are low ionic conductivity and low strength (Chai et al., 2012; Ahmad et al., 2015a; Ramlli et al., 2015). There have been several studies in the literature reporting CMC as a single host polymer that can enhance the nature of the insulating biopolymer cellulose towards ionic conductivity and its

potential to be applied in energy storage when ionic dopant was incorporated into the system (Ahmad et al., 2012; Samsudin et al., 2014; Ahmad et al., 2015b; Noor et al., 2015; El-Gamal et al., 2017).

2.3 Techniques to Enhance Ionic Conduction Properties

Numerous approaches have been suggested in the literature for the ionic conductivity enhancement of solid biopolymer electrolytes. CMC has low ionic conductivity and is very sensitive to humidity, often becoming electrically non-conducting upon drying which can limit the performance of SBEs either in electrical and structural studies or in the fabrication of EDLC. The approaches that are being investigated include blending two polymers, adding ionic dopants, adding ionic liquids as well as adding plasticizers (Osinska et al., 2009; Hu et al., 2018; Kadir et al., 2018; Kuppu et al., 2018).

2.3.1 Polymer Blend

Since the initial finding on ionic conduction of polyethylene by Wright and co-workers in 1975, many studies have been done to improve the ionic conductivity of SBE for application in high energy density batteries (Nik Aziz et al., 2010). In 2011, Khair et al., (2011) published a paper study on polymer blend based starch-chitosan in which they described the ideal ionic conductivity for solid polymer electrolyte is at a range of 10^{-3} to 10^{-2} S cm^{-1} . Many techniques have been developed including polymer blending, use of different polymers for polymer blends, copolymer grafting, addition of ionic dopant or plasticizer and varying the ratios of polymers, salts or plasticizer in order to modify the degree of crystallinity (Nithya et al., 2009; Kadir et al., 2010; Shukur et al., 2014b).

Two or more polymers or copolymers are blended to produce a polymer blend. This well-known and conventional technique was selected to be used in the present study due to its low cost and high potential to enhance the ionic conductivity (Khair et al., 2011; Ramly et al., 2011). Nevertheless, the properties of the SBE system depend on its miscibility. Good ionic conductivity will only be achieved by blends with good miscibility i.e. those that do not exhibit separation between the phases of both polymers. This technique is preferred by many researchers due to its ability to produce the desired properties at a low cost (Sivadevi et al., 2015). Moreover, the technique is easy to

conduct and it is possible to control the film's physical properties and ionic conductivity though they are affected by the polymers' interactions (Kadir et al., 2010; Shukur et al., 2014).

In previous studies, CMC was also blended with other polymers such as starch (Ma et al., 2008), chitosan (Hafiza & Isa, 2014) and PVA (El-Gamal et al., 2017) to improve the product's quality and stability, provide a desirable texture and to control the mobility of water and moisture since it is a water soluble heteropoly saccharide with high molecular weight properties (Bertuzzi et al., 2007; Saadiah et al., 2018). According to Hafiza and Isa (2014), CMC can be improved by adding chitosan which was shown to modify the polymer's chemical structure and enhances its ionic conductivity. Other studies have found that adding PVA into CMC can similarly enhance its ionic conductivity as illustrated in Figure 2.3 (Varnell et al., 1981; Varnell et al., 1983). CMC-PVA is a flexible and semi-transparent blend (Wei et al., 2014; El-Gamal et al., 2017). When these two polymers are blended together, inter-chain H-bonding forms between the PVA's hydroxyl group and the CMC's carbonyl group, which increases its conductivity. The application of polymer blending in polymer electrolyte field has received much attention as tabulated in Table 2.6.

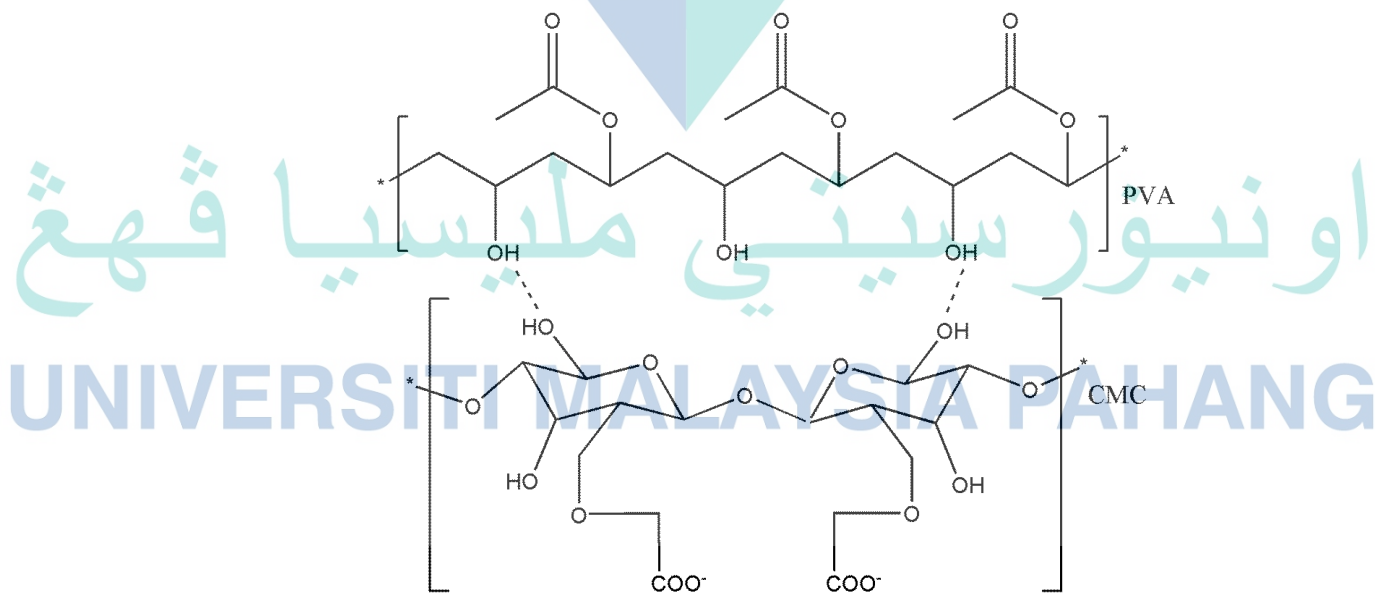


Figure 2.3 Schematic diagram of CMC-PVA polymer blend via hydrogen bonding.

Table 2.6 Previous research on polymer blending based electrolytes.

Sample	Ionic Conductivity (S cm ⁻¹)	References
CMC/PVA	9.12 x 10 ⁻⁶	(Saadiah et al., 2018)
CMC/KC	3.91 x 10 ⁻⁷	(Zainuddin et al., 2018)
MC/Potato starch	1.04 x 10 ⁻¹¹	(Hamsan et al., 2017a)
CMC/chitosan	3.15 x 10 ⁻⁹	(Bakar et al., 2015)
PVA/PVP	1.58 x 10 ⁻⁶	(Rajeswari et al., 2011)

2.3.2 Addition of ionic dopants

Another promising method to enhance the ionic conductivity is by doping using ionic dopants. There are different types of ions which act as charge carriers in polymer electrolyte such as Li⁺, Na⁺, H⁺, Mg⁺, Ag⁺. Table 2.7 shows several charge carriers used in polymer electrolytes from previous works.

The first finding in the usage of proton conductors in polymer electrolytes complexes was discovered by Fenton in 1973. Fenton (1973) reported the basic principle for polymer-dopant salt complexes via dissolving dopant salt in a solvating polymer matrix through direct interaction of cation and electron lone pairs bond of salt. One of the promising proton conductors to be used in polymer complex as dopant salt is NH₄⁺. Due to the considerable hydrogen bonding and coordination interaction of H⁺ to the COO⁻ moiety between host polymer and ammonium salt, the ammonium ion chelates easily, and thus is responsible for the ionic conduction in the polymer complex. The interest in proton conducting using ammonium salt-based polymer electrolytes was first reported by Stainer et al. (1984) who increased the ionic conductivity of PEO based polymer electrolytes by adding NH₄SCN and NH₄SO₃CF₃ which they found to have been caused by the ammonium ion (NH₄⁺) mobility.

Table 2.7 Some examples of charge carriers used in polymer complexes electrolytes.

Polymer	Dopant	Charge carrier	References
PEO/PVA	LiClO ₄	Li ⁺	(Jinisha et al., 2018)
PEO/PVP	NaNO ₃	Na ⁺	(Sundaramahalingam et al., 2018)
PEO/E8	NaIO ₄	Na ⁺	(Koduru et al., 2019)
PVA/PVP	KOH	K ⁺	(Hatta et al., 2009)
PVC/PEO	KCl	K ⁺	(Reddeppa et al., 2014)
PEO/PMMA	AgNO ₃	Ag ⁺	(Sharma et al., 2013)
PVA/PEG	Mg(CH ₃ COO) ₂	Mg ⁺	(Polu et al., 2012)
PAN	LiCF ₃ SO ₃	Li ⁺	(Ahmad et al., 2011)

In 1990, Hashmi claimed that ammonium salt can act as an excellent proton donor in polymer electrolytes (Hashmi et al., 1990). Therefore, ionic dopant materials act as sources of charge carrier in polymer electrolytes, thus playing an important role as the proton conductor. It also can affect the miscibility of polymer pairs and the morphology of the electrolytes through interaction between ions and polymer backbone (Chew et al., 2013; Samsudin et al., 2014). A study by Shukur et al. (2014b) showed that a starch/chitosan blended polymer electrolyte showed increased ionic conductivity of $6.51 \times 10^{-9} \text{ S cm}^{-1}$ from $4.00 \times 10^{-10} \text{ S cm}^{-1}$ and when incorporated with NH₄Cl.

Studies on developing high proton conducting membranes have shown that the ammonium salt is a good proton donor to the matrix ion (Nik Aziz et al., 2010; Ahmad & Isa, 2015; Sikkanthar et al., 2015). According to Ramya et al. (2008), protons or NH₄⁺ cations from ammonium salt in the electrolyte can act as the mobile species that account for the ionic conduction. A considerable amount of literature has been published on ammonium bromide (NH₄Br) as an ionic dopant in biopolymer electrolytes which can provide an increment of ionic conductivity (Hafiza et al., 2014; Bakar et al., 2015; Sikkanthar et al., 2015; Mejenom et al., 2018; Mazuki et al., 2019).

In order to fully investigate the behaviour of a binary dopant salt in polymer electrolytes, the cationic transference number, salt diffusion coefficient and ionic conductivity must be determined (Geiculescu et al., 2006). As protons (H^+) from ammonium salt greatly influence the ionic conductivity of polymer electrolytes, it is necessary to study the amount of H^+ . The protons (H^+) can be determined by using the cation transference number. Commonly, there are two techniques to calculate the cationic transference number which are via the Watanabe technique (Watanabe et al., 1995) and the Bruce and Vincent technique (Evans et al., 1987).

Furthermore, protons (H^+) can be beneficial for developing a proton battery due to the low cost electrode fabrication and electrolyte materials (Samsudin et al., 2014). Thus, proton conducting polymers are being widely studied for potential use in low cost devices (Ng et al., 2008).

2.4 Polymer Electrolytes in electrochemical device application

The biopolymer electrolyte is a crucial component of solid-state energy devices and has been extensively studied. According to Bhargav et al. (2009) and Hatta et al. (2009), ionic conductivity must be sufficient to be applied in electrochemical devices. The basic principle of charge storage depends on the electrostatic charge built-up between the electrode and electrolyte that occurs with no chemical reactions to form a double layer. Electrochemical capacitors (supercapacitor cells) commonly consist of the electrolyte and one pair of electrodes. Numan et al. (2016) and Nadiah et al. (2017) claimed that supercapacitors have the potential to replace batteries in industrial applications due its high power density, excellent cyclic retention and fast charging. Supercapacitors can be divided into two main categories, namely hybrid capacitors EDLCs and pseudocapacitors (Liew et al., 2016). In pseudocapacitors, energy is stored through a Faradaic process while energy is stored in the double layer at the electrode/electrolytes interface in EDLCs without going through the Faradaic process (Liew et al., 2014b; Omar et al., 2016). The EDLCs are proven to be able to store energy at high power densities (Choudhury et al., 2009; Guo et al., 2018) as shown in Figure 2.4.

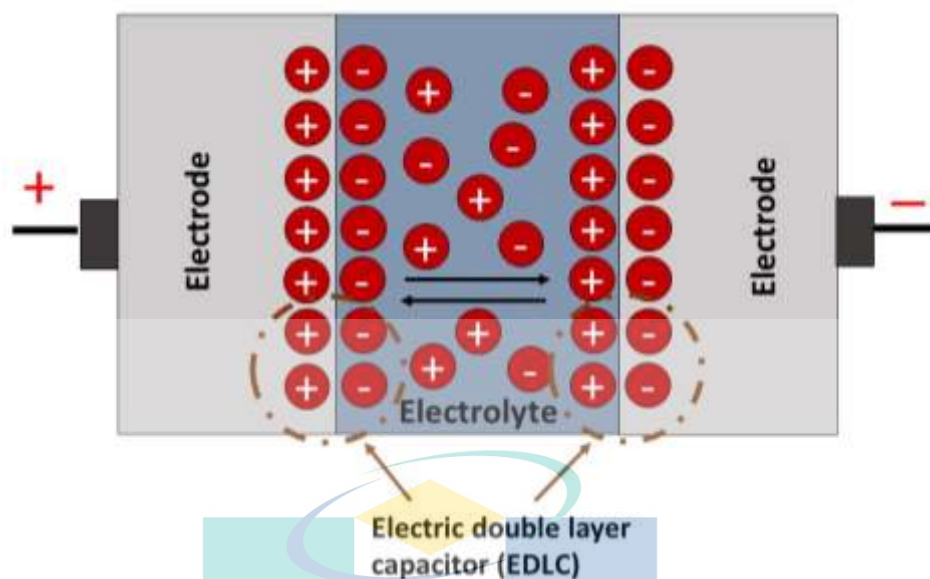


Figure 2.4 Schematic diagram of mechanism in EDLC.

EDLCs have attracted enormous attention worldwide as alternative energy storage systems (Varzi et al., 2015) due to their relatively wide potential window including free maintenance, free of toxic materials, higher power density, large capacitance and longer cycle life compared with batteries (Kibi et al., 1996; Burke, 2000; Zubieta et al., 2000). Figure 2.5 shows a power density comparison of electrochemical devices. To fabricate an EDLC, it requires one electrolyte and two electrodes derived from any suitable material such as graphite (Faraji et al., 2019), activated carbon (Liew et al., 2016), carbon black (Hashmi et al., 1997) and carbon aerogel (Abbas et al., 2018).

Among these active materials, graphene is one of the most popular among researchers for electrochemical application due to several unique properties including high nominal surface area of $2,630 \text{ m}^2 \text{ g}^{-1}$, high electron mobility and high optical transparency (D. A. Brownson et al., 2012; D. A. C. Brownson et al., 2011; Huang et al., 2012; Y. Sun et al., 2011)(Sun et al., 2011; Brownson et al., 2011; Brownson et al., 2012; Huang et al., 2012).

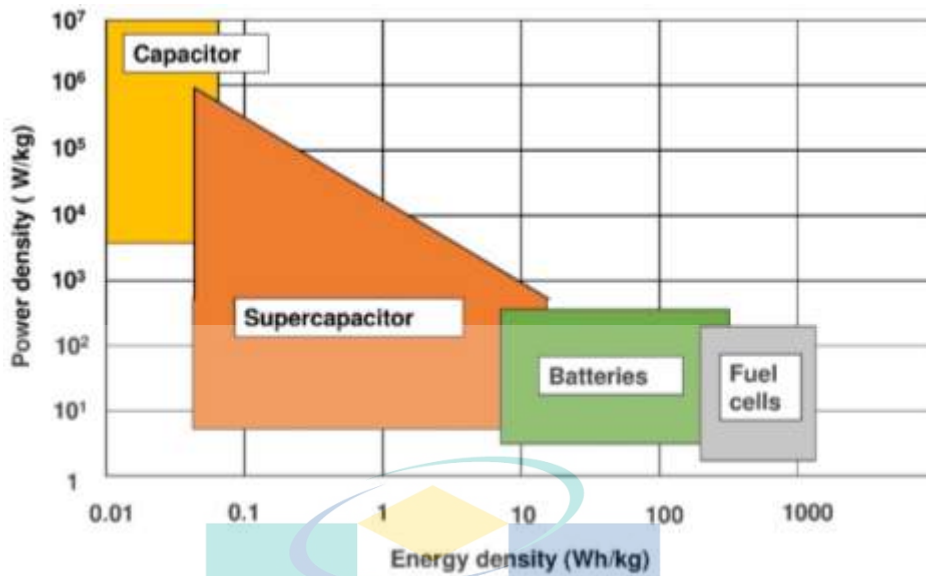


Figure 2.5 Comparison plot for electrochemical devices.

However, graphene is more expensive than other carbon materials for electrochemical devices because of problems in its synthesis related to low levels of quality, yield and reproducibility (Soldano et al., 2010). Another potential material that can act as a promising carbon electrode in EDLC is black carbon which is synthesized from gases, oils or distillates of hydrocarbons via the gas phase thermal decomposition or partial composition (Schütter et al., 2015). In contrast to graphene, the synthesis of black carbon can be better controlled. For example, the surface area of black carbon can be modified from $30 \text{ m}^2 \text{ g}^{-1}$ to more than $1,500 \text{ m}^2 \text{ g}^{-1}$ (Beck et al., 2001). The diameter of black carbon primary particles is 10 nm in diameter but increases to 100 nm when they clump together.

The properties of EDLCs allow them to store high amounts of power (up to 10 kW kg^{-1}), to be rapidly charged and discharged within seconds and to have an impressive half a million cycle life (Böckenfeld et al., 2013; Brandt et al., 2014). EDLCs based on solid and gel polymer electrolytes have the advantages of no leakage and safety issues compared to liquid electrolytes (Teoh et al., 2015). However, the performance of EDLCs also depends on electrode, electrolytes and device configuration (Yang et al., 2019). A comparison of previous studies using biopolymer electrolytes in electrochemical devices is listed in Table 2.8.

Table 2.8 List of biopolymer electrolytes used in electrochemical devices

Materials	Ionic conductivity (S cm ⁻¹)	Electrochemical devices	References
CS/MC-NH ₄ SCN	2.81 x 10 ⁻³	Electrical double layer capacitor (EDLC)	(Aziz et al., 2019)
PVA/Chitosan-NH ₄ NO ₃	2.07 x 10 ⁻⁵	Proton (H ⁺) battery	(Kadir et al., 2010)
CMCKC/CMCE-NH ₄ I	2.41 x 10 ⁻³	Dye sensitized solar cell	(Rudhziah et al., 2015b)
PVA/CH ₃ COONH ₄ -BmImCl	5.74 x 10 ⁻³	Fuel cell	(Liew et al., 2014c)
PVDF-HFP-IL (1-ethyl-3-methylimidazolium thiocyanate)	2.65 x 10 ⁻³	Electrical double layer capacitor (EDLC)	(Tuhania et al., 2018)
PVA-PVP-NH ₄ NO ₃	1.41 x 10 ⁻³	Proton (H ⁺) battery	(Rajeswari et al., 2014)
RS-NaI-MPII	1.20 x 10 ⁻³	Dye sensitized solar cell	(Khanmirzaei et al., 2015)
Chitosan-H ₃ PO ₄ -NH ₄ NO ₃ -Al ₂ SiO ₅	1.82 x 10 ⁻⁴	Fuel cell	(Majid et al., 2009)

اونيور سیتی ملیسیا قهغ

UNIVERSITI MALAYSIA PAHANG

CHAPTER 3

METHODOLOGY

3.1 Introduction

This chapter explains the flow of preparation and characterization done in the present work. The study is divided into five phases. The first phase covers the preparation of the solid biopolymer electrolyte (SBE) by doping the CMC-PVA polymer blend with various amounts of NH_4Br using the solution casting method. The second phase involves the methodologies and characterization of sample preparation. The CMC-PVA- NH_4Br SBEs system was studied to investigate the appropriate content of NH_4Br as an ionic dopant via ionic conductivity analysis. The ionic conduction, thermal properties and structural of CMC-PVA- NH_4Br SBEs system were determined using Electrical Impedance Spectroscopy (EIS) and Transference Number Measurement (TNM), Thermogravimetric Analysis (TGA) and differential scanning calorimetry (DSC) and Fourier Transform Infrared Spectroscopy (FTIR) and X-ray Diffraction (XRD), respectively.

In the third phase, the sample with the highest in ionic conductivity was chosen to measure the potential electrochemical windows via Linear Sweep Voltammetry (LSV). Afterwards, the most conducting sample was used to fabricate electrical double layer capacitor (EDLC) coin cells to understand the performance characteristics of biopolymer electrolyte in EDLC application. The preparation of electrode and fabrication of EDLC is further discussed in phase 4 and the last phase will discuss the EDLC fabrication and characterization. Figure 3.1 depicts an overview of the experiments carried out in the present work.

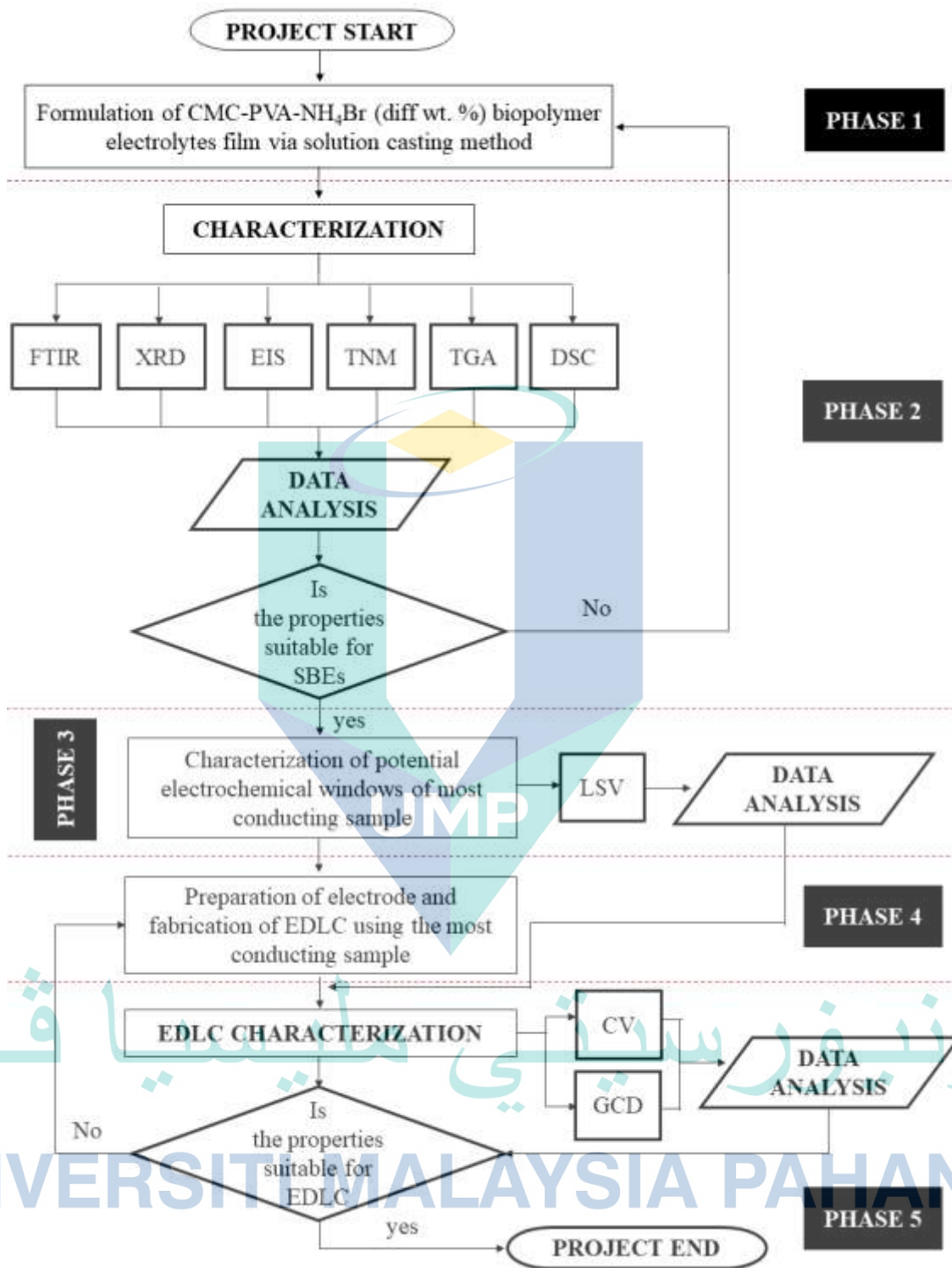


Figure 3.1 General overview of experimental work of this research.

3.2 Preparation of Solid Biopolymer Electrolytes

In the present research, the solution casting technique was used to prepare the carboxymethyl cellulose (CMC) blended with polyvinyl alcohol (PVA) and doped with ammonium bromide (NH₄Br) solid biopolymer electrolyte. The CMC (M.W. 90000) and PVA (M.W. 70000, ~85 % hydrolysis) powdered materials used in this work were both obtained from Across Organic Co. and Merck Co., respectively. Based on a previous work by Saadiah et al. (2019), the 80:20 ratio of CMC-PVA blended polymer was used because it was found to be the most favourable conducting ratio. 1.6 g of CMC was first dissolved in 98 ml distilled water and was stirred with a magnetic stirrer until the solution became homogenous. Then, 0.4 g of PVA was added accordingly into the solution. When the whole solution was completely dissolved, different amounts of NH₄Br (Merck Co.) in the range of 5 to 35 wt. % was added. The beaker was wrapped with aluminum foil at the top in order to prevent contamination by particles or dust. The solutions were continuously stirred until homogenous and then were casted into several petri dishes. For further drying process, the samples were dried in an oven with the temperature at 55 °C for 7 hours. The films were left in a desiccator before they were tested for characterization. The various amount of NH₄Br and designation of SBE systems are tabulated in Table 3.1.

Table 3.1 Designations of CMC-PVA-NH₄Br based SBEs system.

Design	Content of SBEs system				
	Weight (g)		Weight percent	Weight percent	
	CMC	PVA	(wt. %)	NH ₄ Br	(wt. %)
AB0				-	0
AB5				0.11	5
AB10				0.22	10
AB15				0.35	15
AB20	1.6	0.4	80:20	0.50	20
AB25				0.67	25
AB30				0.86	30
AB35				1.08	35
AB40				1.33	40
AB45				1.64	45
AB50				2.00	50

Figure 3.2 shows the preparation process of the CMC-PVA-NH₄Br films-based biopolymer electrolyte via the casting technique.

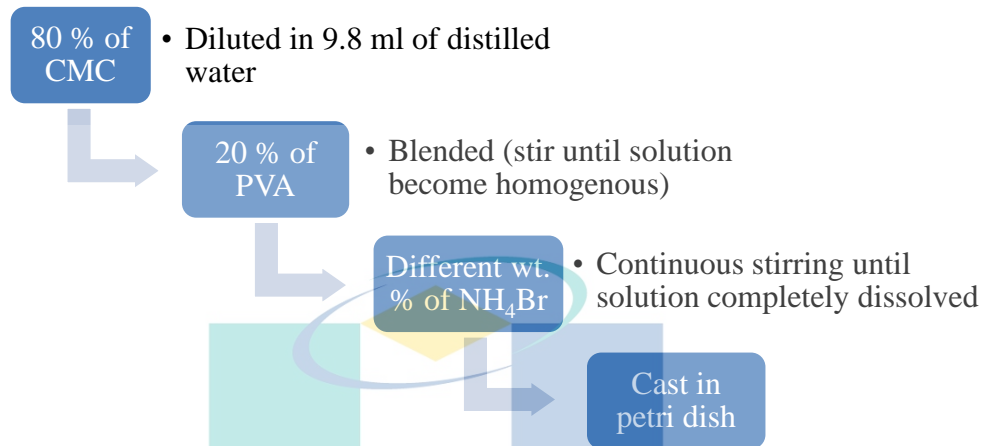


Figure 3.2 Process for making a solid biopolymer electrolyte films sample.

3.3 Characterization of SBEs system

3.3.1 Fourier Transform Infrared Spectroscopy (FTIR)

In the 1880s, chemical infrared spectroscopy emerged as a science and later Connes (1984) reported the study on Fourier transform spectroscopy that began 100 years earlier with the production of the high path difference interference phenomenon that was later used for solar spectrum wavelengths in the near IR. Through gradual advancements, scientists have used Fourier transform spectroscopy in research including the discovery of hyperfine structures and widths of atomic lines, to study the speed of light and invented the interferometer (Connes, 1984). Infrared spectroscopy is currently used to investigate the salt complexation and free ions transport properties of biopolymer-salt complexes.

In addition, FTIR analysis also can detect the presence of impurities and confirm the purity of compounds through a collection of absorption bands. In the present work, the complexation of the CMC-PVA-NH₄Br SBEs system was characterized in the IR spectra using a spectrometer (Perkin Elmer Spectrum 100). This spectrometer was equipped with an Attenuated Total Reflection (ATR) accessory with a

germanium crystal. Infrared light was passed through the sample that was placed on the germanium crystal with the light frequency of 700 to 4000 cm^{-1} and a spectra resolution of 2 cm^{-1} . For pure NH_4Br , the FTIR spectra was determined using potassium bromide (KBr) in pellets form.

3.3.2 X-ray Diffraction (XRD)

According to Thomson (1968), electron diffraction was first discovered in the early 1920s of which crystal analysis by x-ray diffraction supported the classical theory of light. In addition, low-temperature irregularities of specific heats were explained by Planck's theory of radiation. An American physicist, Athur Holly Compton later discovered the Compton effect which demonstrated the particle nature of electromagnetic radiation. The X-ray diffraction (XRD) method, also known as X-ray crystallography is a method to investigate the crystal structures of material. The XRD analytical technique can also determine whether the material is amorphous or crystalline, the degree of crystallinity of materials, structural aspects and the quantitative phase analysis subsequent to the identification (Klug et al., 1974; Hwang et al., 2001). The phenomenon of diffraction occurs when X-rays touch a crystalline target.

XRD was used in this work to determine the nature of the CMC-PVA- NH_4Br complexes. The XRD measurements was carried out using a nickel-filtered $\text{Cu K}\alpha$ ($\lambda = 0.154 \text{ nm}$) XRD-Rigaku MiniFlex II with a radiation of 30 kV, 15 mA at room temperature. The blended polymer films were placed onto a glass slide and then was placed in the sample holder of the diffractometer. The X-rays diffract through the SBE sample and into a detector. The beam and detector were rotated through different angles and the angles at which the crystals diffract the beam into the detector correspond to planes of the samples as illustrated in Figure 3.3. In this present work, CMC-PVA- NH_4Br biopolymer electrolytes were scanned at 2θ angles between 5° and 80° . XRD deconvolution were carried out to determine the full width at half maximum (FWHM) for all SBEs sample by using OriginPro 8.0 software. The XRD spectra were deconvoluted from 5° to 80° . The FWHM were then used to calculate the size of crystallinity of SBEs sample.

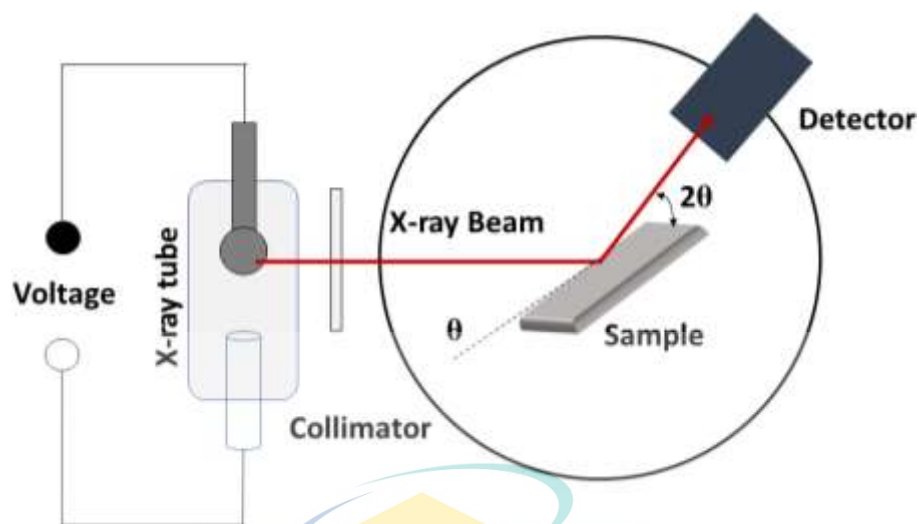


Figure 3.3 A simplified schematic of X-ray diffraction.

3.3.3 Thermogravimetric Analysis (TGA)

In recent years, thermal methods have found a wide application. These methods are known by various names such as thermal analysis, thermo analysis or thermo analytical techniques. They are used for characterization studies such as to characterize elements, compounds and mixtures of systems by measuring ambient temperature changes in physical and chemical properties in response to increasing temperature (Parker, 1983). There are two major methods which include thermogravimetric analysis and differential thermal analysis. Within this definition, other methods has developed which involve the use of changes in electrical resistance, solid volumes, gas pressures or volumes, and ultraviolet (Coats et al., 1963). The materials will undergo phase transitions which involve structural changes and decomposition under increasing temperatures when they are heated. The mass of materials will also change during the decomposition process and measured as a function of temperature/time, with a constant heating rate and under a controlled atmosphere. The thermal stability of the solid biopolymer electrolytes system was measured with a TGA instrument (Mettler Toledo TGA DSC 1). For measurements of CMC-PVA-NH₄Br films, they were heated from 5 to 800 °C at a heating rate of 10 °C min⁻¹ under nitrogen gas atmosphere at a flow rate of 20 ml min⁻¹. The mass of samples used for TGA characterization was ~5 mg.

3.3.4 Differential Scanning Calorimetry (DSC)

The development of an instrument for differential thermal analysis is to measure the transition energy of the sample analyzed (Watson et al., 1964). The measurement of the depression of the sample's melting point are often used to determine the purity of the sample. Differential Scanning Calorimetry (DSC) is routinely used to measure the melting endotherms to detect the occurrence of melting and to determine the samples' melting temperature (Brown, 2001). A computerized differential scanning calorimetry (DSC) (Netzsch Polyma 240) was used for thermal analysis in the present study.

The DSC technique can be employed to determine a crystalline polymer's glass transition or a polymer's response to heating. Moreover, the DSC data can also provide the glass transition temperature, T_g that is very useful in investigating the miscibility of a polymer blend. For the analysis, a prepared sample was first sealed in an aluminum pan. An empty aluminum reference pan was placed in the DSC furnace next to the sample pan. Both pans were then heated by a heating element in the furnace at the same rate. Crystallization or melting thermal transitions cause an absorption or release of heat which result in temperature differences between the sample and reference. The samples were heated and cooled with a $10\text{ }^\circ\text{C min}^{-1}$ heating rate from 30 to $450\text{ }^\circ\text{C}$ using nitrogen gas at 20 ml min^{-1} .

3.3.5 Electrical Impedance Spectroscopy (EIS)

The impedance spectroscopy (EIS) technique is used to study the electrical properties of materials. This technique is widely used in many applications, not only in electrochemical devices but also in medical devices. Islam et al. (2013) reported the usage of EIS in their work which can provide several advantages that include being a comparatively cheap technique, rapid data collection that allows measurement of changes in function and monitoring of physical functions in the long-term. EIS is widely used in the field of electrochemical devices as a tool to investigate the material's electrochemical and electrical properties (Barsoukov et al., 2018).

In the present study, the EIS was used to determine the ionic conductivity of the biopolymer electrolytes. The impedance was measured using a computer-connected HIOKI 3532-50 LCR Hi-TESTER in a frequency range of 50 Hz to 1 MHz.

Furthermore, the ionic conductivity measurement was carried out from room temperature up to 373 K for each sample to investigate the ionic conductivity behaviour. The prepared CMC-PVA-NH₄Br films were cut into four pieces and were placed in between two electrodes made out of stainless steel. The bulk resistance (R_b) value was obtained from the imaginary impedance (Z_i) against real impedance (Z_r) of Nyquist plots (Figure 3.4). Equation 3.1 represents the relation for ionic conductivity, σ :

$$\sigma = \frac{y}{R_b A} \quad 3.1$$

where y is the thickness of the sample and A (cm²) the cross-sectional area of the sample. According to (Arof et al., 2014), the real impedance, Z_r and imaginary impedance, Z_i of polymer electrolytes sandwiched between two blocking electrodes can be expressed as the following relation:

$$Z^* = Z_r + Z_i \quad 3.2$$

$$Z_r = \frac{R_b}{1 + (\omega R_b C)^2} \quad 3.3$$

and

$$Z_i = \frac{\omega R_b^2 C}{1 + (\omega R_b C)^2} + \frac{2}{\omega C_e} \quad 3.4$$

where R_b is bulk resistance, ω is angular frequency, C is bulk geometrical capacitance while C_e is electrical double layer. These two equations above correspond to the Nyquist plots that consist of a perfect semicircle with its center on the Z_r axis and a vertical spike.

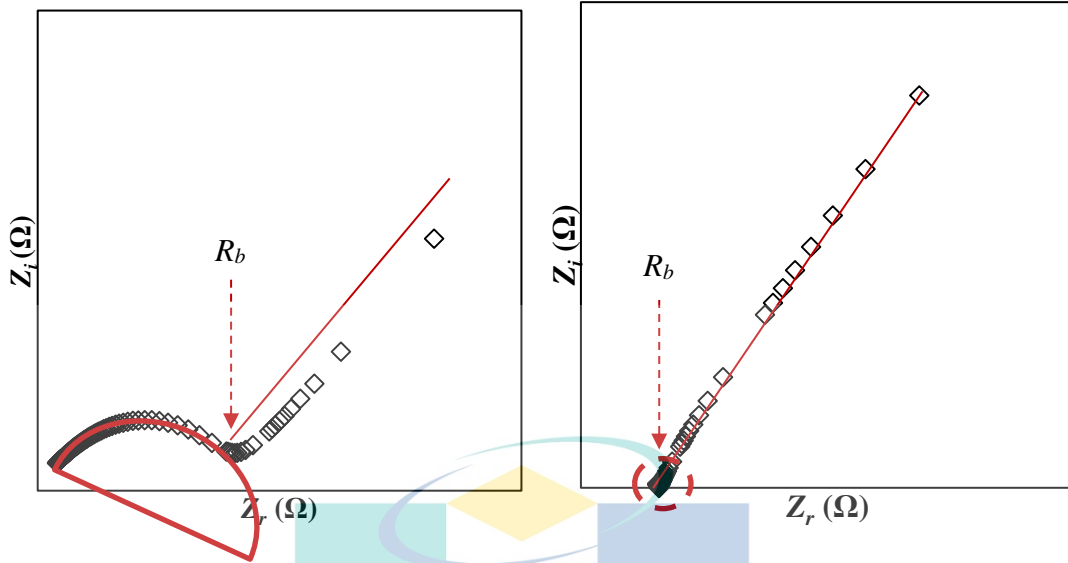


Figure 3.4 General Nyquist plot

The value of dielectric permittivity of dielectric constant, ϵ_r and dielectric loss, ϵ_i can be derived as follows:

$$\epsilon_r = \frac{z_i}{\omega C_o (z_r^2 + z_i^2)} \quad 3.5$$

$$\epsilon_i = \frac{z_r}{\omega C_o (z_r^2 + z_i^2)} \quad 3.6$$

where Z_i and Z_r correspond to the imaginary part and real part, respectively, of complex permittivity, $\omega = 2\pi f$, f is frequency while $C_o = \epsilon_o A/t$, ϵ_o is free space permittivity. The ϵ_r is known as energy storage component and dipole alignment amount in SBEs system. Meanwhile, ϵ_i is known as the energy storage component of mobile charge or dipole alignment during each cycle of the applied field. The real modulus, M_r and imaginary modulus, M_i were calculated in order to detect the relaxation peak in the high frequency region. The complex electrical modulus, M^* can be defined using complex dielectric constant, ϵ^* via the following relation:

$$M^* = M_r + jM_i = \frac{1}{\epsilon_r^*} \quad 3.7$$

where,

$$M_r = \frac{\epsilon_r}{\epsilon_r^2 + \epsilon_i^2} \quad 3.8$$

$$M_i = \frac{\epsilon_i}{\epsilon_r^2 + \epsilon_i^2} \quad 3.9$$

3.3.6 Transference Number Measurement (TNM)

TNM was used in this work to investigate the mechanism of the conducting species in the CMC-PVA-NH₄Br based biopolymer electrolytes system, i.e., indicating that the ionic conductivity of the sample is either being more cationic or anionic. The combination of complex impedance and DC polarization measurement techniques were used in the present work to evaluate the cation transference number (t_{H^+}) (Bhide et al., 2007). The Watanabe technique was employed and MnO₂ was chosen as the blocking electrode (Sukeshini et al., 1996; Woo et al., 2011). 1.2 g MnO₂, 0.18 g black carbon super p and 0.12 g polyvinylidene fluoride (PVDF) were grinded together for the preparation of the electrode and the resulting homogenous mixture was compressed to become a pallet. The H⁺ transference number was measured using the highest conducting sample and was recorded with a *dc* voltage and the impedance analyser (PGSTAT M101 with FRA32M module Autolab). The parameter used for impedance spectroscopy analysis to measure the t_{H^+} was 0.8 V amplitude at a frequency between 0.01 Hz to 100 kHz. Figure 3.5 illustrates the TNM circuit arrangement.

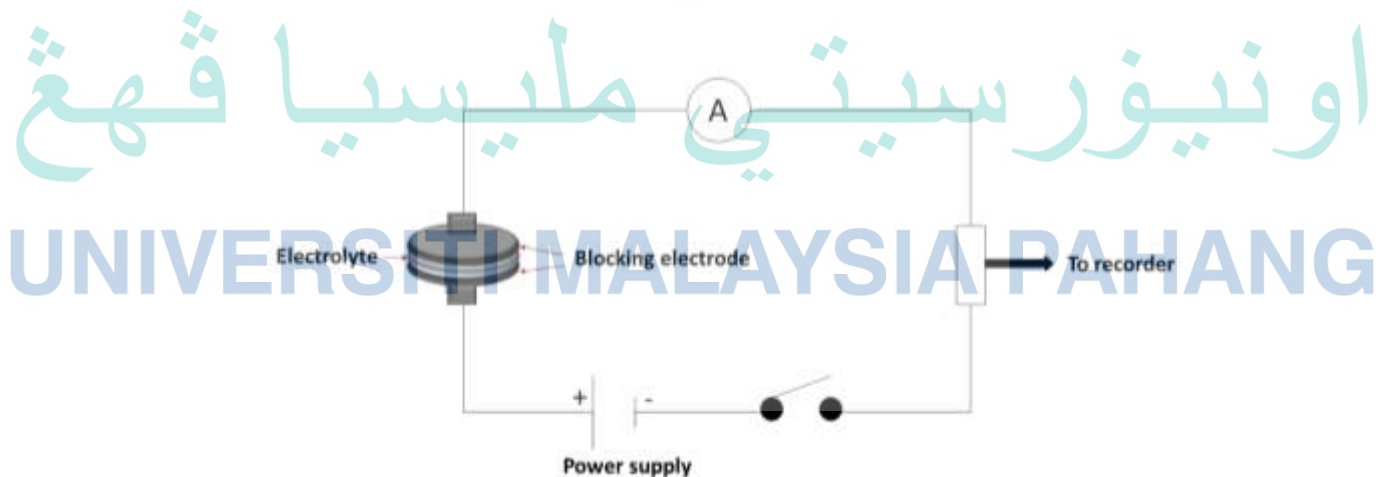


Figure 3.5 Ionic transference number experimental arrangement via *dc* polarization technique.

3.3.7 Linear Sweep Voltammetry (LSV)

For a successful application in electrochemical devices, the most important parameter to evaluate is the electrochemical stability of electrolytes. An Autolab PGSTAT M101 LSV with a FRA32M module Autolab system (Metrohm Autolab B.V., the Netherlands), operated by Nova 1.9 software was employed to determine the electrochemical stability window of the EDLC cell of biopolymer electrolyte-based CMC-PVA polymer blend doped with 20 wt. % NH_4Br . The sample with the highest ionic conductivity value was tested where the SBEs system was sandwiched between two stainless steel blocking electrodes at a scan rate of 5 mV s^{-1} at room temperature. The potential voltage was started from 0 V and ended at 3 V. The circuit setup is shown in Figure 3.6. The voltage breakdown can be detailed from the current onset as shown in Figure 3.7.

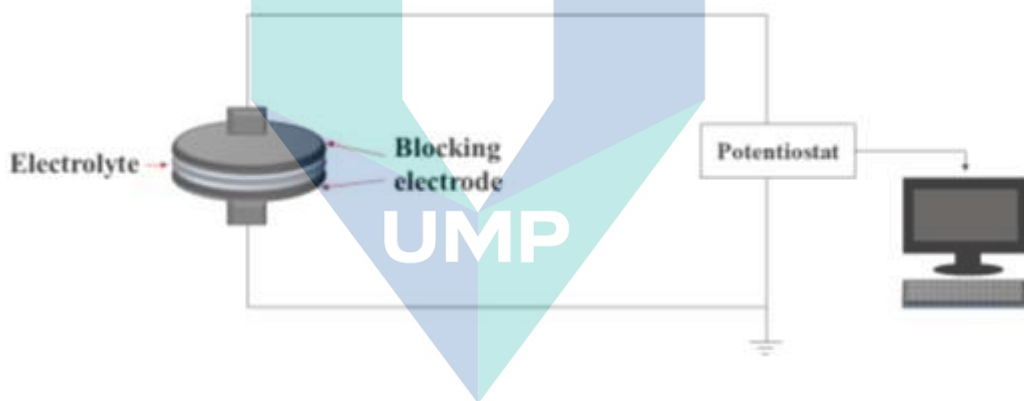


Figure 3.6 Schematic diagram of linear sweep voltammetry circuit.

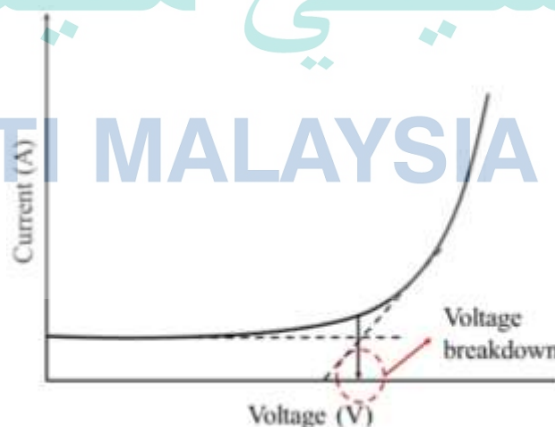


Figure 3.7 Schematic diagram of linear sweep voltammetry.

3.4 Preparation of Electrodes

A ratio of 80:10:10 of activated carbon black powder 20 (AC BP20):super conductive carbon (super P):poly(vinylidene fluoride) (PVdF) in 2.8 ml acetone was used to prepare EDLC electrodes. The BP 20, super P and PVdF were obtained from Kuraray, King First Chemical and Sigma Aldrich, respectively. The mixture was stirred until a slurry was formed followed by an ultrasonic bath treatment for 30 minutes to disperse the molecules and to homogenize them before further stirring on a hot plate for an additional 36 hours. Afterwards, the homogenous slurry was then spread on a graphite sheet via the dropping technique. The slurry spread was heated in a vacuum oven until dried. For further drying, the casted electrodes were placed in a drying cabinet filled with silica gel.

3.5 Preparation of Electrical Double Layer Capacitor (EDLC)

The EDLC was assembled by sandwiching the polymer electrolyte with two activated carbon electrodes as displayed in Figure 3.8. The electrodes were cut using an electrode cutter with area of 1 cm^2 and the mass was $\sim 0.0085 \text{ g}$. The assembled EDLC coin cells were then pressed under pressure to ensure the electrodes and biopolymer electrolyte-based CMC-PVA-NH₄Br were in good contact.



Figure 3.8 Arrangement of EDLC in the present research.

3.6 Electrical Double Layer Capacitor Characterization

3.6.1 Cyclic Voltammetry (CV)

The EDLC coin cell in the present study was characterized via cyclic voltammetry (CV) and galvanostatic charge-discharge studies. CV was carried out using Autolab PGSTAT M101 with FRA32M module Autolab system (Metrohm Autolab B.V., the Netherlands), operated by Nova 1.9 software. The EDLC coin cell was placed into the jig which acted as the sample holder and was tested from 0 to 1 V with a varying scan rate of 2, 4, 6, 8, 10, 20, 30, 40 and 50 mV s^{-1} . Figure 3.9 illustrates the schematic diagram of the CV curve. The C_{sp} was calculated using the following relation (Chen et al., 2010; Chen et al., 2010; Shukur et al., 2014a; Shukur et al., 2015; Hamsan et al., 2017b):

$$C_{sp} = \int_{V_1}^{V_2} \frac{I(V)dV}{2(V_2 - V_1)mv} \quad 3.10$$

where $I(V)$ is the area under the graph which was obtained using OriginPro 8 software, $(V_2 - V_1)$ is the potential window, m is the mass of activated materials in gram and v is the potential scan rate (Vs^{-1}).

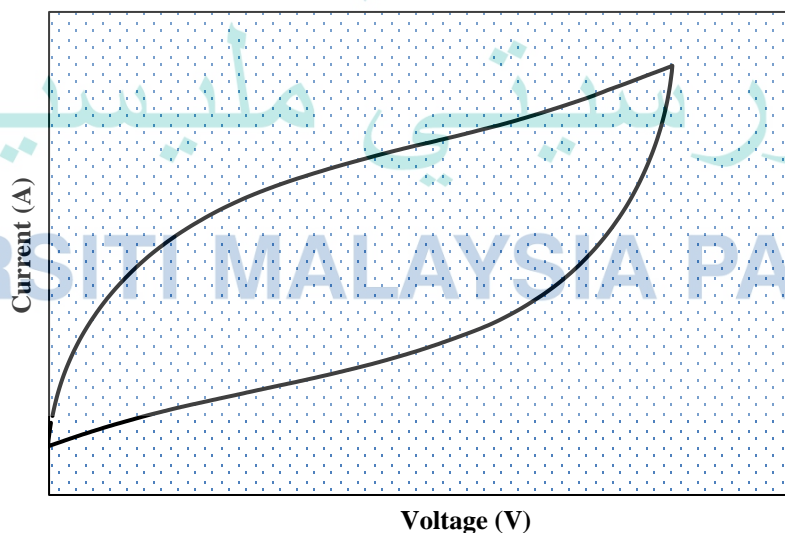


Figure 3.9 Schematic diagram of cyclic voltammetry plots of EDLC coin cell.

3.6.1 Galvanostatic Charge-Discharge (GCD)

The galvanostat Neware battery testing system (Figure 3.17) was used to determine the galvanostatic charge-discharge characteristics of the EDLC. The EDLC coin cell was tested in a voltage of 1 V at a various current densities of 0.5, 0.4, 0.3 and 0.1 mA cm⁻². Using the selected charge-discharged cycle, the specific capacitance was calculated as well as the power density and energy density for the purpose of evaluating the performance of the highest conducting biopolymer electrolyte-based CMC-PVA-NH₄Br in EDLC coin cell.

The specific capacitance can be calculated via the equation:

$$C_{sp} = \frac{it_d}{mV_d} \quad 3.11$$

where I is a constant current density, t_d is discharge time, m is mass of active material and V_d is potential drop obtained from discharging curve. Meanwhile, the ESR of the EDLC can be obtained from the following relation:

$$ESR = \frac{V_d}{i} \quad 3.12$$

The coulombic efficiency is another important parameter needed to further understand the cycling stability of the EDLC coin cell. The coulombic efficiency can be calculated using the following equation:

$$\eta = \frac{t_d}{t_c} \times 100 \% \quad 3.13$$

where t_d and t_c are discharge and charge time, respectively. The energy density, E and power density, P of the EDLC coin cell can be expressed as the following relation:

$$E = \frac{C_{sp}V_d^2}{2} \quad 3.14$$

$$P = \frac{E}{t_d} \quad 3.15$$

where C_{sp} is specific capacitance, V_d is potential drop obtained from discharging curve and t_d is discharge times. Figure 3.10 illustrates the ideal GCD profile.

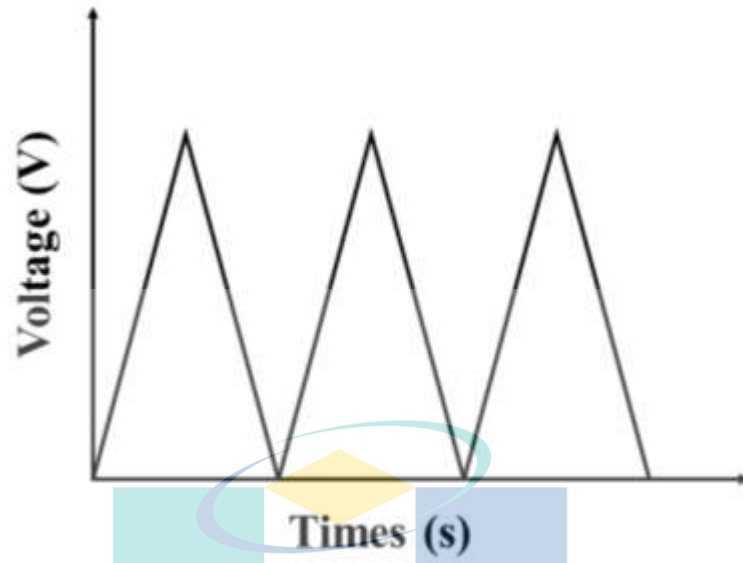


Figure 3.10 Schematic diagram of galvanostatic charge-discharged plots of EDLC coin cell.

اونيورسيتي ملايسيا قهغ

UNIVERSITI MALAYSIA PAHANG

CHAPTER 4

RESULTS AND DISCUSSION

4.1 Introduction

This chapter discusses the results obtained from all of the characterization used in this work including the structural, thermal and conduction properties of the CMC-PVA-NH₄Br biopolymer electrolytes system using Fourier Transform Infrared (FTIR) Spectroscopy, X-ray diffraction (XRD), Differential Scanning Calorimetry (DSC) and Thermo Gravimetric Analysis (TGA). The ionic conduction properties of the biopolymer electrolytes system were measured via the Electrical Impedance Spectroscopy (EIS) and Transference Number Measurement (TNM). A further evaluation on the performance of solid biopolymer electrolytes as an electrical double layer capacitor (EDLC) via Linear Sweep Voltammetry (LSV), Cyclic Voltammetry (CV) and Galvanostatic Charge-Discharge (GDC) are explained in this chapter. All of the findings in this work are compiled to support each other and based on references from previous works in order to achieve the objectives 2, 3 and 4.

4.2 Appearance of Blend Biopolymer Electrolyte

The solid biopolymer electrolytes (SBEs) thin film system-based CMC-PVA polymer blend doped with various amount of NH₄Br had been successfully prepared via the casting method. The physical appearance of SBEs showed a transparent thin film, flexible and free standing as presented in Figure 4.1. The excellent appearance helped the present SBEs to show good compatibility with electrodes, ease the fabrication process, have no leakage, low self-discharge and elasticity. However, the sample was found not to form a solid-state when above 35 wt.% of NH₄Br was introduced. Therefore, these samples that exhibited a different morphology were not further analysed.



Figure 4.1 Solid biopolymer electrolyte film.

4.3 Fourier Transform Infrared Spectroscopy (FTIR) Analysis

Infrared radiation is part of the electromagnetic spectrum between the visible and microwave regions (4000 to 700 cm^{-1}) (Ramesh et al., 2007). FTIR spectroscopy is widely used to investigate the polymer electrolyte backbone structure.

4.3.1 IR spectra of CMC-PVA blend

In the present research, the best conducting ratio of 80:20 for CMC:PVA was used based on previous research conducted by Saadiah et al., (2018). PVA is a water-soluble polymer which contains the hydroxyl group (-OH). The interaction between CMC and PVA was expected to occur via the formation of hydrogen bonding at the carboxyl group (COO^-). Rajendran et al. (2003) agreed that the formation of the polymer blend is assisted by the hydrogen bonding in PVA that originates from the OH group.

The interaction between the CMC-PVA based biopolymer electrolyte was analysed via FTIR spectroscopy in order to identify the structure of the polymer and is illustrated in Figure 4.2. It shows that there are seven absorption bands that were observed at wavenumbers of 901 cm^{-1} , 1057 cm^{-1} , 1325 cm^{-1} , 1428 cm^{-1} , 1590 cm^{-1} , 2919 cm^{-1} and 3316 cm^{-1} which corresponded to C-H rocking, C-O-C bending, C-H stretching, O-H stretching, COO^- asymmetric stretching, C-H stretching and O-H stretching, respectively. The list of functional groups for pure CMC and pure PVA are summarized in Table 4.1

and Table 4.2, respectively. The functional groups for CMC-PVA polymer blend are summarized in Table 4.3.

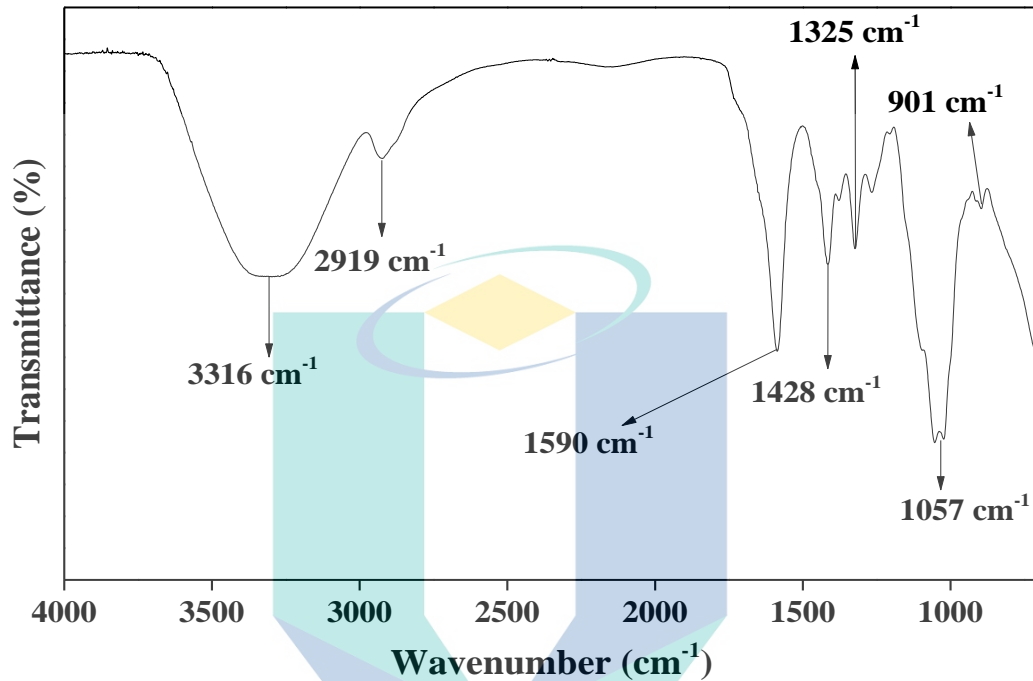


Figure 4.2 FTIR spectra of CMC-PVA solid biopolymer electrolyte.

Generally, CMC interacted with PVA via hydrogen bonding and this is supported by Saadiah et al. (2019) who stated that the shift in wavenumber is caused by the interaction among the two polymer blends. The band assigned to the C=O of carboxyl anion group (COO^-) appears to belong to the CMC-PVA polymer blend. This functional group had been highlighted due to their opportunity to interact with the ionic dopant when introduced into the system. The CMC-PVA polymer blend provided more vacant sites for ions from the ionic dopant to dissociate in the polymer complex and was predicted to help increase the ionic mobility which in turn can increase the ionic conductivity. It is also one of the indicative bands to see if any complexation occurs when CMC-PVA was incorporated with NH_4Br .

Table 4.1 List of functional groups for pure CMC from previous works.

Material	Wavenumber (cm ⁻¹)	Assignment	References
Carboxymethyl cellulose (CMC)	1060	C-O-C bending	(Biswal et al., 2004)
	1329	C-H stretching	(Chai et al., 2013b; Kamarudin et al., 2013)
	1420	O-H stretching	(Chai et al., 2013b; Rani et al., 2016)
	1591	COO ⁻ stretching	(Cuba-Chiem et al., 2008; Samsudin et al., 2011; Samsudin et al., 2012)
	2909	C-H stretching	(Biswal et al., 2004; Ramlli et al., 2016)
Polyvinyl Alcohol (PVA)	3432	O-H stretching	(Biswal et al., 2004; Chai et al., 2013b)
	850	C-H rocking	(Rajendran et al., 2004; Hema et al., 2007; Hema et al., 2009)

Table 4.2 List of functional group of pure PVA from previous works.

Material	Wavenumber (cm ⁻¹)	Assignment	References
Polyvinyl Alcohol (PVA)	1026 and 1091	C-O bending	(Buraidah et al., 2011)
	1430	C-H bending	(Rajendran et al., 2004; Hema et al., 2007, 2009)
	1659	C-O stretching	(Hema et al., 2007)
	1724	C=O stretching	(Hema et al., 2007; Hema et al., 2009; Buraidah et al., 2011)
	2925	CH ₂ asymmetric stretching	(Hema et al., 2007)
	3354	O-H stretching	(El-Sawy et al., 2010; Buraidah et al., 2011; Kadir et al., 2011)

Table 4.3 List of functional groups for CMC-PVA polymer blend.

Materials	Wavenumber (cm ⁻¹)	Assignment
CMC/PVA	901	C-H rocking
	1057	C-O-C bending
	1325	C-H stretching
	1428	O-H stretching
	1590	COO- asymmetric
	2919	C-H stretching
	3316	O-H stretching

4.3.2 IR spectra of Ammonium Bromide (NH₄Br)

The FTIR spectra of pure NH₄Br is illustrated in Figure 4.3. As shown, a broad intensity band at 3133 cm⁻¹ was due to asymmetric stretching vibration of the ammonium ion. According to Yusof et al. (2014), the N-H stretching mode were detected at 3079 cm⁻¹ and 2934 cm⁻¹ which is also in agreement with Zainuddin and Samsudin (2018). Meanwhile, a sharp intense absorption was observed at 1402 cm⁻¹ which was assigned to the N-H bending mode. A similar band was also reported by Samsudin (2014) and according to Hema et al. (2008), the NH₄⁺ is an important functional group acting as the proton donor in the electrolyte of the present study. Table 4.4 tabulates the functional groups of pure NH₄Br.

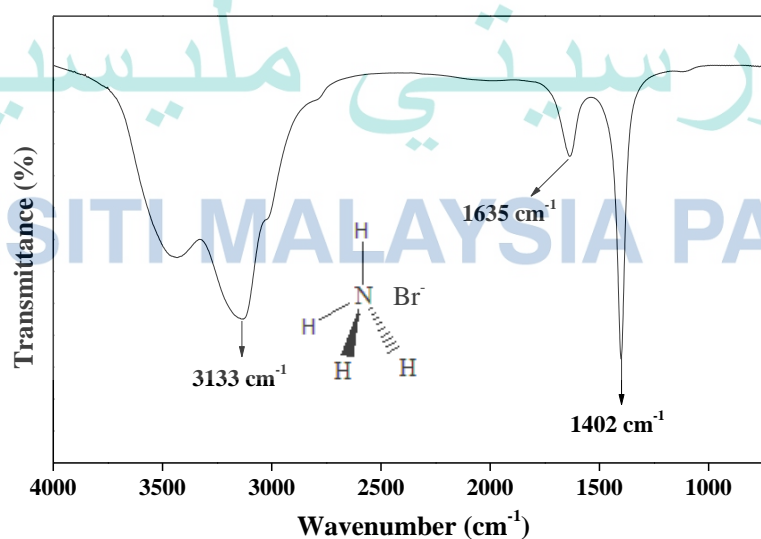


Figure 4.3 FTIR spectra of pure ammonium bromide.

Table 4.4 List of functional groups for pure NH₄Br.

Materials	Wavenumber (cm ⁻¹)	Assignment
NH ₄ Br	1402	NH ₄ ⁺ bending
	1635	N-H bending
	3133	N-H stretching

4.3.3 IR spectra of CMC-PVA doped NH₄Br SBEs

The IR spectra for CMC-PVA polymer blend doped with various amount of NH₄Br was presented in the region of 4000 to 700 cm⁻¹ as shown in Figure 4.4. Information on the structural details of CMC-PVA incorporated with NH₄Br complexes are discussed in this section. In the present research, the CMC-PVA sample (undoped system) had shown the highlighted peak which is believed where the complexation will occur, especially at 1200 to 900 cm⁻¹ (C-O-C bending), 1500 to 1200 cm⁻¹ (O-H bending), 1700 to 1450 cm⁻¹ (COO⁻ stretching and C=O stretching) and 4000 to 2700 cm⁻¹ (C-H stretching and O-H stretching). These peaks have been focusing and presented in different region as shown in Figure 4.5, Figure 4.6, Figure 4.7 and Figure 4.8, respectively.

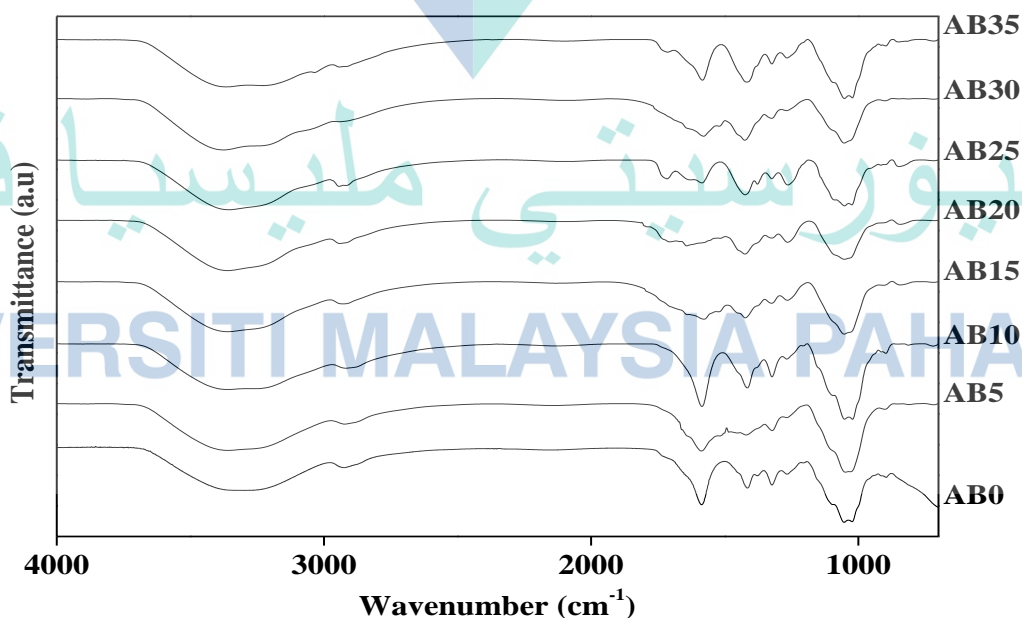


Figure 4.4 IR spectra of CMC-PVA doped with various amounts of NH₄Br at 4000 to 700 cm⁻¹.

Based on Figure 4.5, the characteristic vibrational band at 1057 cm^{-1} was determined to be due to the carboxyl (C-O^-) from C-O-C bending vibration of pure CMC (Samsudin et al., 2014), and a slight shift from higher to lower wavenumber was observed from 1057 to 1049 cm^{-1} after the incorporation of NH_4Br . The shift in wavenumber was expected at this region because of the existence of the highly electronegative oxygen atom originating from the C-O^- group that caused interaction between the CMC with the added PVA and NH_4Br which may change the system's crystallinity (Rasali et al., 2017). Therefore, the changes observed in the C-O^- region can be explained by oxygen from C-O^- interacting with H^+ moieties contributed by NH_4Br .

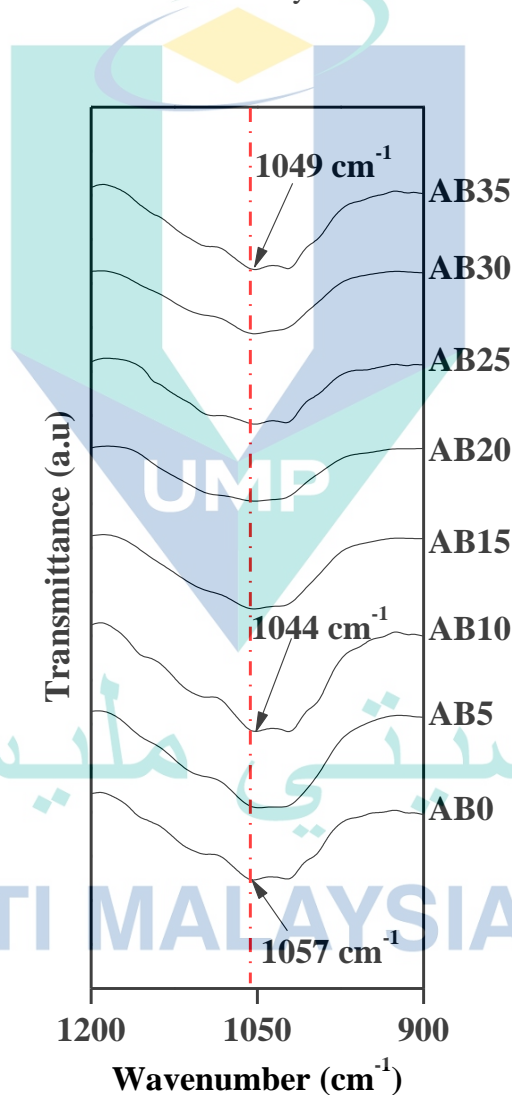


Figure 4.5 IR spectra of CMC-PVA-NH₄Br at region 1200 to 900 cm^{-1} .

Meanwhile, Figure 4.6 shows the hydroxyl (-OH) functional group with bending vibration at the 1320 cm^{-1} wavenumber. Apparently, the peak intensity of this group has decreased while the wavenumber shifted higher to 1325 cm^{-1} after NH_4Br was added. This observation in the present system could be caused by the proton (H^+) from NH_4Br substituting the -OH group and forming H-OH (Ahmad et al., 2016). A similar behaviour was observed in a study carried out by Samsudin et al., (2014) where the shifting in wavenumber also occurred at this region for CMC when the amount of ionic dopant increased, which could be due to the coordination of NH_4^+ ion with the polar group present in the CMC-PVA polymer blend as the NH_4Br was added.

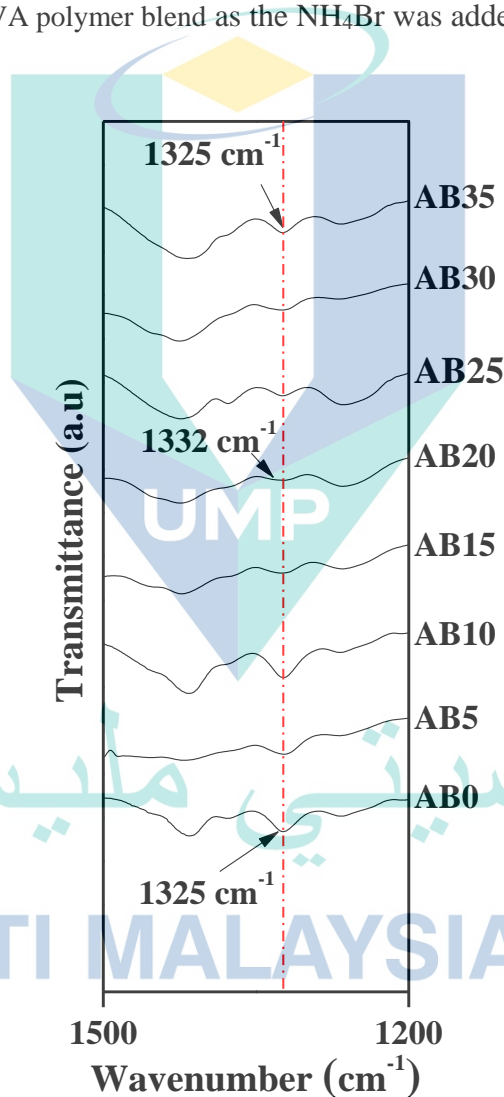


Figure 4.6 IR spectra of CMC-PVA- NH_4Br at region 1500 to 1200 cm^{-1} .

Another obvious change of peak and wavenumber can be observed in Figure 4.7 where the sharp intense absorption at 1590 cm^{-1} that was assigned to the C=O of COO^- stretching moiety of CMC-PVA had a shift to a lower wavenumber of 1581 cm^{-1} due to the protonation process induced by the oxygen's lone pair electrons attracting and attaching the NH_4Br molecule to itself (Ahmad et al., 2015b). In addition, it was observed that the addition of NH_4Br at the AB15, caused peaks to begin to disappear though the peaks re-appeared in AB25 onwards. It is speculated that this phenomenon was caused by the polymer host COO^- functional group having a coordination interaction with the H^+ from NH_4^+ which reflect the CMC-PVA polymer blend's carboxylate group having a protonation reaction with the cations. This is in agreement with Mejenom et al. (2018) who stated that in the polymer blend, the dative bond formed between the nitrogen or oxygen coordinating position and H^+ from NH_4Br caused the observed peak shifting.

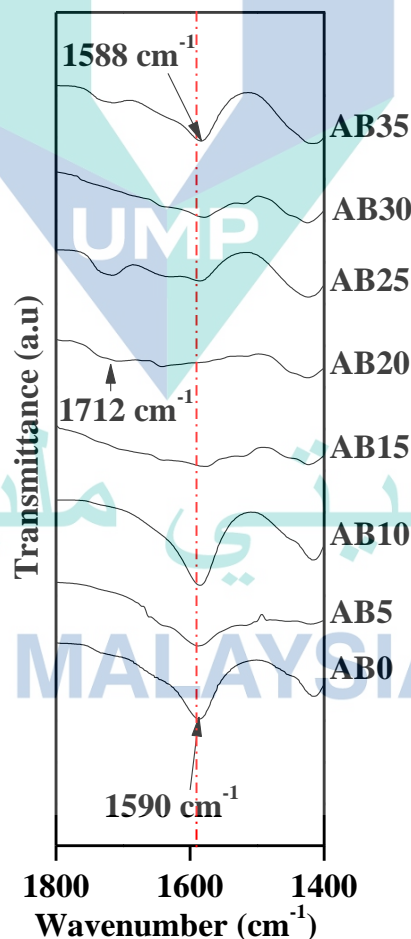


Figure 4.7 IR spectra of CMC-PVA- NH_4Br at region 1800 to 1400 cm^{-1} .

It can be noted here that there was a concomitant increase of H^+ with the increasing amount of NH_4Br , meaning more ions were migrating to the host blend polymer backbone. The ions were driven by this migration to hop from site to site via H-bonds formation (Shukur et al., 2014). This exchange of ions between the complexed sites occurred through a structure diffusion mechanism called the Grotthuss mechanism (Hema et al., 2008). According to (Reed et al., 2006), the $N-H \cdots Br$ bonds were created in ammonium bromide when the N-H bonds within the NH_4^+ tetrahedral ion point directly toward the bromide ion, Br^- . Since ammonium salt was used as a dopant in the present SBE system, it was very likely that the proton migration (H^+) mechanism was the most predominant because in the NH_4^+ ions, two out of four of the hydrogen atoms are identically bound, while for the remaining two hydrogen atoms, one was strictly bound and the other as weakly bound. The latter weakly bound hydrogen atom was easily dissociated into H^+ ions that under a *dc* electric field, can hop site to site, leaving vacant sites that will be filled by other H^+ ions (Du et al., 2010; Kadir et al., 2011).

In the present work, the PVA used was partially hydrolysed. It was observed that for the AB20 sample, a new shoulder peak appeared at the 1712 cm^{-1} wavenumber that was assigned to the C=O stretching in the PVA acetate group (Park et al., 2010). However, the addition of 25 wt. % NH_4Br caused the peak to diminish, though it reappeared in the AB35 sample. According to Ramlli et al. (2015) and Rajendran et al. (2003), changes in the intensity and position of a polymer's polar group were due to the interaction between the host polymer and the proton (H^+) ion from ammonium salt that caused an increase in number of electrons to be attracted towards the CMC-PVA via the C=O group and forming hydrogen.

Figure 4.8, shows the presence of two peaks assigned to the C-H stretching and O-H stretching. The peak at 2919 cm^{-1} that was assigned to the stretching C-H was believed to be from the undoped CMC-PVA that had no changes due to the strong bonding between C and H atoms that was easy to break. This revealed that the C-H of CMC-PVA does not provide anything towards the addition of NH_4Br .

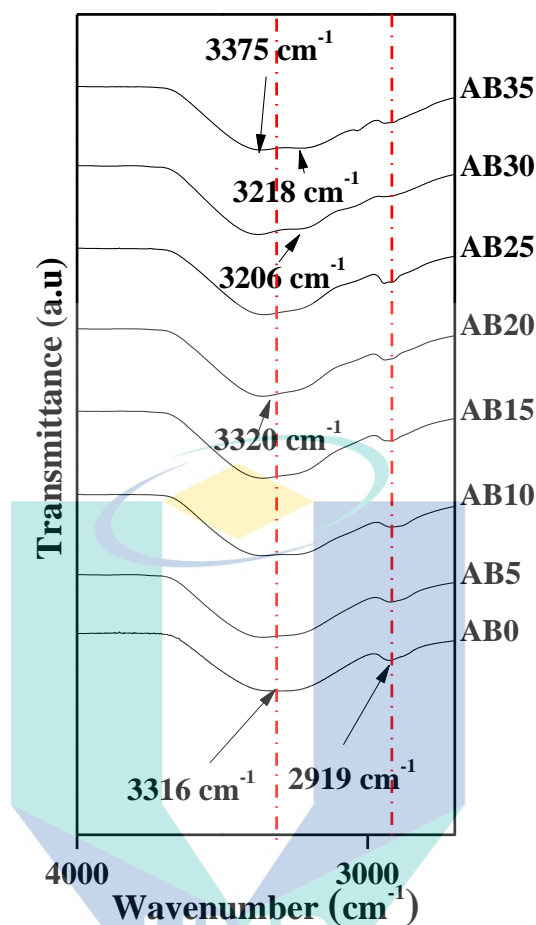


Figure 4.8 IR spectra of CMC-PVA-NH₄Br at the regions of 4000 to 2700 cm⁻¹.

Figure 4.8 also shows the existence of a broad band at 3316 cm⁻¹ that corresponded to the O-H stretching. Upon the increasing addition of NH₄Br, a shift to a higher wavenumber of 3320 cm⁻¹ for the peak assigned to the hydroxyl band was observed in the AB25 sample. This observation might be caused by the CMC-PVA polymer blend interacting with NH₄Br at the O-H band. According to El-Sawy et al. (2010) and Krimm et al. (1956), the O-H stretching absorption band at 3316 cm⁻¹ was generated from PVA which was blended with CMC. A further addition beyond 25 wt. % NH₄Br into the present system caused the appearance of new peaks at 3206 and 3218 cm⁻¹. Shukur et al. (2014) reported in a similar study that the added NH₄Cl interacted with the O-H group between starch and chitosan. This phenomenon can be explained in the present work by the NH₄⁺ ions undergoing a coordination reaction with the CMC-PVA polar groups upon the addition of NH₄Br into the system.

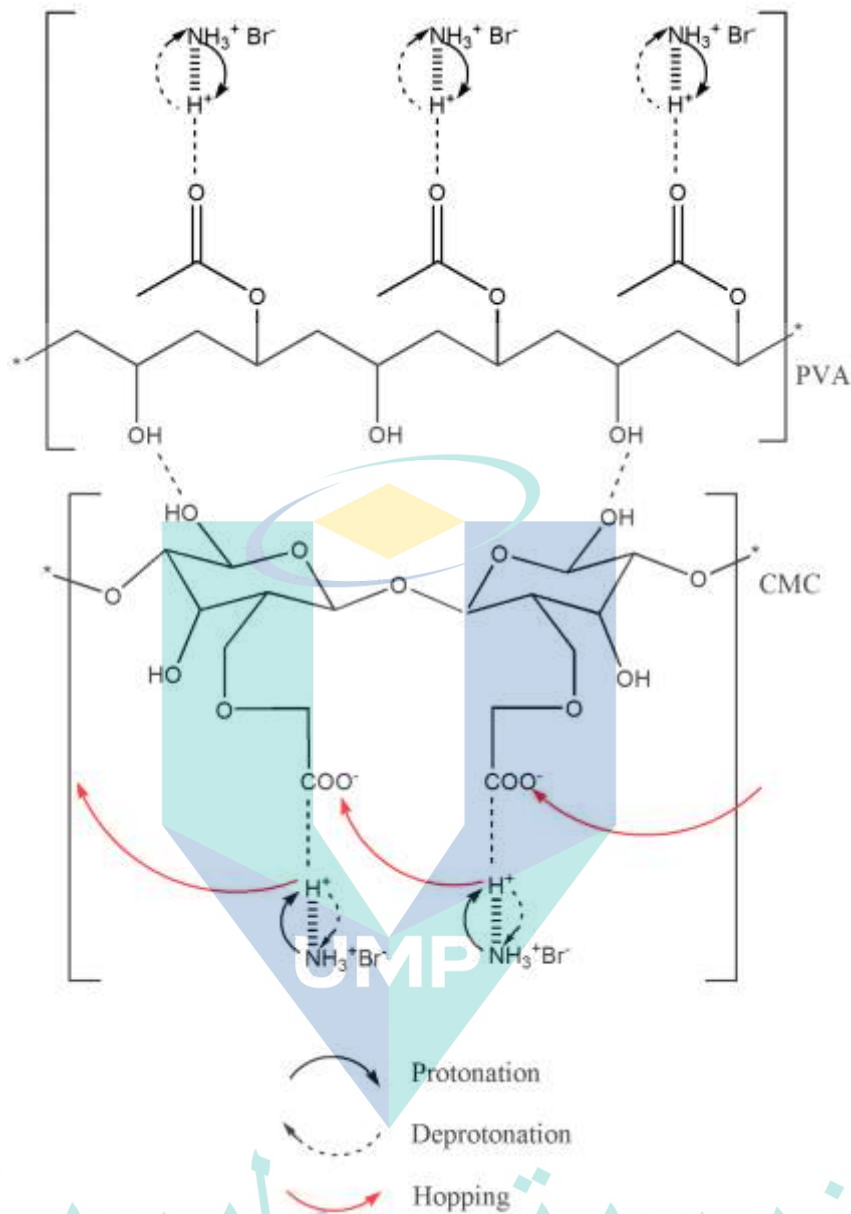


Figure 4.9 Schematic diagram of interaction between CMC-PVA and NH_4Br .

Figure 4.9 shows a schematic diagram of the interaction between the polymer blend host and ionic dopant in the present work. Based on the findings from FTIR analysis, it appeared that the Grotthus mechanism was used to allow H^+ from $\text{NH}_4^+ - \text{Br}^-$ to interact with the oxygen from the CMC-PVA polymer blend, as proven by peak intensity changes and shifts in wavenumbers. The observation from FTIR analysis showed that the complexes has occurred between CMC-PVA polymer blend and NH_4Br which influenced the amorphous phase of present research. The influence of NH_4BR in the amorphous phase of SBEs will be discussed later.

4.4 X-ray Diffraction Analysis

X-ray diffraction (XRD) is a rapid analytical technique usually used to determine the crystalline phase of materials and/or samples. This technique works by applying an X-ray beam with different angles, 2θ and wavelength directed toward the SBE samples. A cathode ray tube was used to generate the X-rays that were then filtered to produce constructive interferences and a diffracted ray, thus allowing the diffraction pattern to appear as result of the sample's structure. In this section, the XRD results are discussed for solid biopolymer electrolyte systems containing CMC-PVA polymer blend and NH_4Br . The XRD analysis was carried out to study the crystallinity of the samples with different content of NH_4Br , thus to ensure that the electrolyte samples show good compatibility with other analysis for fabrication purposes and have good performance.

4.4.1 XRD spectra of CMC-PVA and NH_4Br

The amorphousness of the polymer matrices can be determined via XRD analysis. The XRD spectra of pure CMC-PVA and NH_4Br are illustrated in Figure 4.10.

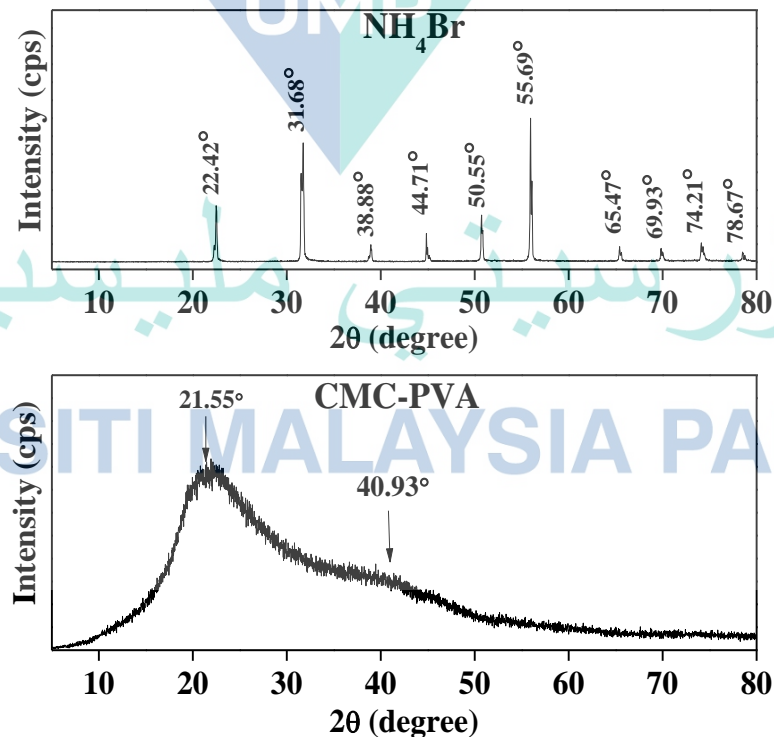


Figure 4.10 XRD patterns for pure CMC-PVA polymer blend and NH_4Br .

It was found that the CMC-PVA diffractograms revealed two diffraction peaks at 2θ , 21.55° and 40.93° , thus confirming that this polymer host was semi-crystalline. Saadiah et al. (2019) has reported that the occurrence of semi-crystallinity was due to the appearance of both crystalline and amorphous regions in the CMC-PVA backbone. In contrast, pure NH_4Br showed sharp diffraction peaks at $2\theta = 22.42^\circ$, 31.68° , 38.88° , 44.71° , 50.55° , 55.69° , 65.47° , 69.93° , 74.21° and 78.67° , which disclosed that the NH_4Br salt was crystalline in nature (Hema et al., 2008; Mejenom et al., 2018).

4.4.2 XRD spectra of CMC-PVA doped NH_4Br

The X-ray diffractograms of the CMC-PVA polymer blend incorporated with NH_4Br are depicted in Figure 4.11. As shown, the peak intensity of the CMC-PVA polymer blend shifted to a lower angle when NH_4Br was introduced into the electrolyte system up to the AB15 sample. The shifting in peak intensity to the lower 2θ may be attributed to the interaction occurring between the ionic dopant and the host polymer blend, in turn enhancing the amorphous phase of SBE systems (Rajendran et al., 2003; Bao et al., 2018; Moniha et al., 2018). According to Hodge et al. (1996), the addition of molecules such as water and salt can destroy the crystallinity by transforming the configuration from crystalline to amorphous. The H^+ might attach to vacant groups on the macromolecules and become free mobile ions as well as hydrogen bonding being relocated in the polymer matrix. Furthermore, the polymer blend has provided more vacant sites and give opportunity to ions to associate in the polymer backbone. An analysis of the XRD pattern revealed the disappearance of most peaks associated with pure NH_4Br in samples with added 5 to 25 wt. % of NH_4Br . This observation could be caused by the ammonium salt being completely dissolved in the polymer blend matrix.

As previously discussed, adding NH_4Br to the CMC-PVA contributes the raising of H^+ protonation which results in an enhancement of the amorphous phase. In addition, the hump becomes more broadened by increasing NH_4Br content and this can be explained by the polymer blend backbone softening when the two polymers were blended together, thus improving its segmental motion. This observation suggested that the ionic dopant readily interacted with the CMC-PVA, reflecting towards the sample's amorphous nature (Samsudin et al., 2012). The results showed that above 20 wt.% of NH_4Br content, there was a decrement of the amorphous phase and the crystallinity peak

started to appear. This might be due to the aggregation of the ionic dopant in the SBEs system which lead to the re-appearance of the NH_4Br peak at 22.23° , 31.50° , 38.77° , 44.94° , 50.59° , 55.84° , 65.39° , 69.83° , 74.00° , 78.44° .

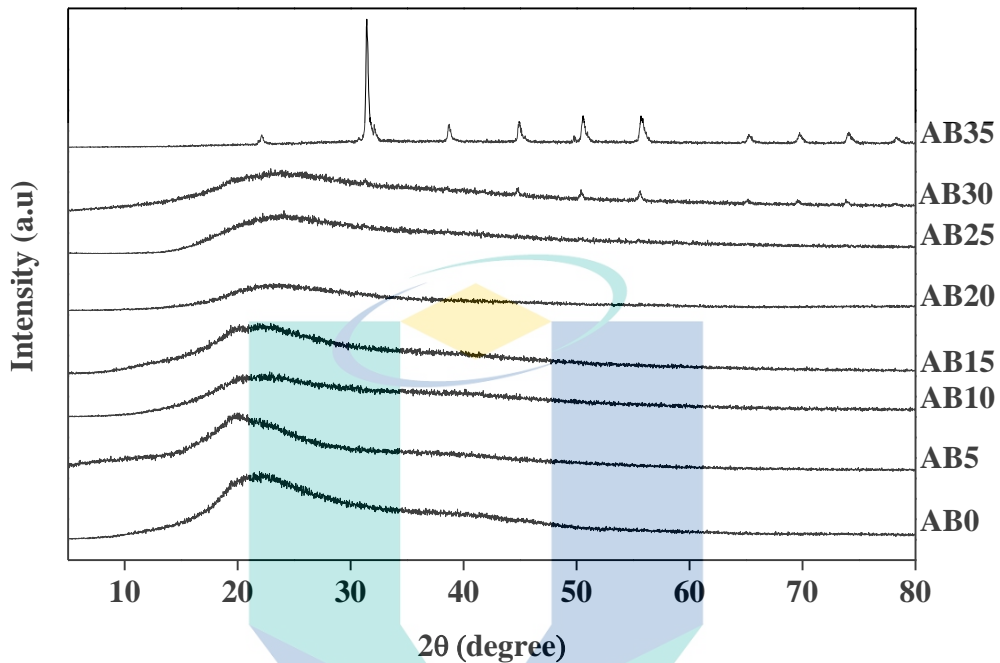


Figure 4.11 XRD patterns of biopolymer electrolytes for all NH_4Br content.

The sizes of crystallinity for the entire sample were calculated from deconvoluted XRD to study the effect of NH_4Br in CMC-PVA SBE based on the peak's full width at half maximum (FWHM) as retrieved using the OriginPro 8.0 software. This parameter was needed to identify the crystallinity changes in the samples of the present system by using the Debye-Scherrer approach (Mahakul et al., 2017; wang et al., 2017).

$$D = \frac{0.94\lambda}{\beta \cos \theta} \quad 4.1$$

where λ is represent to the wavelength of the X-ray used with value of 1.5406 \AA , β is represent to the value FWHM of the peak and θ is represent to the Bragg diffraction angle. The measured sizes of crystallinity of XRD patterns for all of the solid biopolymer electrolyte samples are tabulated in Table 4.5 and the XRD deconvolution are illustrated in Appendix 2. As shown in Table 4.5, the crystallinity value was inversely proportional to the FWHM where the higher value of crystallinity, the lower the value of FWHM (Yang et al., 2015).

Table 4.5 Crystallite sizes of all SBEs system.

Sample	2 θ (degree)	FWHM (rad)	D (Å)
AB0	20.85	0.08	18.29
AB5	21.12	0.12	12.33
AB10	21.7	0.14	10.44
AB15	27.43	0.48	3.11
AB20	23.74	1.26	1.36
AB25	23.99	0.32	4.80
AB30	22.74	0.15	9.75
	47.51	0.73	2.18
	50.42	0.88	1.82
	55.62	0.0051	323.35
	73.93	0.0077	235.92
	79.39	0.13	14.76
AB35	22.15	0.0021	187.81
	31.46	0.0079	191.49
	38.75	0.0056	274.75
	44.97	0.0044	359.06
	50.62	0.0068	235.25
	55.81	0.0077	213.31
	65.3	0.0054	317.77
	69.79	0.0058	306.43
	74.12	0.0059	305.69
	78.34	0.0038	486.29

As reported by Shukur et al. (2014b), the amorphousness of electrolytes is related to the ionic conductivity trend. As the amorphous phase increases, the ionic conductivity will also increase. Based on Figure 4.11, it was expected that the biopolymer electrolyte containing 20 wt.% NH₄Br that showed the lowest crystallinity value would exhibit the highest amorphous phase. The presence of new peaks at AB30 and AB35 proved that the salt had un-dissociated and caused the sample to become more crystalline (Samsudin & Isa, 2012). Furthermore, some of the salt was deposited on the surface of the film because

a significant portion of the salt did not become entrapped in the host polymer. Based on Table 4.5, the crystallinity of SBEs started to decrease when NH_4Br was added and achieved a minimum value for the sample containing 20 wt.% of NH_4Br . This phenomenon could be explained by increased protonation (H^+) and transport in the amorphous phase of the CMC-PVA- NH_4Br SBEs system. Furthermore, the decrement of crystallinity in SBEs upon the addition of NH_4Br was expected and this result was similar to that observed in the FTIR analysis where the added NH_4Br interacted via H^+ towards vacant sites in the CMC-PVA backbone, leading to an enhancement of the amorphous phase in CMC-PVA SBEs system (Buraidah et al., 2011; Rasali et al., 2018). In conclusion, the NH_4Br was proven to improve the amorphous phase of the electrolytes when added to the CMC-PVA polymer blend system.

4.5 Thermal Stability Analysis

Thermal analysis has been widely used in many years to characterize the materials of polymer electrolytes as it can provide information such as miscibility of the polymer blends, stability and stiffness (Rao et al., 2000). The studies of thermal properties of solid biopolymer electrolytes-based CM-PVA blend doped with various amount of NH_4Br were measured via thermogravimetric analysis (TGA) and differential scanning calorimetry measurement (DSC). The TGA analysis were carried out to investigate the thermal stability and decomposition temperature of solid biopolymer electrolyte systems. In addition, DSC analysis was used to determine the thermal behaviour, miscibility and phase transition of the polymer blends. The glass transition temperature which is one of the most important parameters for the biopolymer electrolyte system could also be determined using the DSC analysis.

4.5.1 TGA spectra of CMC-PVA and CMC-PVA doped NH_4Br

The degradation of polymer electrolytes is mainly associated with dehydration and decomposition processes. The TGA thermogram of the present solid biopolymer electrolyte containing CMC-PVA polymer blend is shown in Figure 4.12. As could be seen in Figure 4.12, the CMC-PVA polymer blend went through three stages until it reached the degradation process. The first stage occurred at the 47°C to 110°C range which corresponded to a loss of moieties from the samples due to water loss. Similar

observations were reported by other researchers where the initial drop of the TGA curve was also ascribed to the absorbed moisture and residual solvent being evaporated (Ramesh et al., 2010; Saroj et al., 2012; Arora et al., 2018).

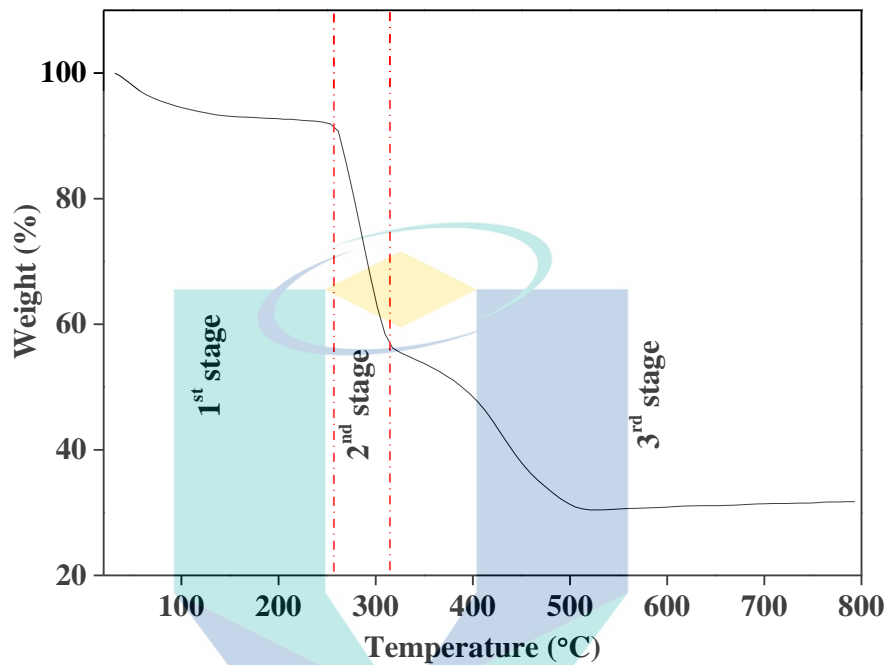


Figure 4.12 TGA curve of CMC-PVA polymer blend.

A sudden drop in weight was observed at the second stage (257 °C to 320 °C) and this observation can be explained by the degradation of CMC that gave off the carboxylate group (Ibrahim et al., 2011). Ramesh et al. (2011) reported that their study on a PMMA-PVC polymer blend also showed a sudden weight loss right after moisture stage that was due to the degradation of unsaturated groups such as C-O and -O- from the PMMA. This is also in agreement with Saadiah et al. (2019), who observed that when two polymers were blended together, it will enhance the flexibility of the polymer backbone, thus leading to an increment of the sample's decomposition at higher temperatures. Lastly, the third stage occurred at the region from 409 °C to 501 °C which was due to the backbone of the biopolymer complexes being degraded (Vöge et al., 2014; Sivadevi et al., 2015). As expected, prolonged heating above the decomposition temperature would cause carbonization and ash formation in the present sample (Ma et al., 2010; Liew et al., 2014c).

Figure 4.13 depicts thermo gravimetric spectra for CMC-PVA doped NH_4Br based solid biopolymer electrolytes system. The distinct decomposition stages for all of the samples in the range of 20-800 °C could be seen. From Figure 4.13, it can be observed that the initial weight loss from the decomposition process was accounted in all the tested samples at the temperature of 30 °C to 120 °C owing to the evaporation of residual solvent and moisture (Hashmi et al., 1990). The initial weight loss was attributed to the presence of a small amount of moisture influenced from the use of distilled water as solvent in SBEs system (Mohamad et al., 2007). Further increase in the temperature to the de-polymerization of the present biopolymer electrolytes. According to the findings, it can be seen that AB5 underwent one-step weight loss process with the decomposition temperature of 317 °C.

The second maximum decomposition temperature was observed from 200 °C to 340 °C for all samples in the SBEs system. This sudden weight loss may be due to the decomposition of carboxylate ($-\text{COO}^-$) group in the present SBEs system (Ma et al., 2010). It could be observed that when NH_4Br was added in CMC-PVA polymer blend SBEs system, the sample that contained the lowest composition provided the highest weight loss in comparison to the un-doped CMC-PVA SBEs system. The increase in weight loss at this region was expected to lead towards the decrease in ionic conductivity (Du et al., 2003). The greatest weight loss was also believed to be due to the disintegration of the intermolecular and partial breaking of the molecular structure (Lewandowska, 2009). As reported by Anjali (2012) and Biswal et al. (2004), the decarboxylation of the polymer chain occurs at the temperature between 300 °C to 340 °C, which in line with present work.

Apart from that, according to Liew et al. (2014c) and Yang et al. (2009), the second weight loss was due to the elimination of the side groups of the polymer backbone of PVA at about 250–350 °C. This showed that with the addition of NH_4Br in the present system, the decomposition temperature for the entire system started to increase. This could be attributed to the formation of the homogenous polymer electrolytes over the entire content, and this would allow CMC-PVA to receive any ionic charge (Rajendran et al., 2012). Based on this mechanism, it was evident that CMC-PVA would provide more vacant sites for ion hopping when NH_4Br was introduced into the system and hence leading to an increase in the decomposition temperature. Su et al. (2010) reported that

when two different polymers blended together, the crosslinking and Millard reaction between two polymers can contribute to the enhancement of the thermal stability by creating more free volume space.

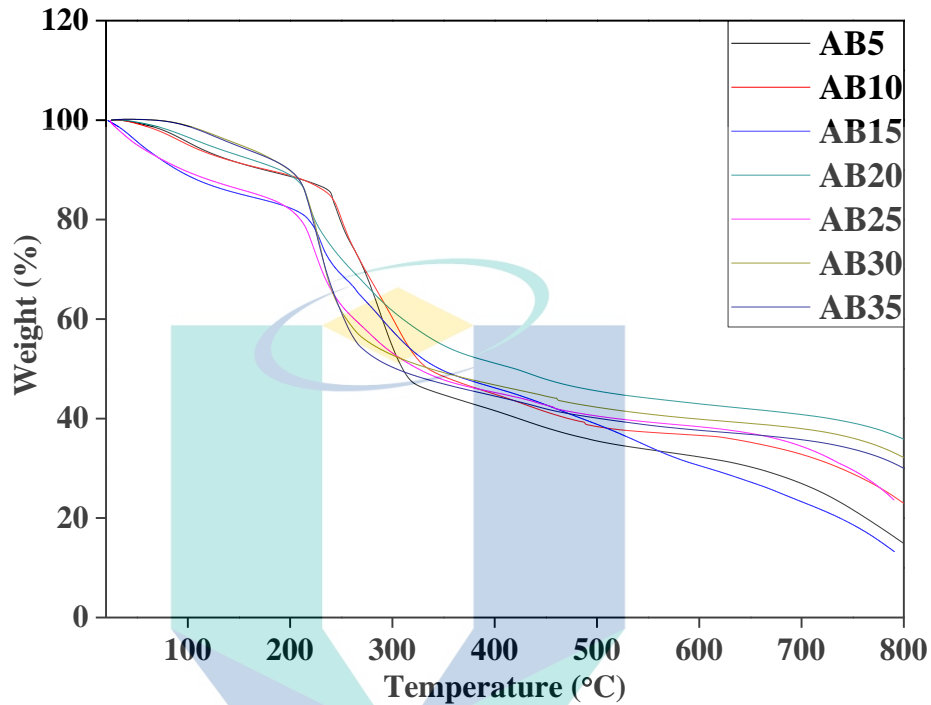


Figure 4.13 TGA curve of biopolymer electrolytes at various amount of NH_4Br .

As demonstrated in Figure 4.13, the sample with 20 wt. % NH_4Br showed the minimum total weight loss of 46.36 % with a maximum decomposition temperature of 358 °C, suggesting that the sample was more thermally stable in comparison to other samples. Table 4.6 tabulated the temperature decomposition and total weight loss for the entire SBEs samples. This observation was supported by the XRD analysis where the most amorphous sample led to an increase in flexibility of the polymer-complexes, thus allowing the ease for ion transportation in the present system. From the observation, it was predicted that the sample with a higher decomposition temperature and lower weight loss will provide higher thermal stability. In addition, the TGA analysis indicated that the solid biopolymer electrolyte can withstand more than 200 °C which is suggested to enhance the performance of the electrolyte at high temperature.

Table 4.6 Maximum decomposition temperature and total weight loss of various content CMC-PVA SBEs system.

Sample	Maximum decomposition temperature, T_d (°C)	Total weight loss (%)
AB0	316	48.93
AB5	318	52.81
AB10	331	50.77
AB15	349	49.46
AB20	358	46.36
AB25	335	51.29
AB30	288	47.31
AB35	278	47.54

4.5.2 DSC spectra of CMC-PVA and CMC-PVA doped NH_4Br

It is well known that one of the methods to study the miscibility of the molecules in polymer blends is to determine the glass transition temperature. Keeping the temperature region in consideration so as not to cause thermal degradation in the first heating run, two cycles of heating and cooling runs were adopted to eliminate the effect of moisture.

Figure 4.14 illustrates the Differential Scanning Calorimetry thermograms (second heating) of SBE containing CMC-PVA polymer blend. The glass transition temperature, T_g was observed at the endothermic peaks and measured at midpoint of the sample content (Hema et al., 2009; Sivadevi et al., 2015; Liew et al., 2016b). The T_g was used in the present work to study the degree of purity and the nature of the substance (Guirguis et al., 2012b). In addition, the T_g value also can provide information about the miscibility and homogenous phase of the sample based on the appearance of the T_g peak as displayed in the DSC thermogram (Ramesh et al., 2010).

The temperature of glass transition (T_g) for CMC-PVA polymer blend without dopant in the present work was detected at 83 °C. Su et al. (2010) have reported in their work that the T_g for pure CMC was observed at 55 °C. Meanwhile, according Saadiah et al. (2018), the T_g for pure PVA was found to be at 89.7 °C. The shifting to lower temperature might be due to the interaction between CMC and PVA polymers via H-bonding and the result is supported by other published reports (Sudhamani et al., 2003; Abd El-Kader et al., 2005; El-Kader et al., 2011). Moreover, Iwamoto et al. (1979) reported that the blending of PVA into water can reduce its crystallinity.

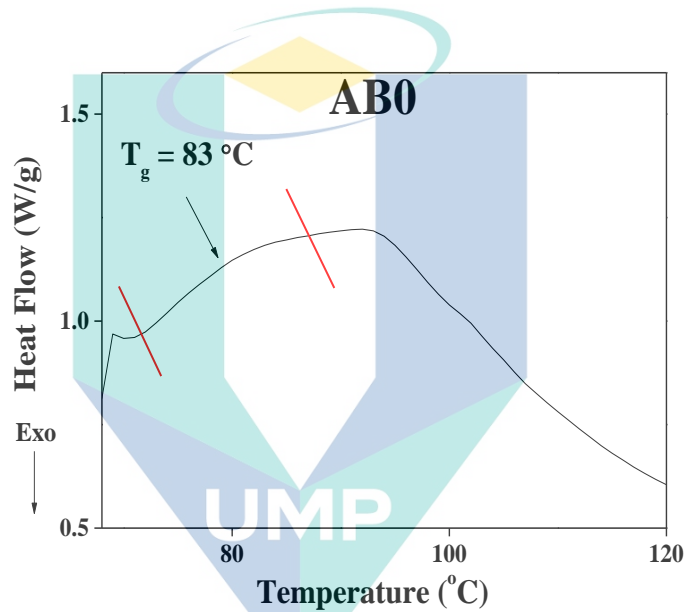


Figure 4.14 DSC spectra of CMC-PVA

The incorporation of NH_4Br into the system was expected to decrease the T_g value as the ionic dopant can provide free conducting ions, thus enhancing the flexibility of polymer blend backbone (Agrawal et al., 2004). According to Du et al. (2009), the addition of ammonium salt into the system can weaken the interactions between hydrogen bonds of the polymer chains and thus would enhance the segmental motions of the polymer blend chains. Figure 4.15 shows the DSC curves for all samples based on solid biopolymer electrolytes. The degree of purity and nature of the substance can be obtained from the T_g parameter (Guirguis et al., 2012a).

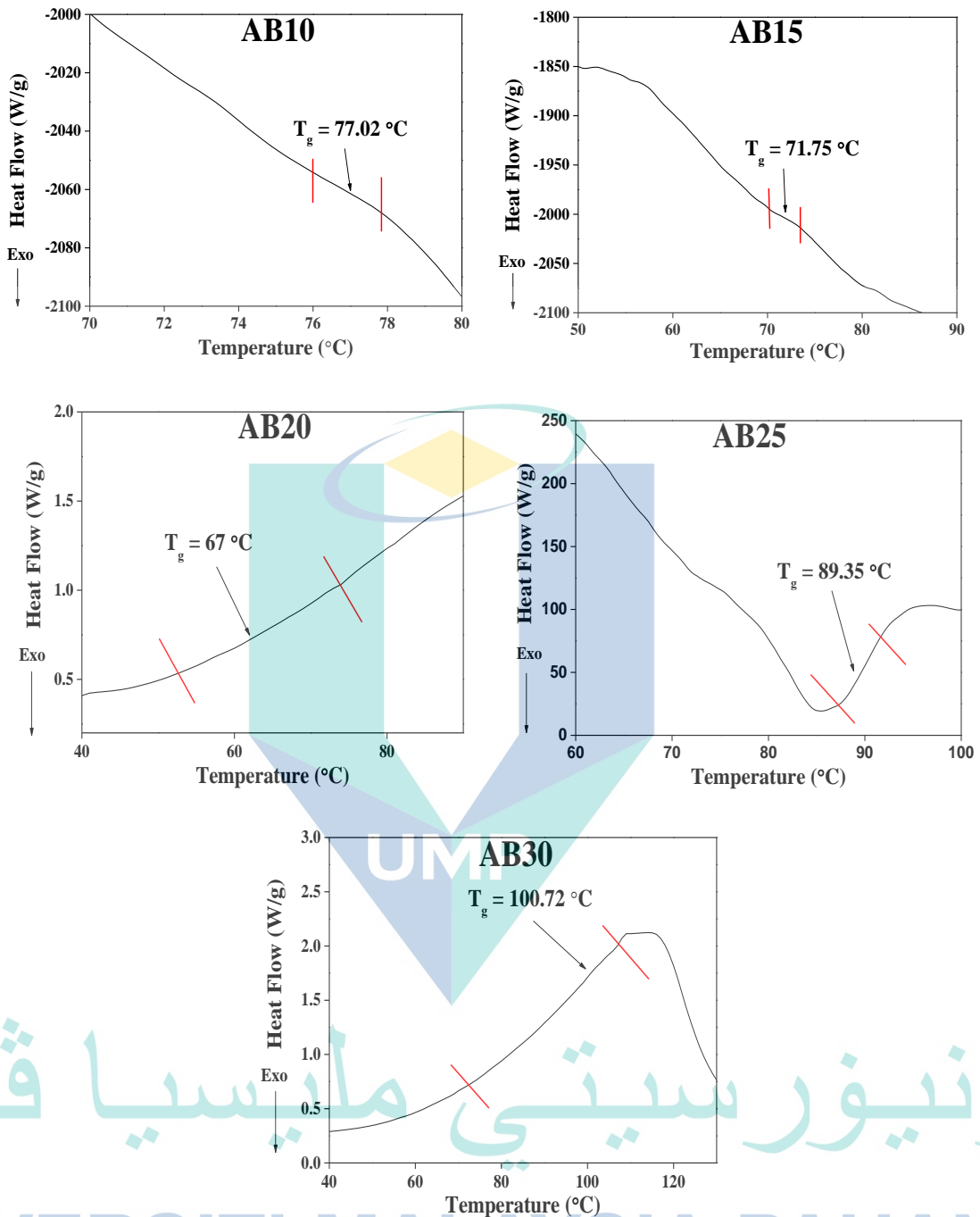


Figure 4.15 DSC Thermograms at selected amounts of NH_4Br .

Based on Figure 4.15, the addition of NH_4Br decreased the T_g of CMC-PVA. The incorporation of NH_4Br has lowered the glass transition (T_g), indicating interaction of the dissociated NH_4Br with the polymer blend host that resulted in the sample becoming highly amorphous due to increased segmental motion as shown in the XRD analysis (Sudhakar et al., 2013) Genova et al., 2015). A similar observation was reported by (Sivadevi et al., 2015), for a PVA-PAN blend polymer electrolyte system doped with

ammonium thiocyanate where a decreasing pattern was seen due to the ionic dopant's effect in the host polymer matrix. Moreover, the addition of ammonium salt into the CMC-PVA matrix weakened the dipole-dipole interaction between the polymer blend host chains, which upon the application of an electric field, will allow the ions to move freely through the network of polymer chain (Vijaya et al., 2013). AB20 exhibited the lowest T_g which inferred a high flexibility of the polymer blend doped system chain, thus it was expected to affect the ionic conductivity. Additionally, an increase in T_g led to an increase in the crystallinity of the biopolymer electrolytes structure. Apart from that, Yuhanees (2017) and Mizuno et al. (1998) have reported that increases in the crystallinity as well as T_g were due to more restriction of the segmental motions which may lead to inter and intrachain hydrogen bonding. As a conclusion, the DSC analysis have proven the miscibility and homogeneity of the CMC-PVA polymer blend and the T_g values verified the ionic conductivity pattern.

4.6 Summary of structural and thermal analysis

As a summary for the structural and thermal part of this research, FTIR analysis proved the interaction between CMC-PVA polymer blend and NH_4Br as shown from the changes in peak intensity and wavenumber at the regions for C-O-C, O-H, COO- and C=O. The region for COO- stretching showed the most obvious complexation, thus suggesting that it has interacted with the ionic dopant when introduced into the polymer blend system via the Grotthus mechanism. From the XRD analysis, it could be observed that the addition of NH_4Br has increased the amorphous phase up to AB20. By evaluating the XRD deconvolution, the size of crystallinity can be calculated and it was found that sample AB20 had the lowest value. Furthermore, from the thermal stability study, sample AB20 has achieved the highest decomposition temperature and lowest weight loss, which suggested that it was the most thermally stable. AB20 was also the most flexible among other samples due to its lowest T_g value. Hence, it could be concluded that the incorporation of 20 wt.% NH_4Br (AB20) into the system was expected to provide highest ionic conductivity which will be discussed further in the impedance spectroscopy analysis in Section 4.7.

4.7 Impedance Spectroscopy Analysis of CMC-PVA doped NH₄Br

The electrical impedance spectroscopy (EIS) analysis was used to investigate the ionic conductivity and electrical properties of the SBE systems. The EIS data were also used to investigate the transport properties of biopolymer electrolytes. The studies on ionic conductivity at ambient and different temperatures were done to understand the electrical conduction trend and transport mechanism in the CMC-PVA-NH₄Br systems. In this section, the effects of adding ammonium salt are discussed based on the ionic conductivity behaviour.

4.7.1 Nyquist Plot of CMC-PVA+NH₄Br

Figure 4.16 shows the complex impedance plot at ambient temperature (303 K) obtained for CMC-PVA-NH₄Br biopolymer electrolytes system. In the present work, only unfinished semicircles with a spike were observed for the Nyquist plot. From the intercept of high frequency semicircle and low-frequency spike on the Z_r axis, the bulk resistance, R_b can be determined (Rajeswari et al., 2014). The existence of R_b could be due to immobile polymer chains.

It can be seen that there was formation of semicircles when NH₄Br was added from 5 to 15 wt. %. The semicircle was related to the relaxation process in the bulk biopolymer electrolyte which triggers the decrement of ionic conductance ability. This phenomenon was obvious for those samples added with 5 to 15 wt. % of NH₄Br due to the motionless polymer chain (Saadiah et al., 2018) and hence increasing the R_b value.

As observed in Figure 4.16, the semicircle started to decrease as more NH₄Br was introduced into the CMC-PVA polymer blend. This can be attributed to the local effective pathway in the liquid phase for ionic conduction, resulting in an increase in the mobility of ions as the electric potential alternates between the positive and negative in an ac field.

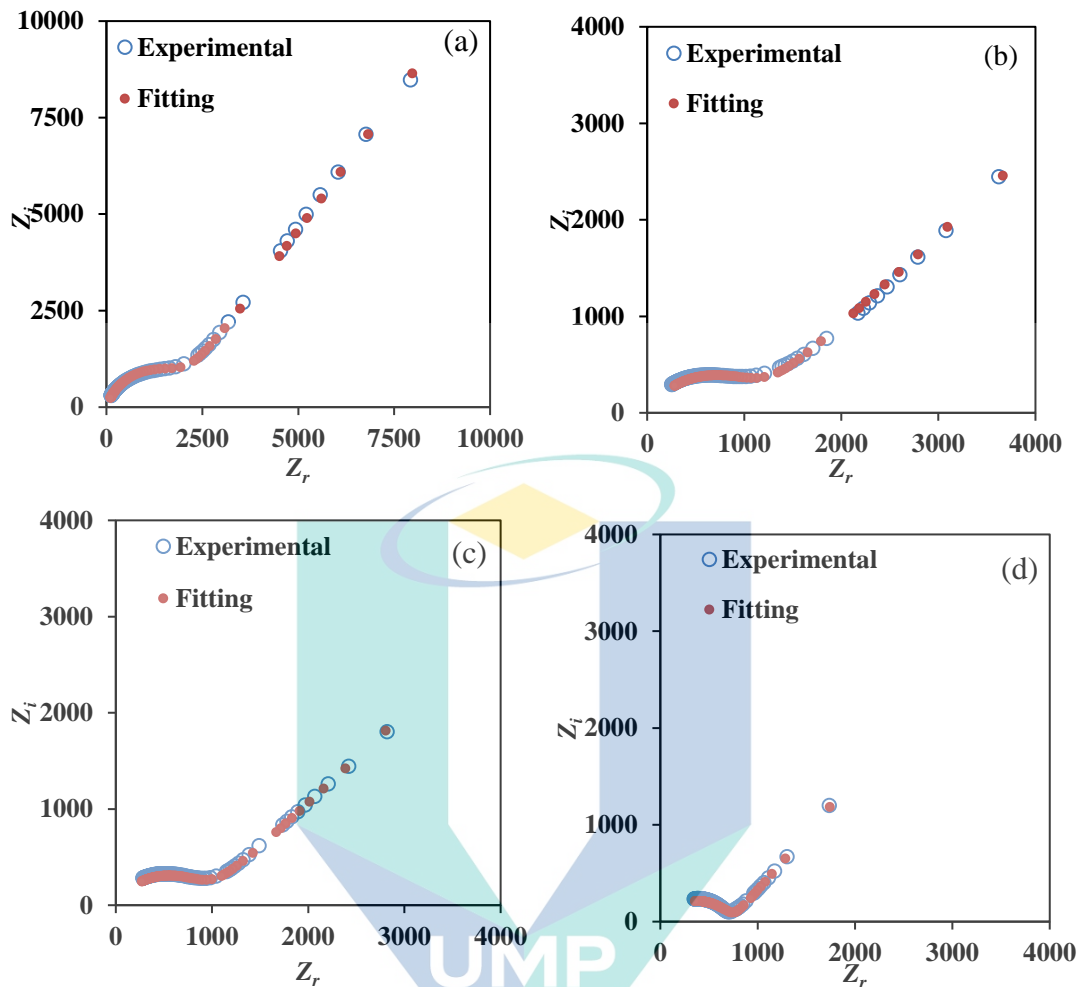
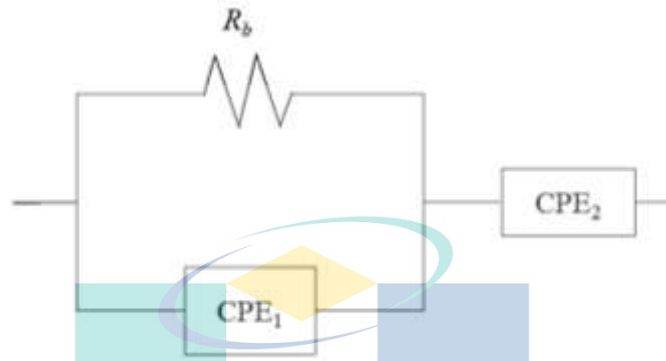


Figure 4.16 Nyquist plot for CMC-PVA-NH₄Br based SBES system, (a) CMC-PVA polymer blend, (b) AB5, (c) AB10 and (d) AB15.

Moreover, the semicircle at high frequency was due to the parallel combination of bulk resistance, R_b and constant phase elements (CPE). CPE is also known as bulk capacitance and as a “leaky capacitor”. The existence of bulk capacitance might be due to the migration of protons in the biopolymer electrolytes system. Since the present work used stainless steel as the blocking electrode, the interface of electrode/electrolyte can be regarded as a capacitor. The connection in a series of bulk resistance and CPE can represent the inclined spike in the plot. The inclined spike at lower frequency also can be caused by the polarization effect at the interface of the electrode/electrolyte (Shukur et al., 2014c). Therefore, the Nyquist plot that consisted of both semicircle and spike can be represented by bulk resistance connected in parallel with CPE_1 and fitted in series by another CPE_2 as presented in Scheme 4.1 (Selvasekarapandian et al., 2010; Teo et al., 2012; Rudhziah et al., 2015a). According to Han et al. (1998), the electrical equivalent

circuit was usually used in impedance spectroscopy analysis because it is simple, fast and can provide a complete picture of the biopolymer electrolyte system. The equivalent circuit of the present study was observed to be similar with those observed by other researchers (Mobarak et al., 2013).



Scheme 4.1 Model of the equivalent circuit

The Z_r and negative Z_i impedance of CPE can be represented via the equation (Shuhaimi et al. 2012; Arof et al., 2014; Shukur et al., 2014b; Saadiah et al., 2018):

$$Z_r = \frac{\cos\left(\frac{\pi p}{2}\right)}{k^{-1}\omega^p} \quad 4.2$$

and

$$Z_i = \frac{\sin\left(\frac{\pi p}{2}\right)}{k^{-1}\omega^p} \quad 4.3$$

where k^{-1} is the bulk geometrical capacitance of biopolymer electrolyte, ω is angular frequency ($2\pi f$) and p is referred to the deviation of the plot from the axis. Hence, the real and imaginary parts for Nyquist plot containing a semicircle and title spike can be expressed as (MAzuki et al., 2018):

$$Z_r = \frac{R_b + R_b^2 k_1^{-1} \omega^{p_1} \cos\left(\frac{\pi p_1}{2}\right)}{1 + 2R_b k_1^{-1} \omega^{p_1} \cos\left(\frac{\pi p_1}{2}\right) + R_b^2 k_1^{-2} \omega^{2p_1}} + \frac{\cos\left(\frac{\pi p_2}{2}\right)}{k_2^{-1} \omega^{p_2}} \quad 4.4$$

$$Z_i = \frac{R_b + R_b^2 k_1^{-1} \omega^{p_1} \sin\left(\frac{\pi p_1}{2}\right)}{1 + 2R_b k_1^{-1} \omega^{p_1} \cos\left(\frac{\pi p_1}{2}\right) + R_b^2 k_1^{-2} \omega^{2p_1}} + \frac{\sin\left(\frac{\pi p_2}{2}\right)}{k_2^{-1} \omega^{p_2}} \quad 4.5$$

where R_b is bulk resistance, k_1^{-1} is the bulk geometrical capacitance of biopolymer electrolyte, k_2^{-1} is the electrical double layer capacitance at electrode/electrolyte interface during the impedance measurement, p_1 is the ratio of the angle between the diameter of the semicircle and the imaginary axis and p_2 is the skew parameter that controls the degree of the tendency of the title spike from the real axis. Figure 4.17 depicts the Nyquist plots for biopolymer electrolytes containing 20 wt. %, 25 wt. %, 30 wt. % and 35 wt. % at room temperature.

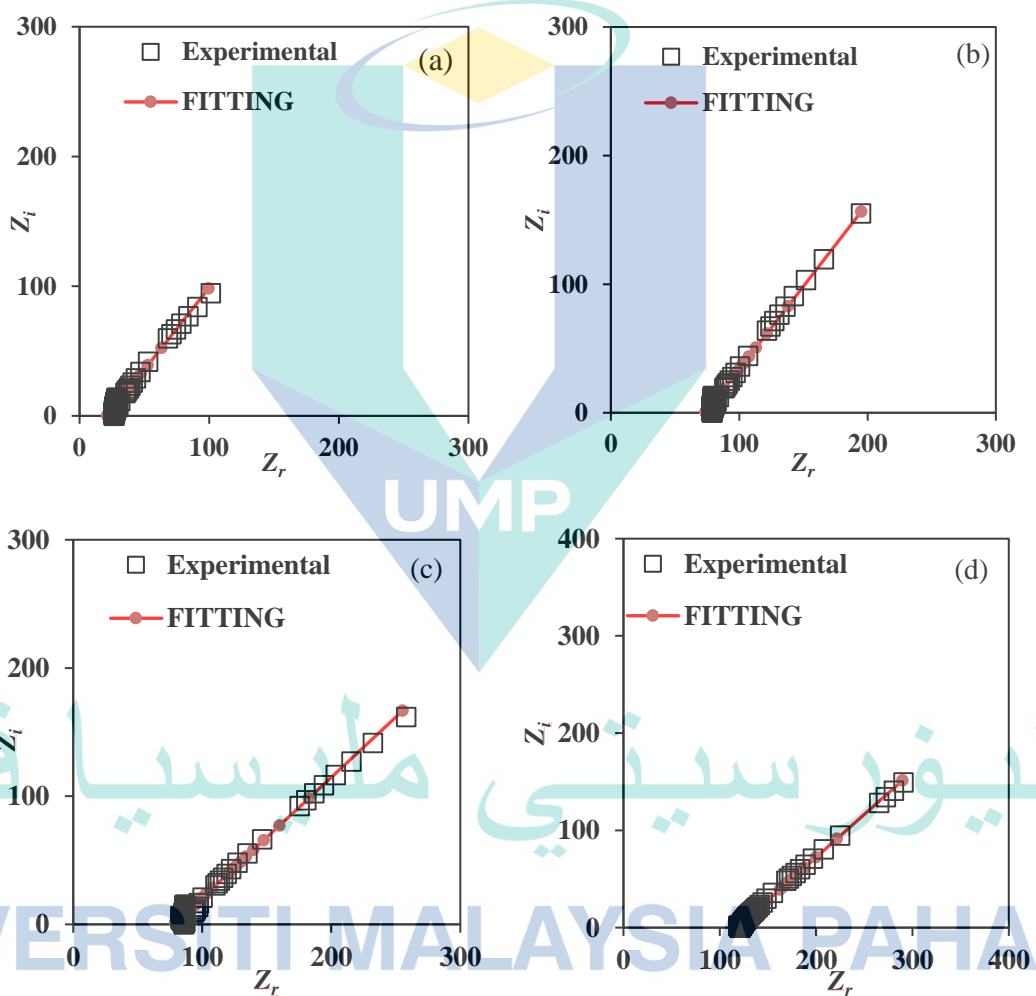
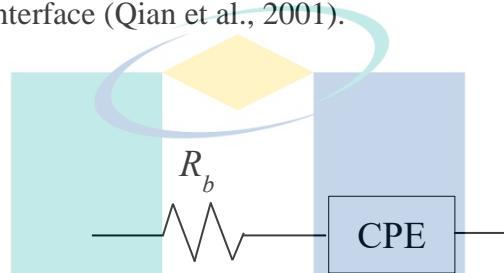


Figure 4.17 Nyquist plot for (a) AB20, (b) AB25, (c) AB30 and (d) AB35.

It can be noted here that between 20 wt.% to 35 wt.% of NH_4Br , the semicircle started to disappear in the impedance plot and was replaced by a tilted spike, suggesting that only the resistive component of the polymer remained (Rajeswari et al., 2014). The value of R_b can be determined from the interception of the line with the real impedance axis. The R_b value decreased with the increment of NH_4Br content where sample AB20 had the lowest R_b value at room temperature. This decrement of R_b value might be due to the mobile charge carrier increase (Shukur et al., 2014b). The Nyquist plots consisting of a tilted spike were triggered due to ion migration and inhomogeneity of the electrode/electrolyte interface (Qian et al., 2001).



Scheme 4.2 The equivalent circuit of SBE system for Nyquist plots consists of tilted spike.

Samples containing AB20 to AB35 showed the spike did not begin at origin, thus the equivalent circuit of spike in this study consisted of R_b and CPE that combined in a series as illustrated in Scheme 4.2. This equivalent circuit is also similar with the previous work by Shuhaimi et al. (2012). This combination in series at Z_i axis was attributed to the double layer capacitance at the blocking electrodes (Baskaran et al., 2004; Ramya et al., 2006). The imaginary part, Z_i and real part, Z_r that are associated to the equivalent circuit can be expressed as:

$$Z_r = R + \frac{\cos\left(\frac{\pi p}{2}\right)}{C \omega^p} \quad 4.6$$

$$Z_i = \frac{\sin\left(\frac{\pi p}{2}\right)}{C \omega^p} \quad 4.7$$

Table 4.7 lists the parameters for the circuit element of all of the SBEs system studied at ambient temperature. The values obtained from the fitting method were try and error substitutions based on the impedance equivalent circuit equation from Equation 4.4 to 4.7 until all of the fitting points completely filled up the impedance plot which is in agreement with the experimental result (Fadzallah et al., 2016). It can be observed that the value of R_b for the fitting gave an almost similar value to the experimental R_b value. The R_b value decreased as the amount of NH_4Br increased in the system. This could be caused by the improvement of the polymer chain segmental motion and salt dissociation.

In Table 4.7, the k_1 and k_2 is inverse k^{-1} used in the complex impedance equation was assigned as capacitance (Linford, 1988). It was noticeable that the capacitance at the lower frequency region was smaller than at the higher frequency region and this decreasing pattern occurred due to the increase in the salt content. Moreover, at AB20 and above, no values for p_2 and C_2 were detected due to the disappearance of the semicircle at low frequency which was replaced with a spike.

Table 4.7 The parameter for CMC-PVA- NH_4Br

<i>Sample</i>	R_b (<i>experimental</i>) (Ω)	R_b (<i>theoretical</i>) (Ω)	p_1 (<i>rad</i>)	C_1 (F)	p_2 (rad)	C_2 (F)
AB0	2.44×10^3	1.70×10^3	0.85	8.26×10^{-9}	0.6	1.13×10^{-6}
AB5	1.21×10^3	1.06×10^3	0.68	5.56×10^{-8}	0.48	1.04×10^{-5}
AB10	9.83×10^2	8.83×10^2	0.68	5.56×10^{-8}	0.48	1.41×10^{-5}
AB15	7.32×10^2	7.32×10^2	0.68	5.56×10^{-8}	0.55	2.72×10^{-5}
AB20	2.83×10^1	2.16×10^1	-	-	0.579	2.95×10^{-4}
AB25	7.98×10^1	7.38×10^1	-	-	0.578	1.80×10^{-4}
AB30	8.46×10^1	7.79×10^1	-	-	0.48	2.60×10^{-4}
AB35	1.27×10^2	1.18×10^2	-	-	0.46	2.90×10^{-4}

4.7.2 Ionic Conductivity Analysis of CMC-PVA+NH₄Br

Figure 4.18 depicts the ionic conductivity of the SBEs system at different NH₄Br contents in ambient temperature (303K). Ionic dopant is known as a charge carrier's provider and the concentration of charge carrier can influence the biopolymer electrolyte systems' ionic conductivity behaviour. Thus, changes to the ionic conductivity are expected after the addition of ionic dopants into the polymer electrolytes (Kumar et al., 2012). As shown in Figure 4.18, the ionic conductivity was increased gradually as the amount of NH₄Br increased up to 20 wt. %. The increasing pattern of ionic conductivity with the addition of NH₄Br could be caused by ion dissociation between H⁺---NH₃⁺ Br⁻ which increased the number of mobile ions and ionic mobility (Ramly et al., 2011; Ramlli et al., 2015).

The increase in NH₄Br content led the ion content to increase and the tendency for the complexation to transpire within the CMC-PVA blend matrices was higher as more ions migrated towards the CMC-PVA system and led to the formation of inter or intra-interaction as discussed in the FTIR analysis in the previous section. This observation was also supported by the XRD results where the sample with 20 wt. % of NH₄Br showed the lowest crystallinity of the SBEs system, hence enhancing the ionic conductivity (Samsudin & Isa, 2012). Apart from that, ionic dopants can increase the decomposition temperature, T_d and decrease the glass transition temperature, T_g , of biopolymer electrolytes as proven in the TGA and DSC analysis. Previous work done by Samsudin et al. (2011) showed that the optimum ionic conductivity was achieved at $1.12 \times 10^{-4} \text{ S cm}^{-1}$ for sample containing 25 wt. % NH₄Br when introduced in the single biopolymer as host in the polymer electrolytes. However, the present research revealed that the optimum ionic conductivity achieved was $3.21 \pm 0.005 \times 10^{-4} \text{ S cm}^{-1}$ for the sample containing 20 wt. % NH₄Br, suggesting that CMC-PVA blend has improved the conduction when incorporated with the ionic dopant. The enhancement of ionic conductivity was substantiated with the results attained from the FTIR, TGA, DSC and XRD analyses where the changes of the structural and thermal properties with the addition of NH₄Br aligned with each other and led to the increment in the ionic conductivity of the present SBEs system.

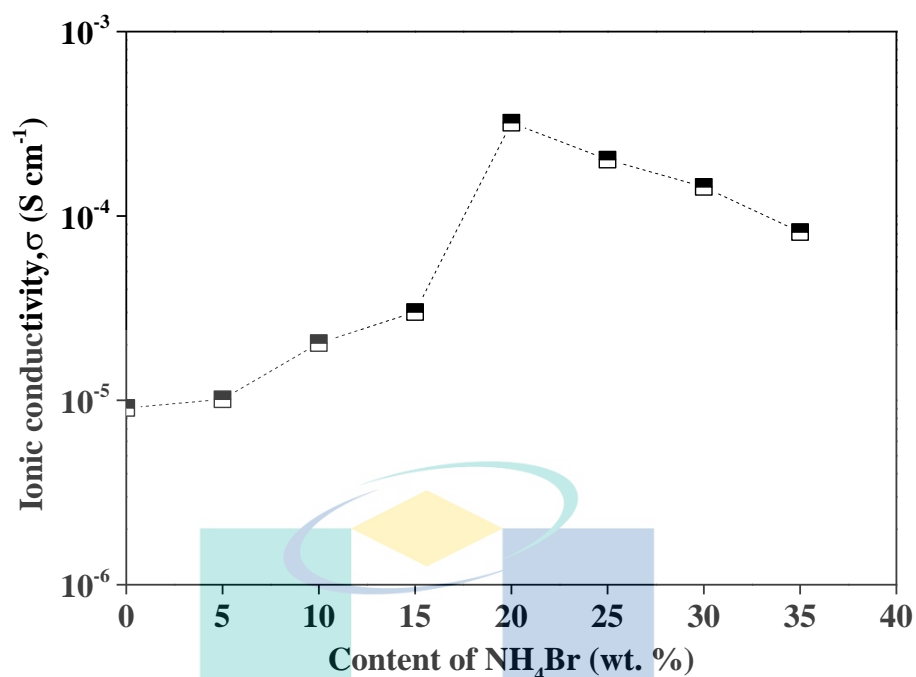


Figure 4.18 Ionic conductivity of solid biopolymer electrolytes system.

It was found that when more than 20 wt. % NH₄Br was incorporated in CMC-PVA solid biopolymer electrolyte, the ionic conductivity seemed to decrease. This phenomenon might be due to formation of neutral ion pairs in the biopolymer electrolytes. A too high salt content contributes more free ions which restricts the movement of other free ions to move freely from one side to another. As the ions mobility were decreased, the resulting ionic conductivity also became reduced. These findings are supported by Samsudin et al. (2011) who similarly found a decreasing pattern at higher contents of ionic dopant that was attributed to the dipole interaction between proton ions and the biopolymer electrolyte medium, thus causing the transports properties to decrease.

Another explanation for the observed decrease in ionic conductivity with the addition of more than 20 wt. % NH₄Br was the re-crystallization of the sample as shown in the XRD analysis. A crystallized sample will block the ion migration and cause the ions to overcrowd in the polymer-salt complexes that in the end will lead the NH₄Br to re-associate, thus reducing the movement of ions and limiting the segmental motion of the polymer chain, resulting in a lowered ionic conductivity. The re-crystallization of biopolymer electrolytes in samples above AB20 also caused them to be thermally stable as well, as seen in the thermal properties study in the previous section.

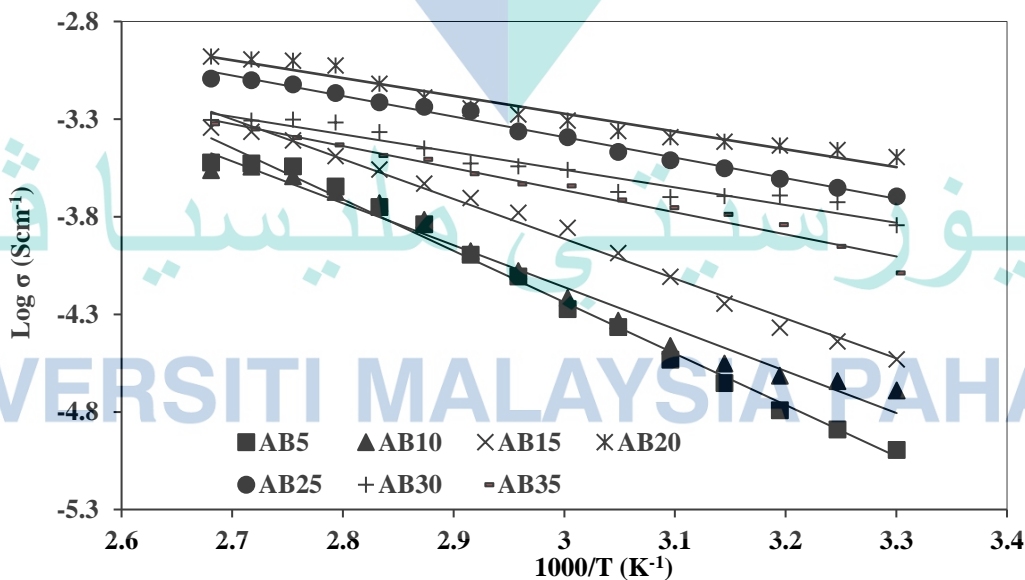
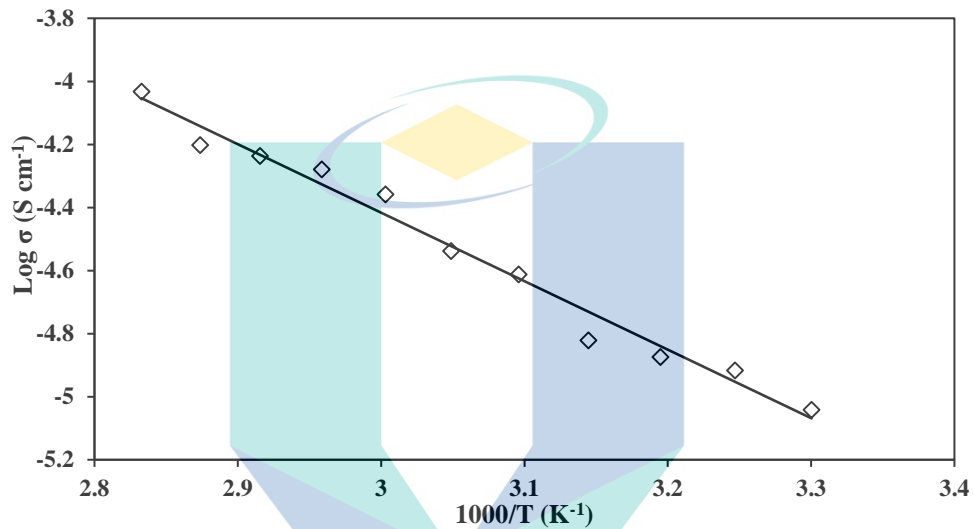
Table 4.8 Previous studies of single polymer and polymer blend-salt complexes electrolytes

Sample	Ionic Conductivity (S cm ⁻¹)	References
PVA/Chitosan – NH ₄ Br	7.68×10^{-4}	(Yusof et al., 2014)
Chitosan/PVA – NH ₄ I	1.77×10^{-6}	(Buraidah et al., 2011)
Starch/Chitosan- NH ₄ NO ₃	3.89×10^{-5}	(Khiar et al., 2011)
Starch/PEO-NH ₄ NO ₃	2.81×10^{-7}	(Ramly et al., 2011)
MC/potato starch- NH ₄ NO ₃	4.37×10^{-5}	(Hamsan et al., 2017a)
CMC-SA	4.02×10^{-7}	(Ahmad et al., 2012)
Starch-NH ₄ NO ₃	2.15×10^{-6}	(Azlan et al., 2011)
PVA-CH ₃ COONH ₄	5.62×10^{-6}	(Hirankumar et al., 2005)
CMC-NH ₄ SCN	1.00×10^{-5}	(Noor et al., 2015)
Chitosan-MC- BMIMTFSI	1.51×10^{-6}	(Misenan et al., 2018)
PVA-Chitosan- NH ₄ NO ₃	2.07×10^{-5}	(Shaffie et al., 2018)
PVC-PEMA- LiN(CF ₃ SO ₂) ₂	1.75×10^{-5}	(Zakaria et al., 2010)
PVA-PVdF-LiCLO ₄	3.04×10^{-5}	(Rajendran et al., 20114)
CMC-PVA-NH ₄ Br	$3.21 \pm 0.005 \times 10^{-4}$	Present work

A comparison was done with previous work that used single and dual blend polymer systems and is summarised in Table 4.8. It could be observed that the findings on ionic conductivity of the present study are comparable with the compared previous works and thus suggests the potential of the CMC-PVA blend to function as a host in polymer electrolytes of electrochemical devices.

4.7.3 Temperature Dependence Analysis of CMC-PVA+NH₄Br

The mechanism of ionic conduction in the present SBEs system was analysed based on temperature analysis. The temperature dependence of CMC-PVA with various contents of NH₄Br (5 to 35 wt. %) at the temperature range of 303K to 373K is illustrated in Figure 4.19.



(b)

Figure 4.19 (a) Temperature dependence plot of CMC-PVA polymer blend and (b) log ionic conductivity versus 1000/T plot for different NH₄Br content.

Figure 4.19 shows that the ionic conductivity increased with temperature up to 353 K for the pure CMC-PVA polymer blend. Meanwhile, for CMC-PVA incorporated with various amount of NH₄Br, the ionic conductivity increased up to 373 K. Thus, it can be inferred that as NH₄Br was introduced into the CMC-PVA polymer blend, the polymer blend became more flexible when the temperature was increased from 303 K to 373 K. This was due to CMC-PVA polymer blend providing more vacant sites for ion hopping which can improve the movement of ion to hop from one site to another as the temperature increased, resulting in an enhancement of ionic conductivity. It is well-known that temperature plays an important role in the enhancement of the ionic conductivity. This is because the electrolyte becomes less viscous at high temperatures, thus leading to the increment of the chain flexibility. This situation was further supported by TGA and DSC analyses with the enhancement in decomposition temperature and decrement of the glass transition. A temperature increase will result in a concomitant increase of thermal movements of the biopolymer chain segments, thus increasing the dissociation of NH₄Br as well as improving the amorphousness of the CMC-PVA–NH₄Br SBEs. The end result was an increase in ionic conductivity (Ulaganathan et al., 2011).

There was no abrupt jump with temperature observed in Figure 4.19, suggesting the absence of phase transition in the structure of the biopolymer electrolytes within the temperature range investigated (Mazuki et al., 2018). Deka et al. (2011) reported that the increase in ionic conductivity due to temperature increase is caused by an increase in the polymer blend chain flexibility, thus providing more free volume that in turn leads to an increment in polymer segmental mobility. The regression values for all of the samples were approaching unity ($R^2 \sim 1$) as shown in Table 4.9. Thus, this suggested that the biopolymer electrolytes-based CMC-PVA polymer blend doped with varying amounts of NH₄Br obeyed the Arrhenius behaviour. This indicated the thermal assistance to the ionic conductivity mechanism (Samsudin & Isa, 2014) by the relation of:

$$\sigma = \sigma_0 \exp\left(\frac{-E_a}{kT}\right) \quad 4.8$$

where σ_0 represents pre-exponential factor, E_a is activation energy, k is the Boltzmann constant and T is temperature in Kelvins.

Table 4.9 Regression value of CMC-PVA-NH₄Br.

Sample	Regression value, R^2
AB0	0.98
AB5	0.99
AB10	0.98
AB15	0.99
AB20	0.98
AB25	0.99
AB30	0.95
AB35	0.98

The variation of activation energies at ambient temperature (303 K) were calculated from the slope of $\log \sigma$ versus $1000/T$ and were plotted as shown in Figure 4.20. It was noticeable that activation energy was inversely proportional to ionic conductivity trends, as the value of activation energy decreased when more NH₄Br content was added into the SBEs system up to AB20 and increased again at high NH₄Br contents.

This showed that the sample with the highest ionic conductivity possessed the lowest activation energy value which can be explained by the optimum amount of NH₄Br giving a lower activation energy for ions migration from one site to another in polymer blend matrix due faster ion migration rate and hence boost the ionic conductivity to the maximum value.

Therefore, the decrement in activation energy due to increasing salt content also can be related with the interaction between polar molecules in the polymer blend and ions of the salt (Baskaran et al., 2006). The increment of amorphous nature with increasing salt content up to AB20 facilitated the fast movement of H⁺ ion in the biopolymer system that contributed to the decrement of the activation energy (Schantz et al., 1993; Kopitzke et al., 2000; Srivastava et al., 2000; Selvasekarapandian et al., 2005).

This observation is aligned with Buraidah et al. (2009) where they believe the activation energy is required to move the ions and thus presupposing that the structure would not change. In the present study, the highest ionic conductivity was found in the

CMC-PVA SBEs system containing 20 wt.% of NH_4Br which also had the lowest activation energy of 0.08 ± 0.002 eV. However, beyond AB20, the activation energy started to increase and this might be due to the high ion content in the biopolymer electrolytes which hindered the movement of ions, thus requiring more energy to move the ions. The values of E_a for CMC-PVA- NH_4Br obtained for the present study were in the range of 0.25 ± 0.005 to 0.08 ± 0.002 eV.

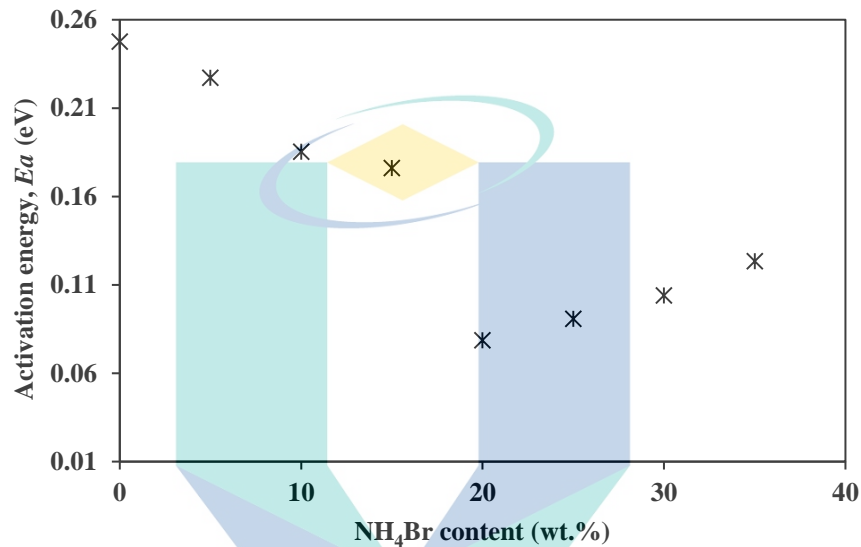


Figure 4.20 The activation energy plot of biopolymer electrolytes system.

4.7.4 Dielectric Analysis of CMC-PVA+ NH_4Br

In order to determine the dielectric constant, the reduction of coulomb interaction of the ion pair in polymer electrolytes had to be measured. Meanwhile, the dielectric loss is a direct measure of energy dissipated and generally consists of contributions from ionic transport (Rajeswari et al., 2014). The behaviour of dielectric properties provides important insights into the ionic transport phenomenon and of the effects on the electrode/electrolytes interface by polarization (Chai et al., 2012; Rani et al., 2015).

Figure 4.21 depicts the dielectric constant (ϵ_r) of CMC-PVA incorporated with various NH_4Br content at room temperature (303K). According to the Figure 4.21, the ϵ_r value at low frequency increased with increment of NH_4Br and was found to follow the ionic conductivity trends. As the NH_4Br content increased, the amount of mobile ions increased as well. This increment meant a related increase in the number of mobile ions

which resulted in the dielectric constant value to rise asymptotically. This further supported the increment of room temperature transport properties and ionic conductivity of the CMC-PVA-NH₄Br SBEs system. It can be seen that the dielectric constant gave the highest value at a low frequency due to the presence of more space charge effect attributed to charge carriers accumulating near the electrodes (Armstrong et al., 1974; Radha et al., 2013). There were two types of dipoles within the frequency study, including the free mobile charge that was being dissociated from the ionic dopant and the localized molecular polar group which led the charge imbalance inside the SBEs (Ravi et al., 2011; Saroj et al., 2012).

It is also can be seen in Figure 4.20, that the dielectric constant was sharply decreased as the frequency increased. This was caused by the electrode polarization which the accumulation was related with the decreasing dielectric constant that indicated a non-Debye behaviour with no single relaxation time. The constant value of dielectric constant at high frequency was believed to be caused by periodic reversal of the field occurring so quickly that the charge carriers were distressed to orient themselves in the field direction, in turn leading to a decrement in the dielectric constant (Hema et al., 2007).

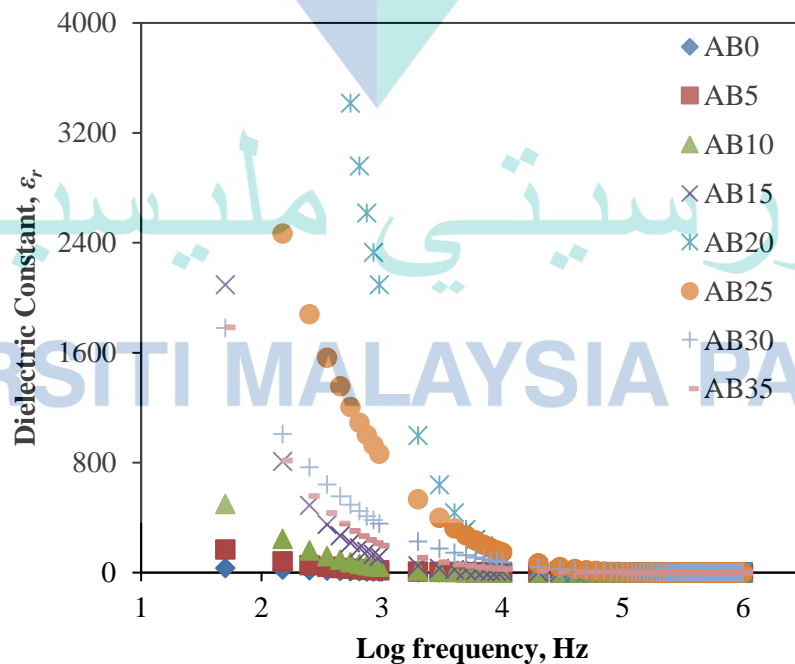
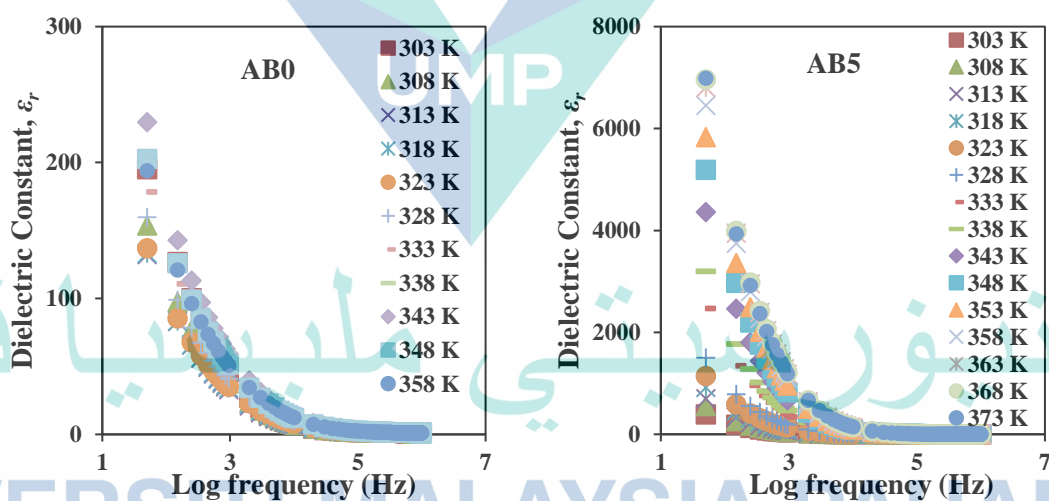


Figure 4.21 Frequency dependence on dielectric constant for CMC-PVA-NH₄Br systems.

Figure 4.22 shows the dielectric constant pattern of CMC-PVA polymer blend doped with various content of NH_4Br at different temperatures. It was found that the ϵ_r value increased as temperature increased, implying that the increment of ϵ_r was temperature assisted. This situation could be explained by the dissociation of neutral ion aggregates due to energetic vibrations from the thermal energy supply upon heating as supported in the temperature dependence study. Furthermore, this increasing pattern can also be related to the increased in flexibility due to the segmental motion of the polymer blend chain (Khiar et al., 2010). As a result, single and triplet ions which can contribute to the improvement of ionic conductivity may have formed. The un-dissociated ammonium salt molecules released an additional number of ions when heated, leading to the enhancement of ionic conductivity which reflected the ϵ_r value as ionic conductivity increased. Moreover, in the higher frequency, the charge had no time to build up at the interface as frequency increased due to increasing rate of reversal of the electric field. Hence, the polarization that occurred due to charge accumulation became decreased when ϵ_r was decreased (Molak et al., 2005).



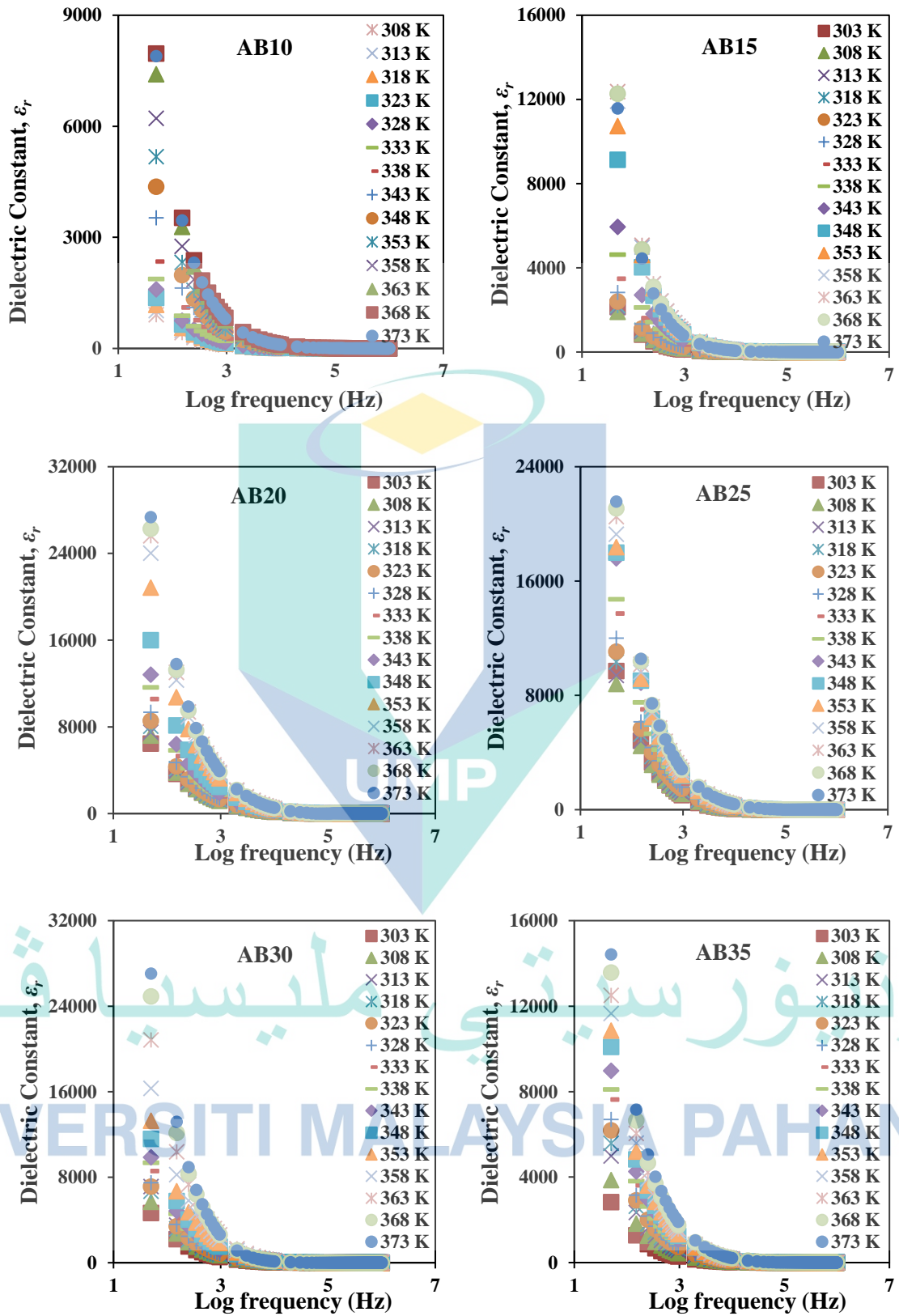


Figure 4.22 Dielectric constant, ϵ_r patterns for SBEs system at various temperature.

Figure 4.23 depicts the dielectric loss (ϵ_i) of various NH_4Br content at room temperature (303K). It was noticeable at low frequency, the ϵ_i value increased when more NH_4Br content was introduced into the system up to AB20. This trends could be due to free charge motion within the present electrolytes system (Pandey et al., 2010). The addition of NH_4Br content into the system gave higher ϵ_i value which reflected the improvement of charge carrier mobility, causing the ionic conductivity to increase (Buraidah et al., 2009). This pattern of dielectric loss was found to be similar with the dielectric constant and showed a non-Debye characteristic without single relaxation properties as observed in the present system.

On the other hand, it could be observed that the ϵ_i decreased as frequency increased. This phenomenon might be due to the fast rate that occurred in the electric field which led to the decrement of ionic conductivity. Another reason can be explained where in high frequency, most of the ions was in the bulk sample and lesser ions can pile up at the interface of each sample, leading to the decrement of ϵ_i value with increasing of frequency.

Meanwhile, the very high value of dielectric loss at low frequency also can be explained as free charge carrier motion that built up within the materials and electrolytes interface (Rani et al., 2015). Moreover, the incorporation of NH_4Br into the CMC-PVA polymer blend complexes caused an increase in the degree of proton ion (H^+) dissociation and was expected to improve the number of mobile ions. It was also observed in Figure 4.23 that dielectric loss increased as more amount of NH_4Br contents were added into the biopolymer electrolyte system. This was believed to be due to the increase in number density of mobile of ions which increased the charge storage.

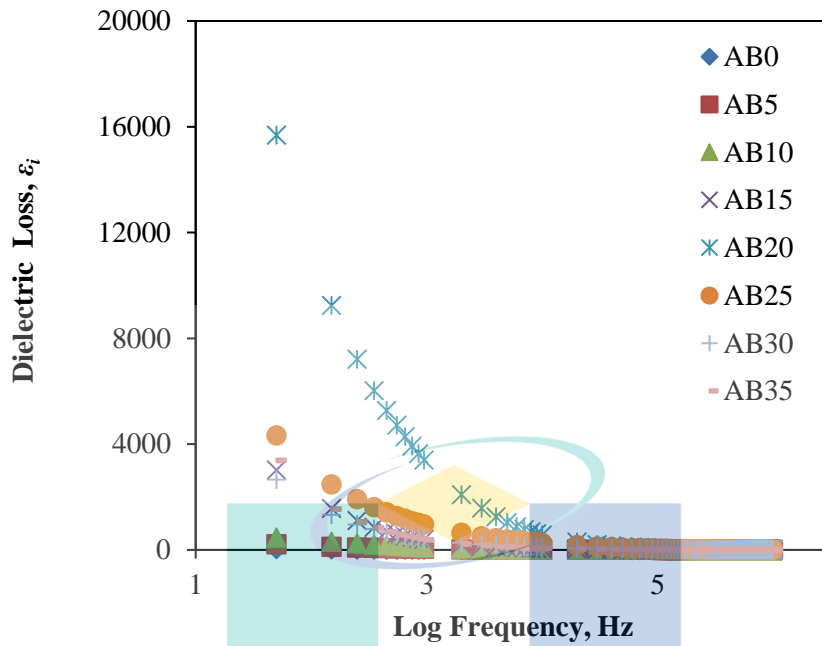
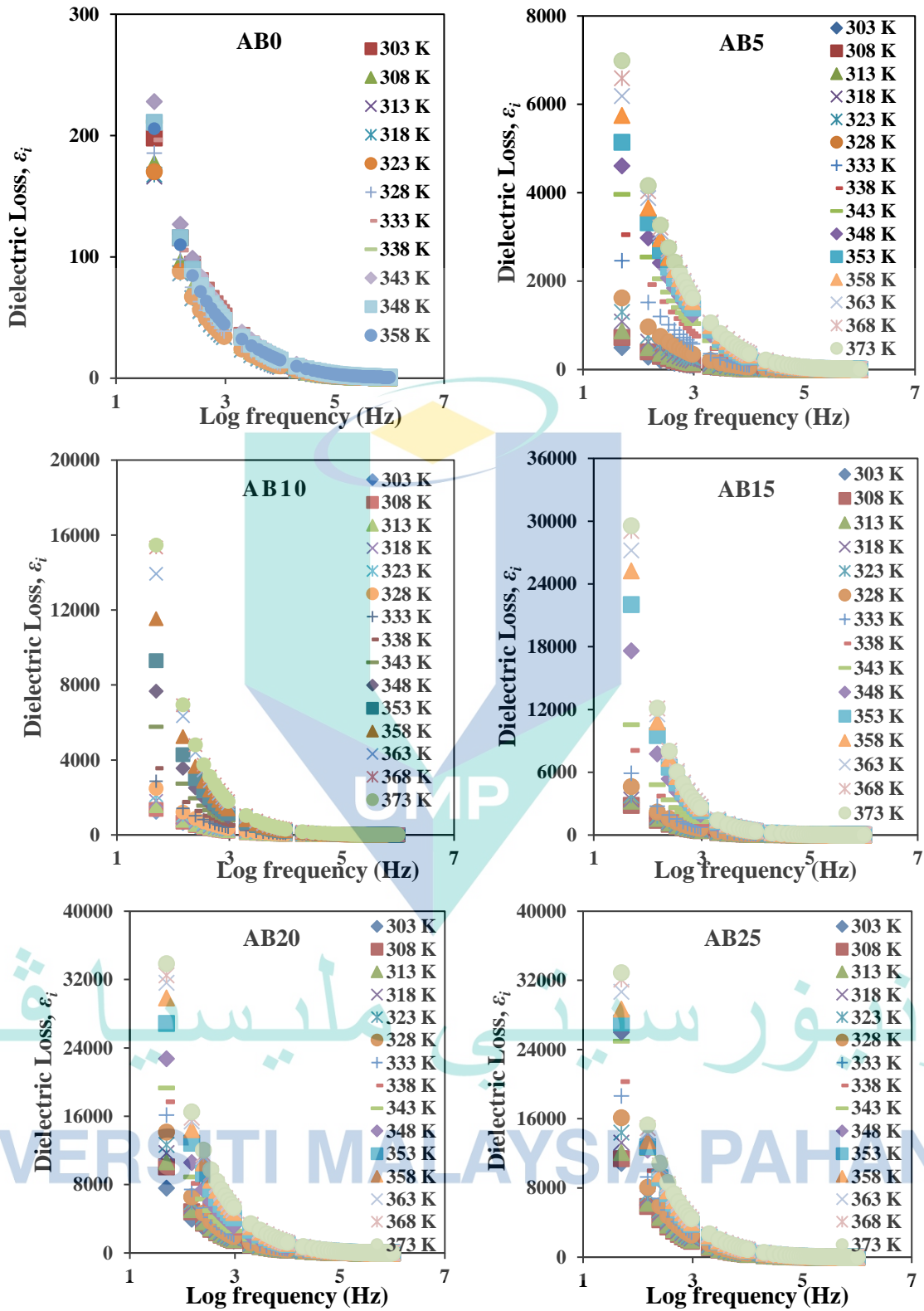


Figure 4.23 Frequency dependence on dielectric loss for CMC-PVA-NH₄Br systems.

Figure 4.24 indicates the dielectric loss pattern of CMC-PVA polymer blend doped with various content of NH₄Br at different temperature. The dielectric constant and dielectric loss gave almost similar pattern where both were increasing at low frequency with increasing NH₄Br content. This indicated the occurrence of electrode polarization and space charge effects which confirmed non-Debye behaviour (Chai et al., 2013a). It also can be seen in Figure 4.24 that the ϵ_i increased as temperature increased, implying that the temperature influenced the behaviour of ϵ_i of the samples. According to Rani et al. (2015), the increment of ϵ_i at low frequency could be attributed to the migration polarization of mobile ion. There were also three main factors that impact the rising of ϵ_i value at low frequency, including trace of moisture from the films, effects of electrode polarization and charge effects which are normally seen in ionic glasses (Mishra et al., 1998).



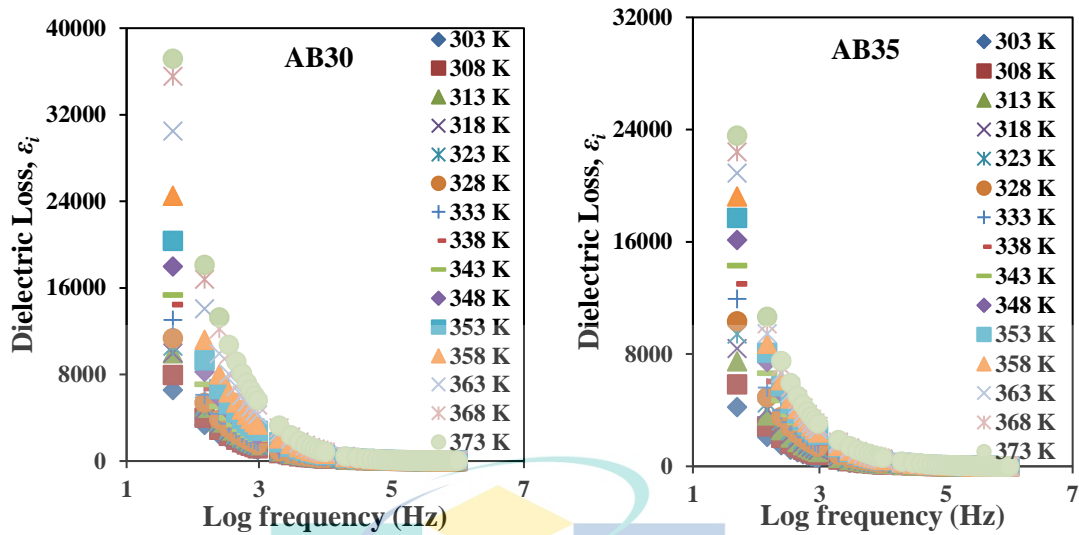


Figure 4.24 Dielectric loss, ϵ_i patterns for sample SBEs system at various temperature.

4.7.5 Modulus Analysis of CMC-PVA+NH₄Br

The dielectric modulus will give a better analysis of electric behaviour. The real modulus, M_r and imaginary modulus, M_i , can inhibit the effect of electrode polarization to give a clear indication of the electric property of the polymer electrolyte. According to Khiar et al. (2006) and Ramly et al. (2011), by plotting the electrical modulus spectra, the bulk dielectric behaviour and the effect of electrode polarization in the biopolymer electrolytes system can be used to investigate the electrode/interfacial polarization imprint. This can be used further to analyse the relaxation phenomenon of the CMC-PVA-NH₄Br SBEs system.

Figure 4.25 illustrates the frequency dependence on electrical modulus of a real part for biopolymer electrolytes-based CMC-PVA doped with varying amounts of NH₄Br at ambient temperature. It was noticeable in real part of the plot, that the value of the real modulus was decreasing with the incorporation of NH₄Br into the electrolyte system. At high frequency, the M_r increased and a long tail was observed at low frequency, indicating that a relaxation phenomenon has occurred that suppressed both direct current conduction and electrode polarization (Mishra et al., 1998; Matos et al., 2015).

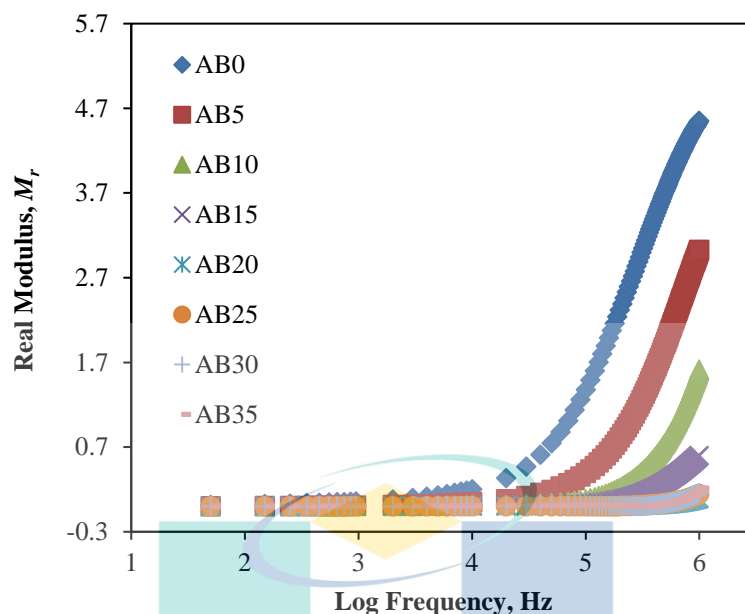
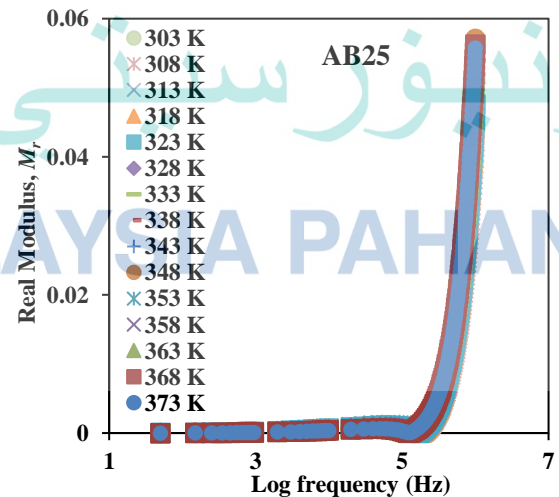
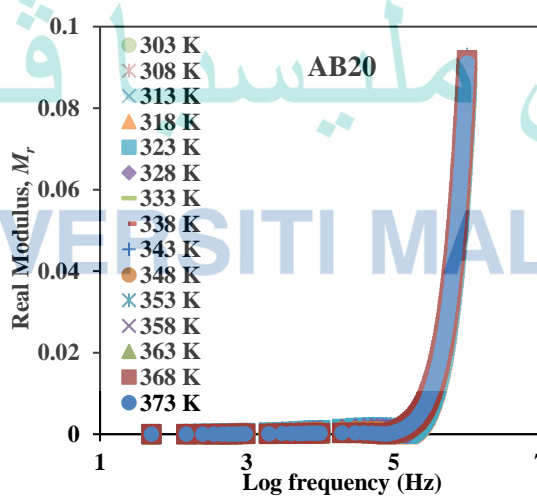
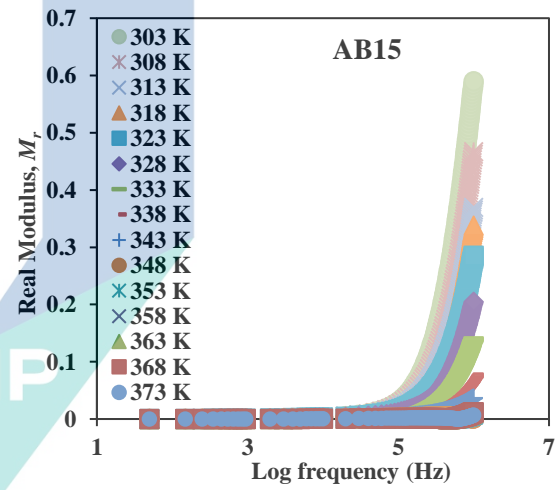
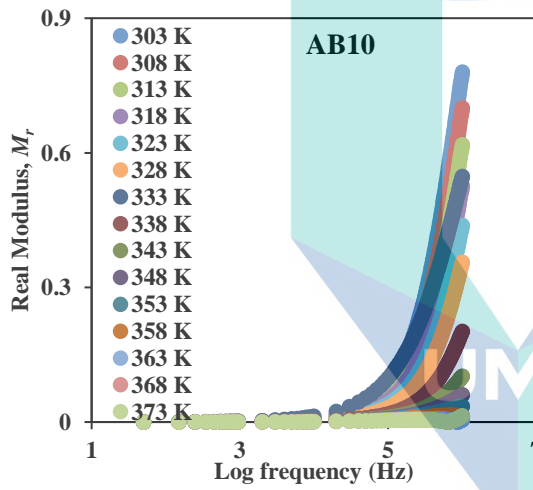
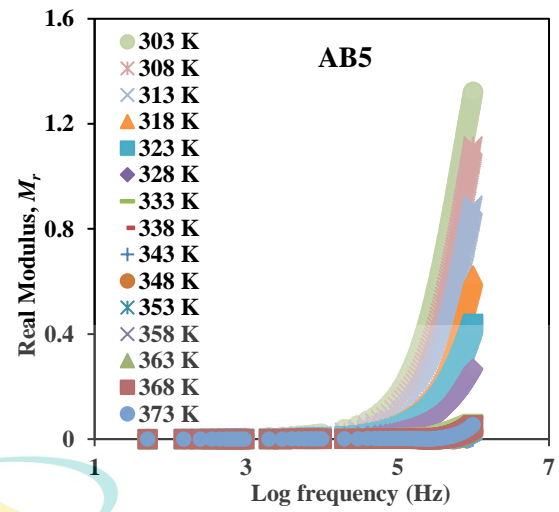
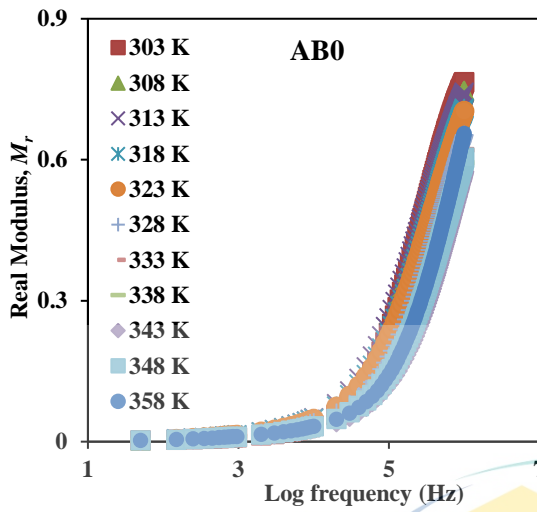


Figure 4.25 Real modulus versus frequency for biopolymer electrolytes containing different NH_4Br content.

Figure 4.26 presents the real part of M^* for CMC-PVA- NH_4Br SBEs system at different temperatures. The fact that at a higher frequency, M_r reached an optimum constant value $M_\infty = 1/\epsilon_\infty$ while at low frequency, M_r approached to zero, suggested that the electrode polarization made an insignificant contribution (Chowdari et al., 1987). This situation can be explained as a lack of restoring force governing the charge carrier's mobility under the action of an induced electric field. The M_r value increased at higher frequencies, suggesting the effect of frequency and temperature. It is also can be observed from Figure 4.26 that the M_r decreased as the temperature increased and this may be due to the plurality of the relaxation mechanism (Sivadevi et al., 2015). It could also be attributed to the ion mobility increasing at higher temperatures where the ions had a shorter relaxation time compared when at low temperatures. This is why at a sufficient high frequency, the ions or charge no longer possesses the ability to polarize. Moreover, Saha et al. (2006) have discussed the increasing patterns of M_r value with increasing frequency approaching to M_∞ for all temperatures can be supported by the conduction phenomena, attributed to short range mobility of ions carriers.



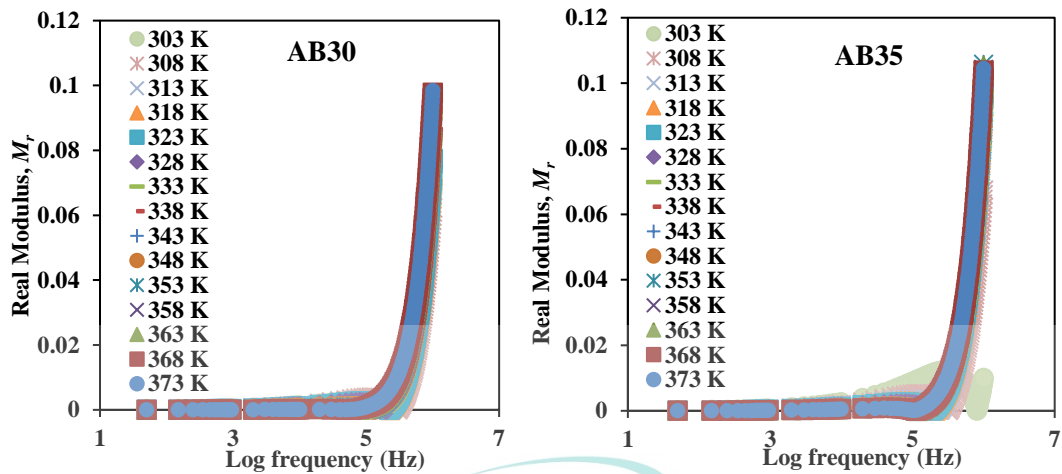


Figure 4.26 Real modulus, M_r patterns for CMC-PVA-NH₄Br SBEs system at various temperature.

Figure 4.27 illustrates the frequency dependence on electrical modulus of the imaginary part for solid biopolymer electrolytes-based CMC-PVA doped with varying amounts of NH₄Br at ambient temperature. As observed in the imaginary plot, the value of M_i was in the vicinity of zero at low frequency. This indicated the negligible contribution of electrode polarization (Ramesh et al., 2002; Padmasree et al., 2006). The appearance of a long tail noticed at the low frequency region also provided evidence of a large capacitance associated with the electrodes (Hema et al., 2009). However, in the imaginary plot, there was a presence of a peak at high frequency that suggested the samples were ionic conductors (Ramly et al., 2011; Noor et al., 2015).

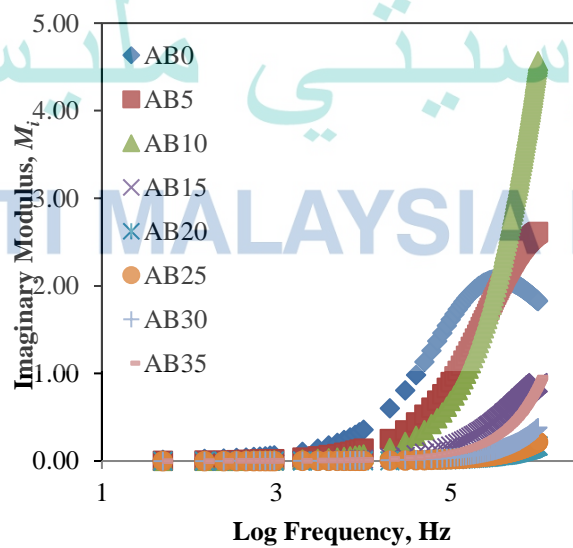
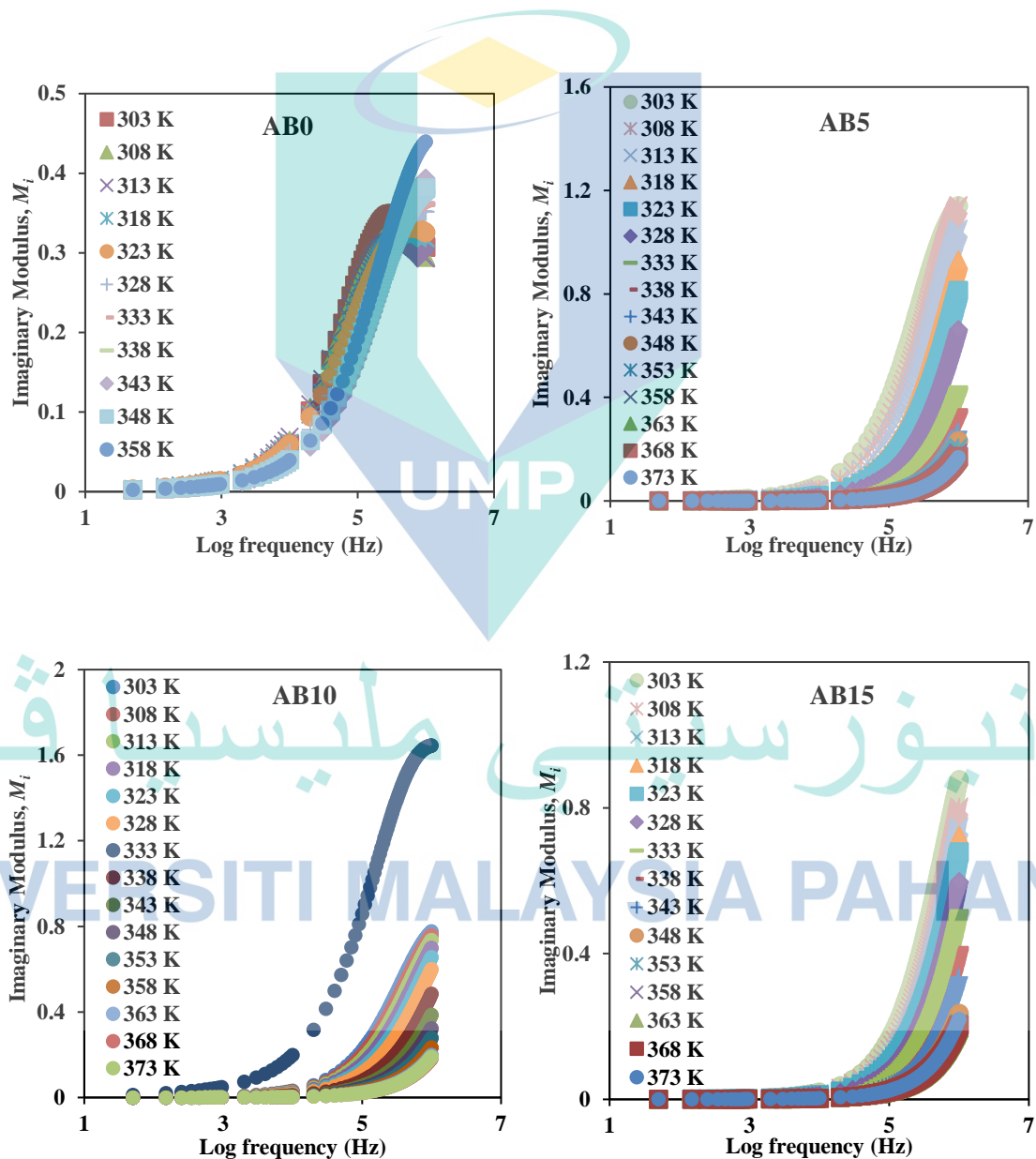


Figure 4.27 Imaginary modulus versus frequency for biopolymer electrolytes containing different NH₄Br content

Figure 4.28 illustrates the imaginary part of M_i for CMC-PVA-NH₄Br SBEs system at different temperatures. The long tail observed at low frequency was related to the electrodes' high capacitance values, indicating charge carriers accumulation happening at the interface of electrode/electrolytes (Aziz et al., 2010). The increase in M_i value at the high frequency could be due to the bulk effect (Hema et al., 2008). As the temperature increased, the peak intensity decreased which implied a relaxation time plurality, thus confirming that the SBEs system obeyed a non-Debye behaviour (Ramlli et al., 2013).



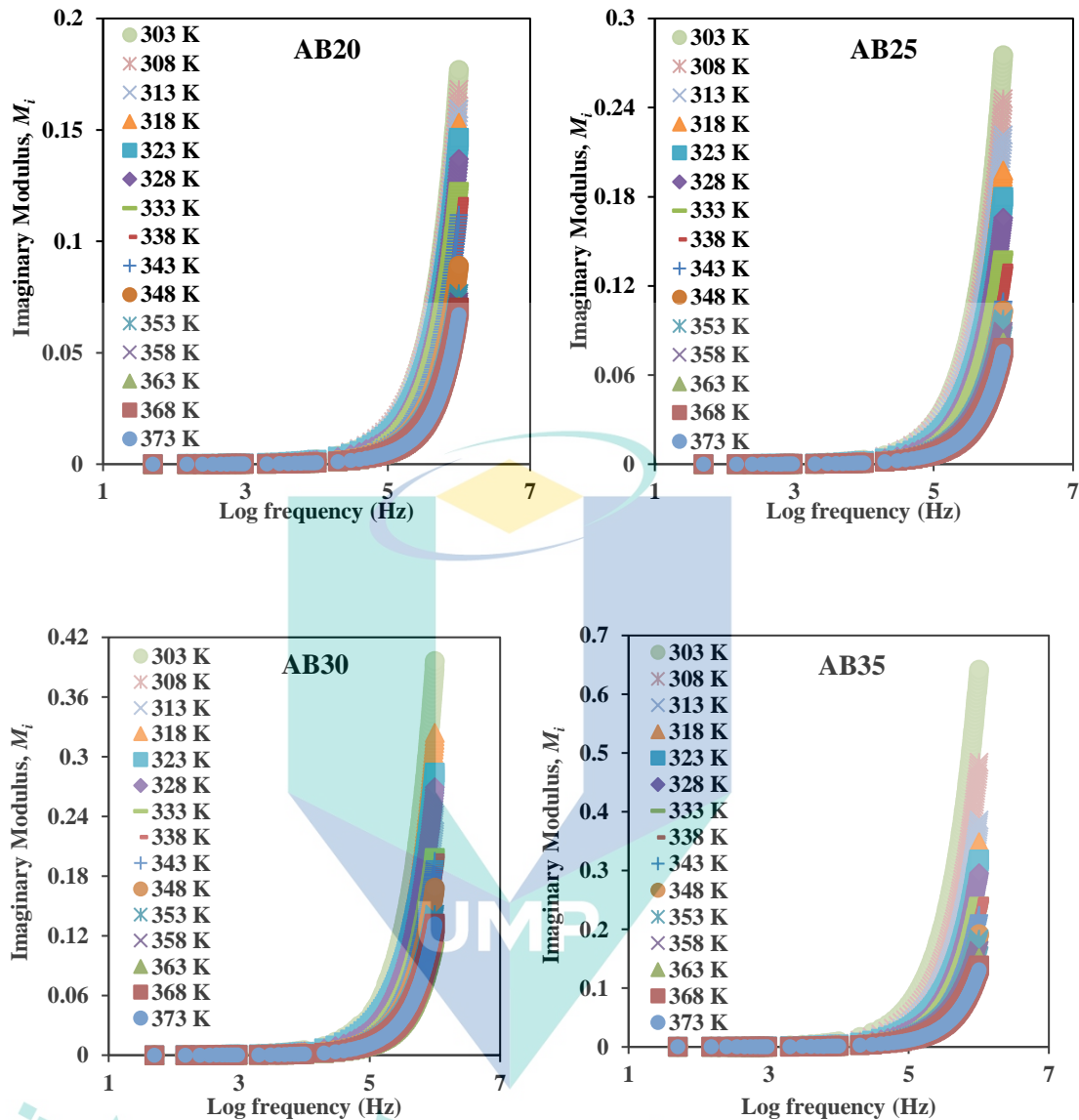


Figure 4.28 Imaginary modulus, M_i patterns for CMC-PVA- NH_4Br SBEs system at various temperature.

By comparing both electrical moduli, it can be observed that at low frequency, the values of M_r and M_i values are low and then it started to increase as the frequency increased. These increment at high frequency can be explained by the electrode polarization phenomenon. At low frequency, the values of real and imaginary parts were in the vicinity of zero, indicating a negligible contribution by the electrode polarisation which is the main advantage in moduli studies. The long tail observed at low frequency was caused by the large capacitance associated with the electrodes (Bakar et al., 2015; Mazuki et al., 2019).

4.8 Transport Properties Analysis of CMC-PVA+NH₄Br

Although there has been a number of research carried out on polymer electrolytes and their application, only a few studies have focussed on the ionic mobility properties, principally due to the difficulty in establishing the transportation of ions (Long et al., 2016). As reported in the literature (Arof et al., 2014), the information from the impedance analyser can be used to study the characteristics of polymer electrolytes and their transport parameter in ionic conduction. There are several approaches that can be carried out using data from the impedance analyser in order to determine the number of mobile ions (η), ionic mobility (μ) and diffusion coefficient (D) such as the Nyquist fitting method (Noor et al., 2019), Rice and Roth model method (Rice et al., 1972) and Broadband Dielectric Response (BDR) method (Bandara et al., 2011). The Rice and Roth model method is a conventional technique which is often applied to define the transport parameters in various biopolymer electrolyte systems based on the impedance spectroscopy data; nonetheless, it is worth to note that it is restricted to temperature-conductivity of the Arrhenius behaviour systems (Rice et al., 1972; Kadir et al., 2010) and in addition the calculated value is also questionable. As for the BDR method that was developed by Bandara-Mellander (Bandara et al., 2011), this method is only relevant for the Nyquist plot that consists of both semicircles as well as spikes. Furthermore, this method is limited for ions that have a single relaxation time and is not appropriate for Nyquist plots that only consist of a spike. Meanwhile, the fitting method which is also known as the Arrof-Noor (A-N) method was found to be the most suitable method to be applied in the present work as it is able to extract the transport parameters from both semicircle-spike and spike provided by the Nyquist plot.

In the present research, these methods were carried out based on data from the impedance spectroscopy (Arof et al., 2014). The parameters of the transport properties were calculated via the following equation:

$$D = \frac{(k_2 \varepsilon_r \varepsilon_0 A)^2}{\tau_2} \quad 4.9$$

$$\mu = \frac{eD}{k_b T} \quad 4.10$$

$$\eta = \frac{\sigma}{e\mu} \quad 4.11$$

where k_b is the Boltzmann constant ($1.38 \times 10^{-23} \text{ J K}^{-1}$), T is ambient temperature in Kelvin (303 K), $\tau_2 = 1/\omega_2$ also being the minimum imaginary impedance with ω_2 corresponding to the angular frequency, e is electric charge constant with a value of $1.602 \times 10^{-19} \text{ C}$, k_2 is capacitance k_2^{-1} that obtained from the Nyquist plot, ϵ_o is permittivity constant ($8.85 \times 10^{-14} \text{ F cm}^{-1}$), A is area of the sample, ϵ_r is obtained from dielectric constant data from the previous section and σ is the ionic conductivity of the SBEs system. However, Eq. 4.9 is only valid for Nyquist plots that consist of a semicircle and title spike. The value of D for the Nyquist plot containing only the title spike can be expressed as (Noor, 2016):

$$D = D_o \exp[-0.0297 (\ln(D_o))^2 - 1.4348 (\ln(D_o)) - 14.504] \quad 4.12$$

where D_o is

$$D_o = \frac{4k_2^4 d^2}{R_b^4 \omega_2^3} \quad 4.13$$

where d is thickness of electrolyte and R_b is the bulk resistance. Figures 4.29 and 4.30 show the graphs of μ and D and η , respectively for CMC-PVA-NH₄Br based biopolymer electrolyte system.

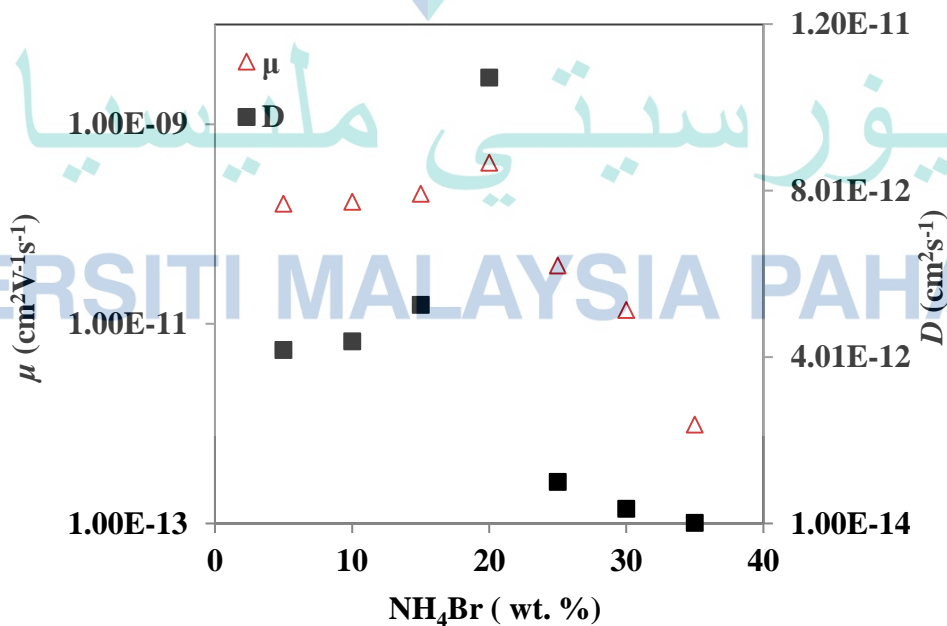


Figure 4.29 Mobility of charge carriers, μ and diffusion coefficient, D versus varied amount of NH₄Br.

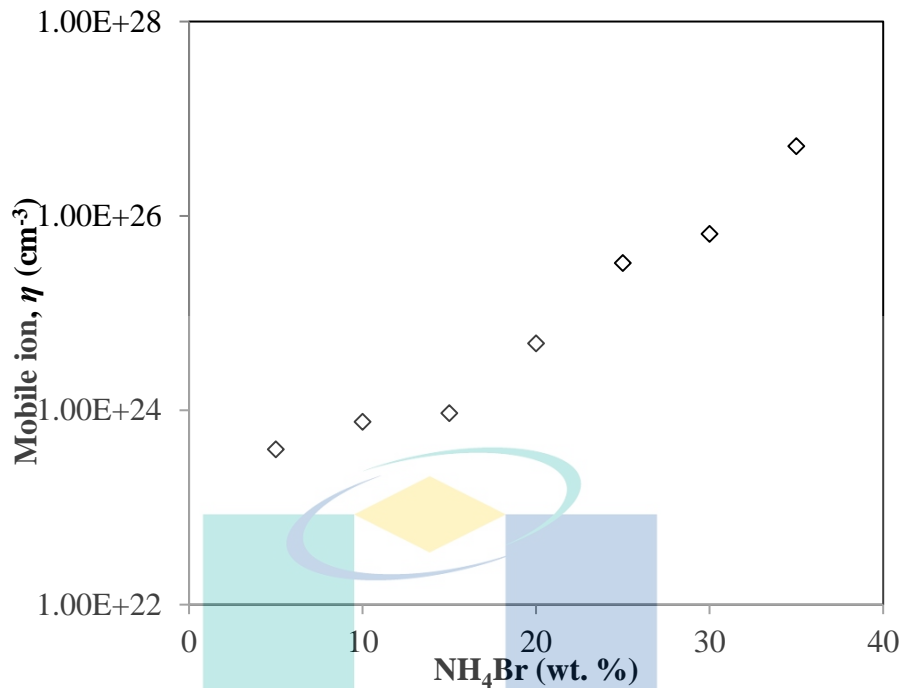


Figure 4.30 Number of ions, η versus varied amount of NH_4Br .

In general, the ionic conductivity totally reflected the η and μ values. However, it was found in the present research that the value of η showed an increasing pattern as the NH_4Br content increased which did not follow the behaviour of ionic conductivity. The number of mobile ions kept increasing even though the ionic conductivity decreased for samples above AB20 and this phenomenon might be attributed to the formation of ions aggregates which hindered the movement of the ions due to the limitation of vacant sites. In addition, at high NH_4Br content, overcrowding of H^+ occurred and huge amounts of trapped ions required more energy in order to hop from one site to another, thus, leading to a decrease in ion diffusion and ionic mobility of the present system. It is believed that when more NH_4Br was introduced, it will supply more H^+ ions into the system as well, leading to the space limitation due to overcrowded H^+ ions, in turn reducing the ionic conductivity. This finding is similar with previous works on transport properties (Idris et al., 2009; Ahmad & Isa, 2015; Chai et al., 2016; Ramlli et al., 2016). This observation is also supported by the FTIR and XRD analysis as discussed in the previous section where the H^+ ions from NH_4Br interacted with the COO^- of the CMC-PVA polymer blend more efficiently as the sample became more amorphous with resultant enhancement of ionic conductivity along with transport properties until it reaches the optimum value.

Furthermore, the μ and D were observed to be aligned with the ionic conductivity trend (Samsudin & Isa, 2012; Ahmad et al., 2015). The drop of μ and D at high content can be explained by the present electrolyte system being overcrowded with H^+ ions dissociated from the NH_4Br (Ramlli et al., 2016; Rasali et al., 2017). The overcrowded ions then caused a high crystallinity phase which then created the blocking pathway and made the movement of ions between one site to another in host polymer difficult. In turn, higher energy value was needed for ions to migrate from one site to another. The findings were further supported by the TGA and DSC analysis where it was believed that AB20 had achieved movement stability of proton ions hopping, in turn, increasing the decomposition temperature and decreasing the glass transition temperature, thus increasing the thermal stability. The drop of μ and D at high NH_4Br content can be explained by the present electrolyte system being overcrowded with H^+ ions dissociated from NH_4Br (Samsudin et al., 2011). The overcrowded ions, in turn, caused a high crystallinity phase which created the blocking pathway and made the movement of ions between one site to another in host polymer difficult, suggesting that high energy was required for migration.

4.9 Proton (H^+) Transference Measurement Analysis

Electronic and ionic transference number measurements were conducted in order to determine the mechanism of conducting species of the SBEs systems, indicating the ionic conductivity of the sample either being more cationic than anionic or otherwise (Azlan et al., 2011). The current relation curve during *dc* polarization and complex impedance after polarization for SBE containing AB20 using reversible electrodes are illustrated in Figures 4.31 and 4.32, respectively. Figure 4.31 shows that the decrement of the initial total current, I_i corresponded to the increase of time until it became saturated and constant in the fully depleted situation. At the steady state, electrons migrated across the electrolyte and interface and triggered the cell to polarize and for current to flow. This might have occurred due to ionic currents passing through an ion-blocking electrode falling drastically with time if the electrolyte is primarily ionic (Koksbang et al., 1995; Sundaramahalingam et al., 2018). Since ionic can be attributed to cation and anion, the possible ionic mobility in biopolymer electrolyte systems might due to H^+ or NH_3^+ or NH_4^+ or Br^- from NH_4Br (Hafiza et al., 2017). Further studies on cationic transference number (t_{H^+}) was done to determine the t_{H^+} ion conduction in the CMC-PVA polymer

blend doped with 20 wt. % solid biopolymer electrolyte system. It was also important to investigate the performance of the SBE film in terms of its application (Manjuladevi et al., 2017). The H^+ transport number was identified via a combination of complex impedance and transference number measurement.

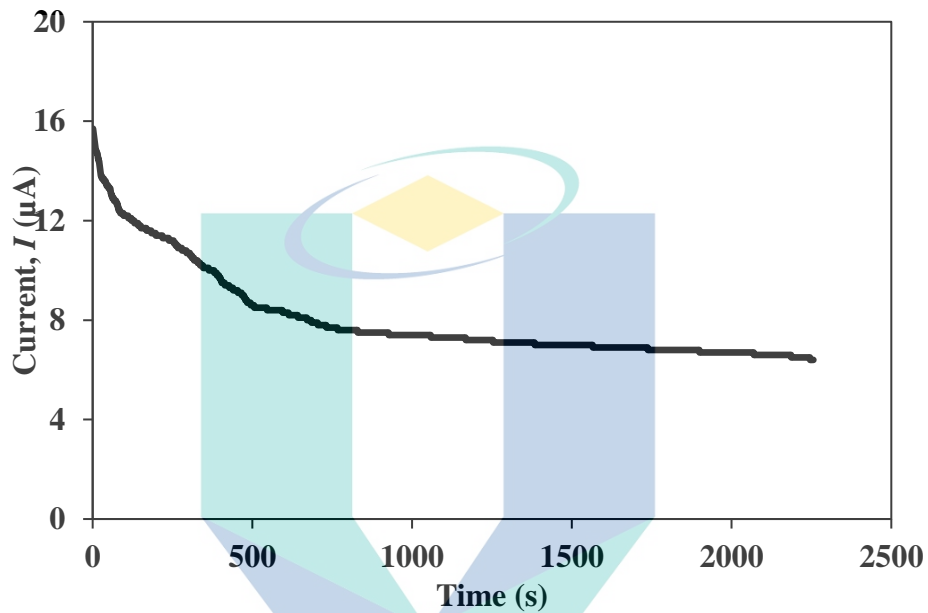


Figure 4.31 Current relaxation curve during *dc* polarization

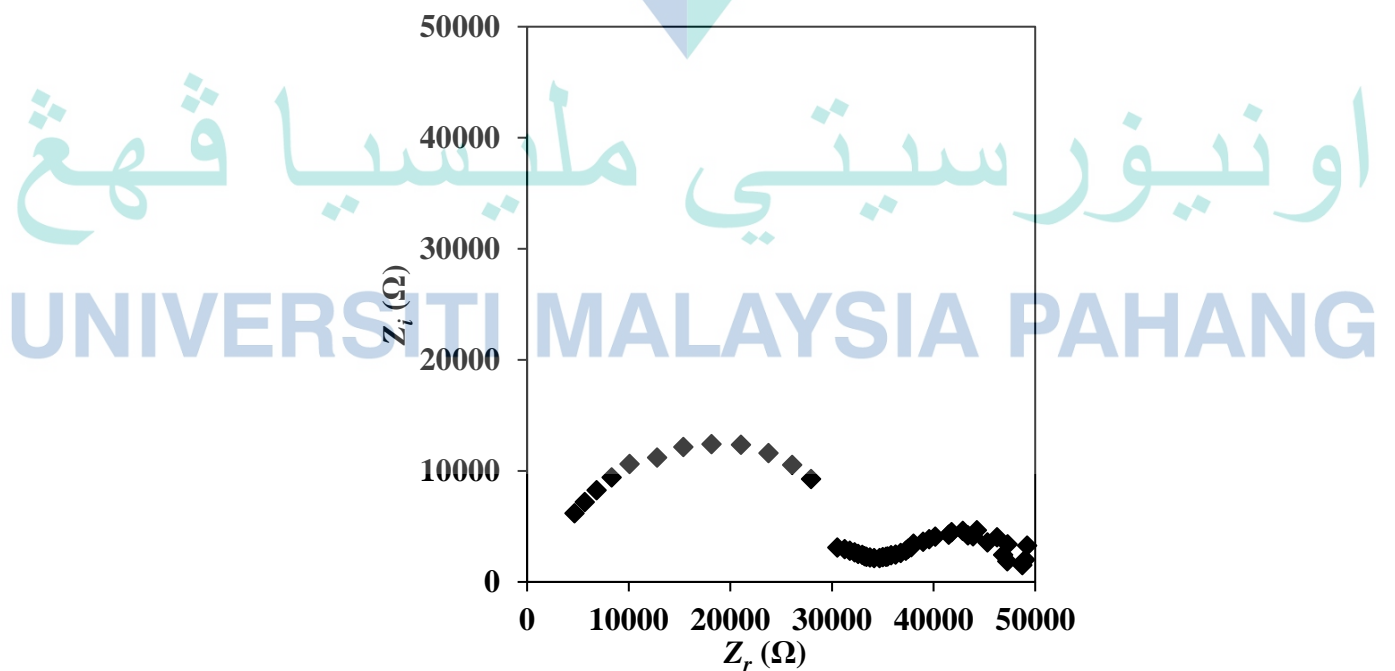


Figure 4.32 Nyquist plot for CMC-PVA+20 wt. % NH_4Br biopolymer electrode using non-blocking MnO_2 electrode.

From the curves, the cationic transference number was calculated using the following equation (Bhargav et al., 2009; Manjuladevi et al., 2017):

$$t^+ = \frac{R_b}{\left(\frac{\Delta V}{I_{ss}}\right) - R_c} \quad 4.14$$

where R_b is bulk resistance ($3.41 \times 10^4 \Omega$), R_c is the resistance of electrode/electrolyte interface ($1.46 \times 10^4 \Omega$), ΔV is the potential voltage applied in DC and I_{ss} is the current at steady state. Watanabe et al. (1995) have pointed out that this method will not give the exact value of cation transport number in a condition where the ionic association occurred in the polymeric network as it is likely to happen in such a relatively low polarity media.

The CMC-PVA+20 wt. % NH_4Br biopolymer electrolyte was sandwiched between two manganese electrodes. In the present work, manganese was chosen as the reversible electrode since the proton was expected to be a mobile species in the polymer blend complex. In addition, manganese is widely used as an electrode for the intercalation of proton in proton batteries (Ng et al., 2006; Kadir et al., 2010; Shukur et al., 2013; Samsudin et al., 2014). The semicircle curve as shown in Figure 4.32 was attributed to the reversible nature of the manganese electrodes and hence confirmed the H^+ ion conduction in the biopolymer electrolyte (Kumar et al., 2011).

The value of cation transference number was calculated to be 0.31, suggesting that the total ionic conduction was predominantly anionic conduction. Based on the findings reported by (Geiculescu et al., 2006), the transference number for the cation never reached the unity value which suggested that even for very large and multiple charged anions, there was still an anionic contribution to the overall ionic conductivity.

4.10 Linear Sweep Voltammetry (LSV) Analysis

Linear sweep voltammetry measurement was carried out in the present work in order to investigate the stability of the electrochemical operating window of the highest conducting CMC-PVA- NH_4Br SBE (Shukur et al., 2013; Shukur et al., 2014a). The electrochemical stability which is also known as the working cell potential range of the SBE is one of the important parameters to be determined for its application in

electrochemical devices such as any storage energy and proton battery (Samsudin et al., 2014; Noor et al., 2019). Figure 4.32 shows a plot of the potential window for the AB20 sample.

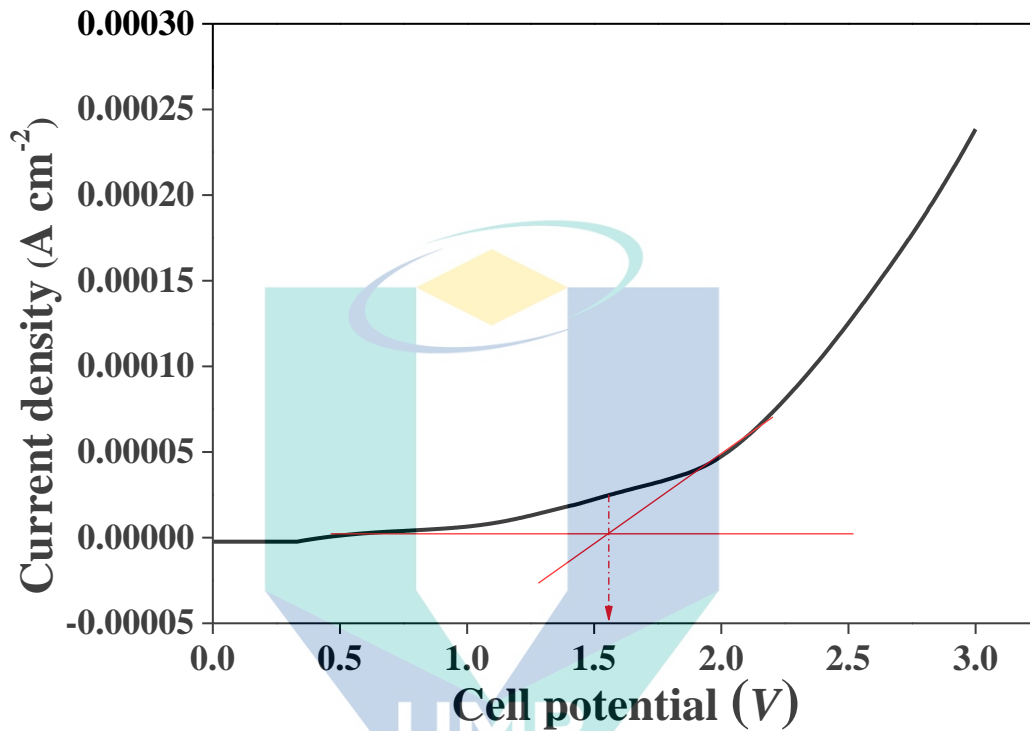


Figure 4.33 LSV response of SBE system of highest ionic conductivity.

It can be seen from Figure 4.33 that no obvious current was detected through the electrode potential from the open circuit potential to 1.55 V. The electrochemical stability of the CMC-PVA polymer blend doped with AB20 biopolymer electrolyte was found to be stable up to 1.55 V on the stainless-steel electrodes. In addition, the current onset was observed at 1.55 V which indicated at that point the breakdown voltage of biopolymer electrolyte has occurred (Kadir & Arof, 2011). The present finding is in agreement with a previous report by Yusof et al. (2014) who found that a polymer blend of PVA-chitosan doped with NH_4Br possessed the breakdown voltage of 1.57 V.

In addition, Kadir and Arof (2011) also reported that their work on a PVA-chitosan blend polymer electrolyte membrane containing NH_4NO_3 exhibited the breakdown voltage of ~ 1.70 V at ambient temperature. The observed operating window voltage for SBE containing AB20 was suitable to be applied in devices such as energy storage and

protonic batteries since the minimum requirement electrochemical window for devices is ~ 1 (Rauh, 1999; Pratap et al., 2006; Ng et al., 2008). Hence, the potential windows showed that the present SBE system was practicable for the construction of an EDLC device.

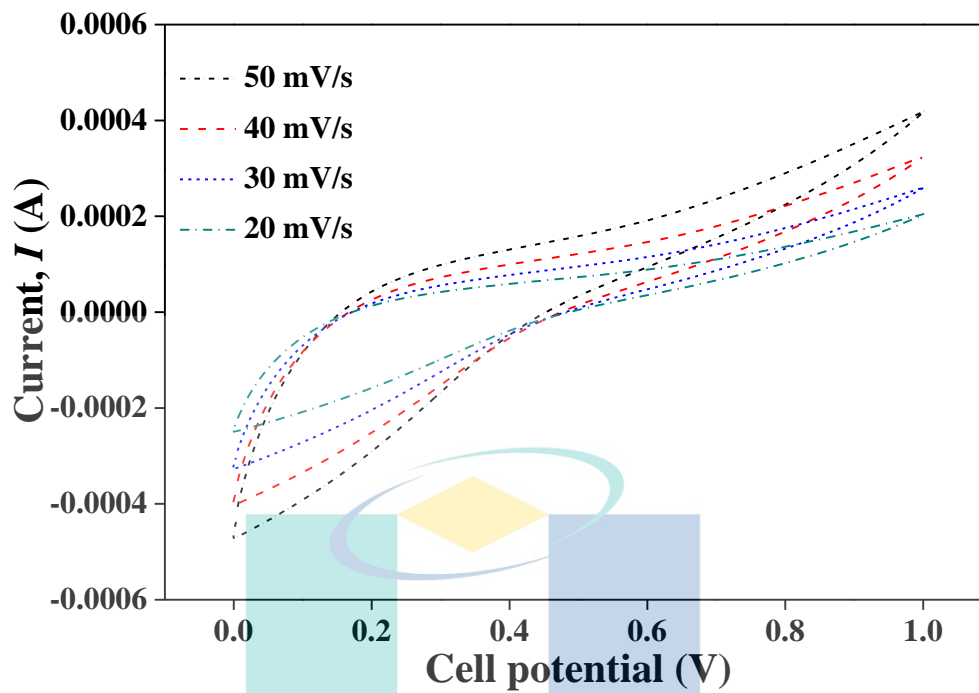
4.9 Electrochemical Properties of Electrical Double Layer Capacitor (EDLC)

The feasibility of the highest conducting solid biopolymer electrolytes-based CMC-PVA incorporated with 20 wt. % NH_4Br for application in electrical double layer capacitor (EDLC) was characterized using cyclic voltammetry (CV) and galvanostatic charge-discharge (GCD) analyses.

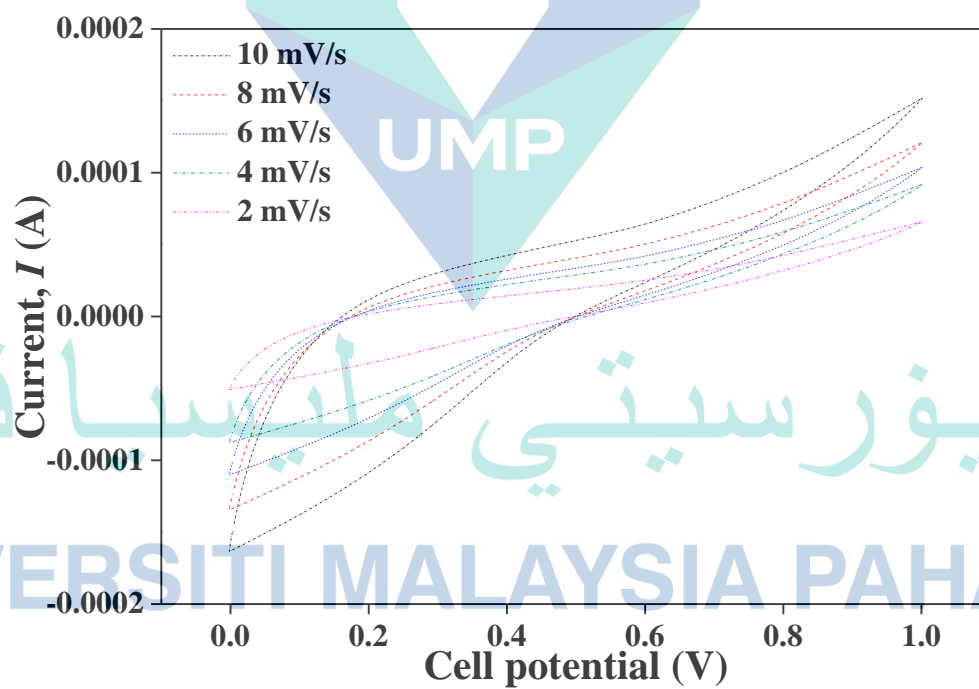
4.9.1 Cyclic Voltammetry (CV) Analysis

The potential dynamic electrochemical measurement is the basis of cyclic voltammetry measurement and involves the determination of electrode potential that corresponds linearly to the time for EDLC performance. Hence, the electrode potential is plotted linearly versus time (Aziz et al., 2019).

Figure 4.34 portrays the CV curve for the SBE system at different scan rates. A non-Faradaic current was detected in the figure, confirming the construction of an electrical double layer capacitor in the present work (Liew & Ramesh, 2015). In EDLC, the energy storage mechanism is non-Faradaic, which refers to that portion of the current observed in an electrochemical system which cannot be attributed to any redox processes occurring at an electrode surface. The electrons from the electrode and ions from the electrolyte are held by the intense electric field, which exists as development of a charge double layer, where the energy is stored as potential energy (Kadir & Arof, 2011).



(a)



(b)

Figure 4.34 Cyclic Voltammetry of the highest conducting SBE at (a) 20 to 50 mV s⁻¹ and (b) 2 to 10 mV s⁻¹ scan rate.

Figure 4.34 shows that the CV curve of the surface area decreased when scan rate was decreased, indicating a decreasing stored charge on the electrode surface, which in turn enhanced the energy loss in the EDLC (Shukur et al., 2015). The increasing of surface area with increases in the scan rate could be attributed to the voltammetry current being directly proportional to the scan rate, thus explaining that the EDLC was scan rate dependent which is a characteristic of capacitor cells. It clearly can be seen that there were no cathodic and anionic peaks observed in all of the CV curves and it is suggested that this might be due to the type of materials used in the present work. From the CV curve, the specific capacitance, C_{sp} can be obtained and the values are tabulated in Table 4.10.

It was noticeable in Table 4.10 that the C_{sp} value decreased as the scan rate increased and this can be explained with the inaccessible portion of H^+ ion from $NH_4^+ - Br^-$ diffusing at the electrode/electrolyte interface (Nadiah et al., 2017). In the present EDLC, a slight deviation was observed and according to Kadir and Arof (2011), this situation was due to the internal resistance and carbon porosity. In addition, Yuhanees (2017) reported that the smaller surface area of the CV profile was attributed to the poor contact of electrode/electrolyte interfaces, which hindered the ions from being absorbed onto the electrode surface. The C_{sp} of the lowest scan rate possessed the highest value of C_{sp} (17.47 F g⁻¹).

Table 4.10 List of specific capacitances obtained from CV curve.

Scan rate (mV s ⁻¹)	C_{sp} (F g ⁻¹)
2	17.47
4	12.01
6	9.40
8	8.59
10	6.87
20	6.07
30	5.18
40	4.84
50	4.63

The performance of EDLC depends on the ionic conductivity which can influence the C_{sp} value. The most conducting sample can promote a higher mobility of charge carriers in the high conductive polymer matrix (Yu et al., 2013). Thus, it can enhance the

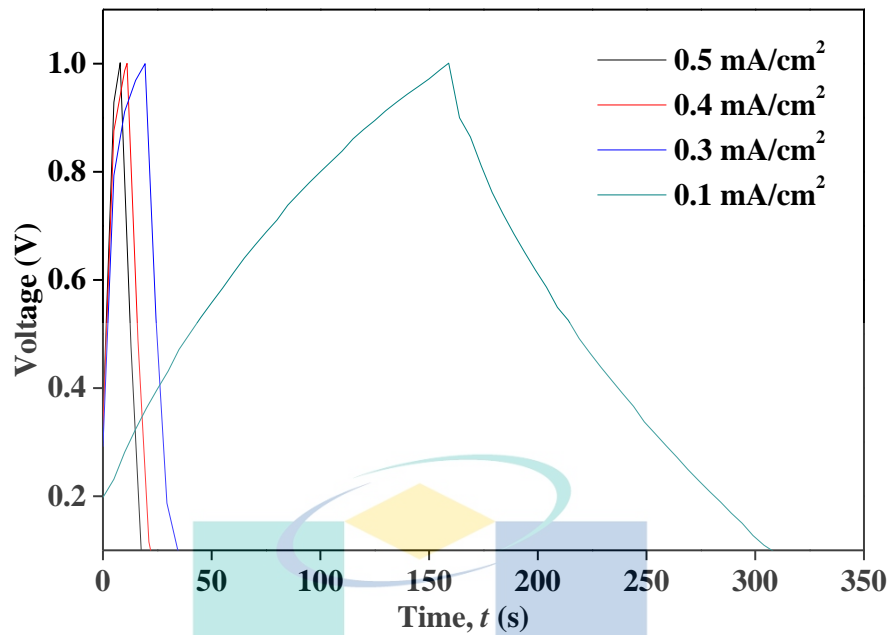
formation of a double layer electrode and improve the energy storage capability in the EDLC.

4.9.2 Galvanostatic Charge-Discharge (GCD) Analysis

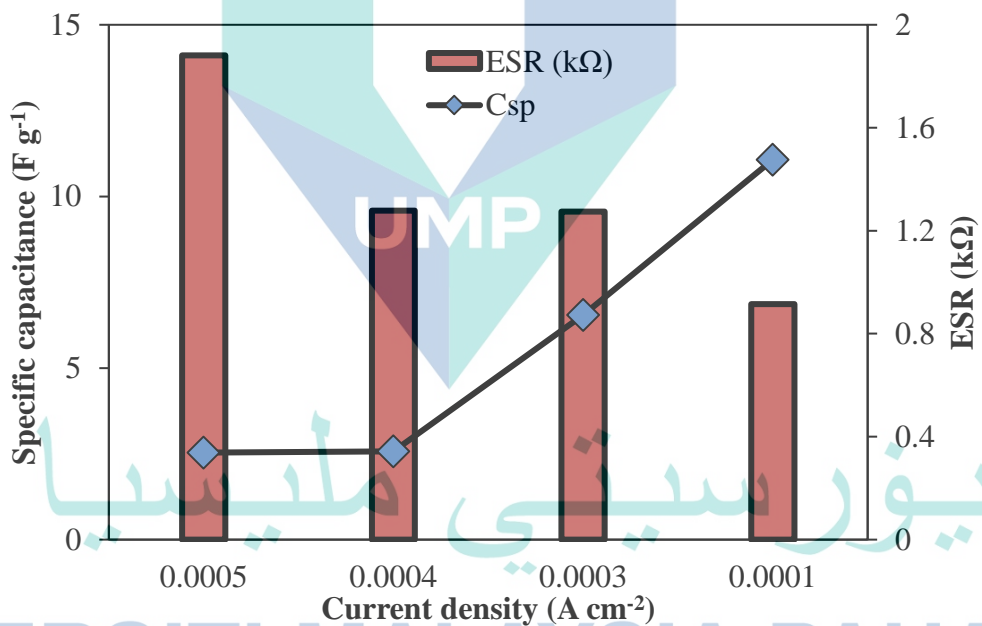
The electrochemical properties of the fabricated EDLC was further investigated via charge-discharge characteristics of the EDLC coin cell containing the highest conducting sample-based CMC-PVA polymer blend SBE. Figure 4.35 demonstrates the galvanostatic charge-discharge profile of the SBE system at different current densities and specific capacitance and equivalent series resistance (ESR) values versus current density.

It can be seen clearly from Figure 4.35 (a) that at the discharge curve, the sudden drop in voltage increased when a high current density was applied in the present work. The sudden drop at discharge curve is known as the internal resistance (I_R), referred to as the ESR of the cell. It can be explained that the different patterns of galvanostatic charge-discharge for each current density could be due to the presence of internal resistance which can reduce the specific capacitance. At high current density, the rapid voltage drop at discharge profile could be attributed to the I_R caused by resistance from the crosslinked structure between the electrode and the present SBEs as discovered by other researchers (Pandey et al., 2011; Shuhaimi et al., 2012). Further, a significant amount of voltage drop occurring across the resistance will reduce the portion of the useful energy in the application. In addition, a high ESR value degrades the performance and this might be attributed to the I^2R losses, noise and higher voltage drop.

In order to further investigate the performance of the charge discharge, the equivalent series resistance (ESR) were calculated and plotted in Figure 4.35 (b). The internal resistance can be determined from the voltage drops at the discharging profile. The internal resistance value was used to calculate the ESR and it was found that the current density for 0.1 mA cm^{-2} was $0.91 \text{ k}\Omega$ which was unusually low for a solid state supercapacitor design compared to other current densities (Pandey et al., 2012). Moreover, it was also observed that the specific capacitance (C_{sp}) was inversely proportional to the ESR value. Thus, it can be concluded that reducing the ESR value will improve the C_{sp} .



(a)



(b)

Figure 4.35 (a) GCD plot for varied current density and (b) specific capacitance and ESR versus current density of highest conducting sample.

Figure 4.36 illustrates the typical galvanostatic charge-discharge characteristics of EDLC fabricated at various cycles with fixed current density of 0.1 mA cm^{-2} . In the present research, the fabricated EDLC was tested at different cycles and by using 0.1 mA cm^{-2} of current density due to its low I_R value and that it can help to enhance the value of

specific capacitance compared to other current densities. In a previous work done by Gu et al. (2000), their EDLC based on PC-EC-LiClO₄ and 25 wt. % PVDF-HFP polymer electrolytes was tested at a current density of 0.1 and 1 mA cm⁻² and was found to have the lowest charge current showing GCD profiles almost triangular with the lowest voltage drop at the discharge profile corresponding to the lowest I_R value as well as being high in specific capacitance. The GCD plot profile showed an almost perfect symmetrical pattern up to the 1600th cycles, implying the excellent capacitive performance of the fabricated EDLC. It can be observed that the cell potential limits were set to be between 0 to 1 V. However, the cell potential was started at 0.18 V in the present study, indicating that the presence of internal resistance of the cell which increased from the interface of electrode/electrolyte and the present SBEs (Arof et al., 2012; Mitra et al., 2001). Similar results were observed at the discharge curve due to the existence of this resistance during the process of discharging.

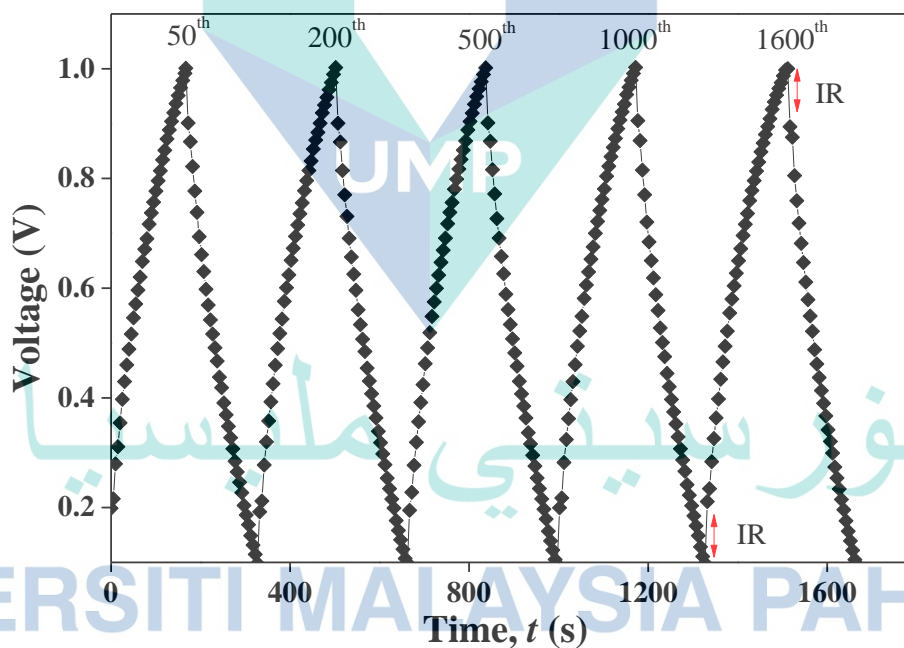


Figure 4.36 Charge-discharge performances of EDLCs at selected cycles.

The charge-discharge profile, the columbic efficiency (η), ESR, C_{sp} , power density and energy density were calculated based on Equations 3.15 to 3.19 in Chapter 3. The cycle stability test of the fabricated EDLC is an important parameter to evaluate the reliability of the EDLC. Figure 4.37 reveals that the charge-discharge performance up to 1600 cycles of the fabricated EDLC containing CMC-PVA incorporated with 20 wt. % of

NH₄Br SBE at 0.1 mA cm⁻². The coulombic efficiency for the present EDLC remained in the range of ~88 % over 1600 cycles, inferring that the electrode and electrolyte have intimate contact with each other. This suggested that the EDLC cell was stable under these charge-discharge conditions. The finding was found to be similar to those observed from previous works (Lim et al., 2014a; Liew et al., 2015; Teoh et al., 2015).

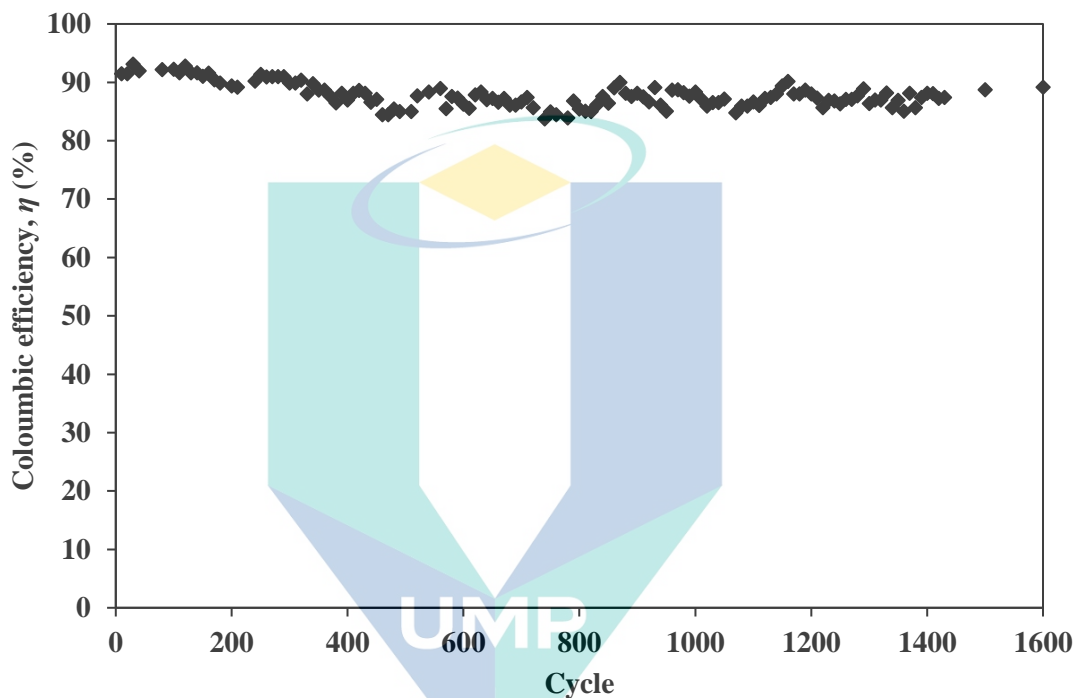


Figure 4.37 Coulombic efficiency as a function of the charge-discharge cycles at a constant current density of 0.1 mA cm⁻².

The specific capacitance and equivalent series resistance (ESR) of EDLC for current density of 0.1 mA cm⁻² were calculated and presented in Figure 4.38. It was noticeable that the long term cycling performance of the EDLC cell containing SBE system with 20 wt.% NH₄Br was operated up to 1600 cycles and the specific capacitance showed an almost constant value, which confirmed the fabricated EDLC capacitive behaviour (Hashmi et al., 2007; Shukur et al., 2015). It was found that the specific capacitance was at ~11 F g⁻¹ and had the potential to be applied in energy storage application (Arof et al., 2012).

Furthermore, there have been several studies in the literature reporting that the value of specific capacitance relies on ionic conductivity (Pandey et al., 2010; Liew et

al., 2014a; Liew et al., 2014b). The relationship between C_{sp} and ionic conductivity was suggested due to the ionic mobility being an important parameter of transport properties, thus it can influence the performance of EDLCs (Yu et al., 2013).

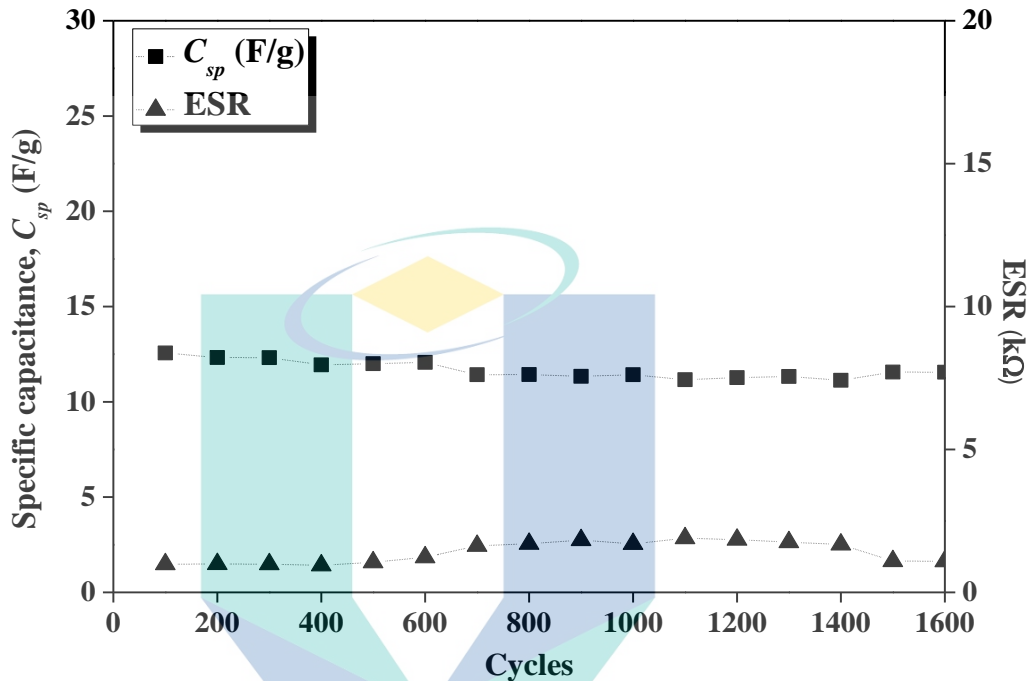


Figure 4.38 Specific capacitance and ESR performance for 20 wt. % NH_4Br electrolytes at 0.1 mA cm^{-2} .

The ESR value have a correlation with ionic conductivity where the lowest ESR gave higher ionic conductivity (Lim et al., 2014a). This can be explained by the concentration of ions from electrolytes and ionic conductivity from the electrode. The ESR was calculated from the voltage drop and was found to be at $\sim 0.91 \text{ k}\Omega$ in the present work. Figure 4.38 reveals the ESR value to be almost consistent, suggesting that the nature of cations in the biopolymer electrolyte does not significantly affect the internal resistance of the EDLC (Lim et al., 2014b). The slight fluctuations in values of specific capacitance have been observed in Figure 4.38. This phenomenon may be attributed to the irreversible charge consumption because of some faradic reactions associated with possible oxidation and reduction of loosely bound surface groups, particularly hydroxyl groups at the interfaces of electrode and electrolytes (Hashmi et al., 1007; Hashmi et al., 2007).

Table 4.11 Previous work on EDLC based polymer electrolytes.

Materials	Ionic conductivity, σ (S cm ⁻¹)	Specific capacitance, C_{sp} (F g ⁻¹)	Charge-discharge cycles	References
Starch-Chitosan-NH ₄ Br-EC	1.44 x 10 ⁻³	~1.172	500	(Shukur et al., 2014c)
Chitosan-H ₃ PO ₄ -NH ₄ NO ₃	10 ⁻⁴	0.216 to 0.220		(Majid, 2007)
Chitosan-Dextran-LiClO ₄	5.16 x 10 ⁻³	8.7	100	(Aziz et al. 2019)
PMMA-LiBOB	3.27 x 10 ⁻³	~0.685	50	(Arof et al., 2012)
MC-NH ₄ NO ₃	2.10 x 10 ⁻⁶	1.67	15	(Shuhaimi et al., 2009)
Starch-Chitosan-NH ₄ Cl	5.11 x 10 ⁻⁴	~3.44	500	(Shukur et al., 2015)
CMC-PVA-NH ₄ Br	3.21 x 10 ⁻⁴	~11	1600	Present work

In addition, there were several factors that can influence the existence of ESR including interfacial resistance between electrode and electrolyte and also between current collector and active material used in the present research (Aziz et al., 2019). Furthermore, the increment of internal resistance contributed to the increasing amount of number of ions which in turn depleted the biopolymer electrolyte. According to Arrof et al. (2012), the internal resistance can be reduced by increasing the percentage efficiency of EDLC to more than 90%. Table 4.11 shows the relation of ionic conductivity and performance of EDLC from the literature. It can be observed that the present work is comparable with the previous findings of EDLCs based polymer electrolytes. The

calculated value of the present EDLC cell showed good performance in terms of ionic conductivity, cycle durability and specific capacitance. Furthermore, blending CMC with PVA can help in the enhancement of specific capacitance of the fabricated EDLC due to the excellent hydrophilic property of the PVA polymer (yang et al., 2005).

Figure 4.39 demonstrates the power density and energy density versus the number of cycles using a current density of 0.1 mA cm^{-2} . The values of power density and energy density has been evaluated and were observed to be at $\sim 31.36 \text{ W kg}^{-1}$ and $\sim 1.19 \text{ Wh kg}^{-1}$, respectively. A decreasing trend was observed with each cycle and showed the capability of the EDLC started to drop. This could be due the increment of the ESR value and might be due to the exhaustion of the EDLC. However, these parameters dropped gradually in the 600th to 800th cycles and remained almost unchanged above the 800th cycles for both energy density and power density. Therefore, the electrochemical stability of the EDLC coin cell became more stable upon the 800th cycles when applied with the charge-discharge process. The reason for the reduction of electrical properties was due to the depletion of the electrolyte, with the ions mobility tended to decrease as the number of cycle increased and also could be due to the formation of ion aggregates (Liew et al., 2016).

In a galvanostatic charge-discharge process, the mobile ions should be in pairs or aggregated after the rapid processes of charge-discharge so that these paired up ions can block the migration of ions in the biopolymer electrolyte matrix. This causes the ions to diffuse into the carbon pores, in turn reducing the formation of ion adsorption at the interface of electrode/electrolyte (Arof et al., 2012). A comparison of energy density and power density between proton batteries and supercapacitors using H^+ ions as carrier from previous research (Lakshmi et al., 2002; Johari et al., 2009; Shuhaimi et al., 2012; Liew et al., 2014a, 2016; Samsudin et al., 2015; Ambika et al., 2018) was carried out and plotted in Figure 4.40. The comparison showed that the present work is comparable with the previous works and have the potential to be used in energy storage application due to the higher value in energy density and power density.

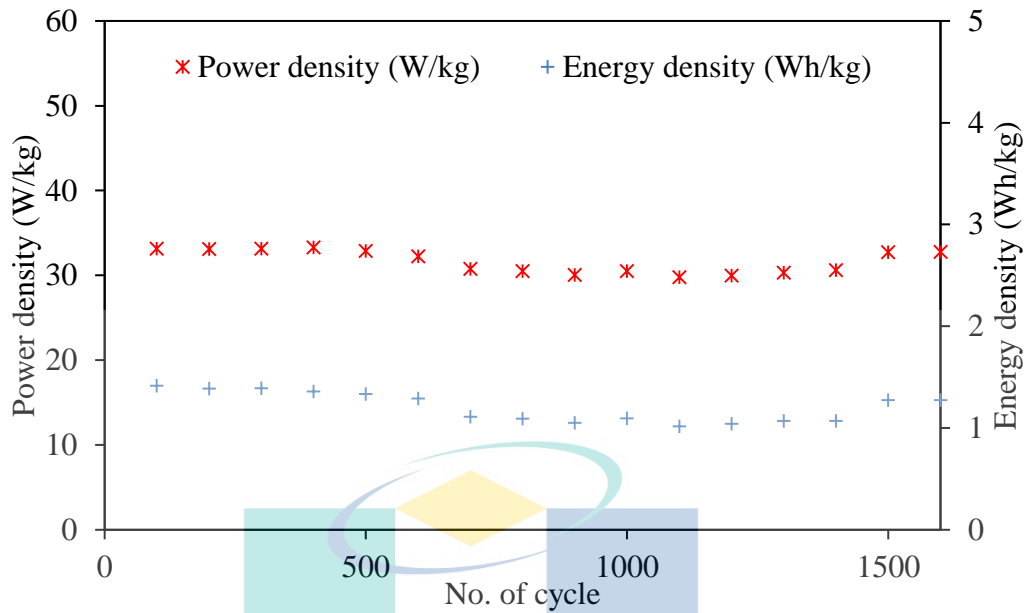


Figure 4.39 Power density and energy density versus number of cycles of cell EDLC.

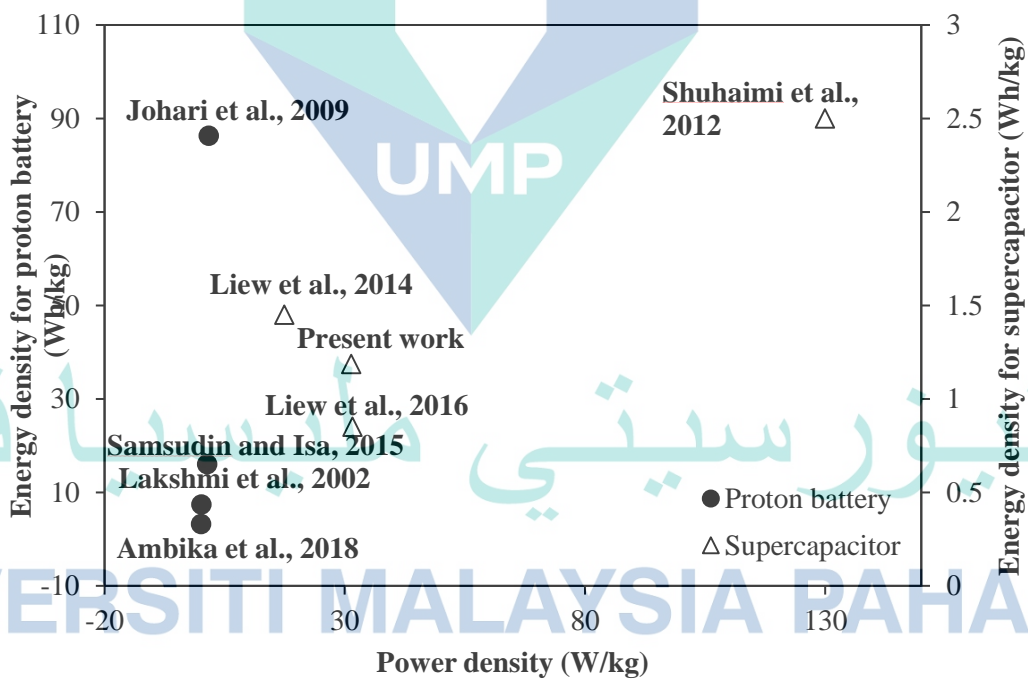


Figure 4.40 Comparable studies of energy density and power density from previous research

CHAPTER 5

CONCLUSION

5.1 Introduction

This chapter, concludes the findings obtained from present work and is expected to support the objectives as stated in Chapter 1. This section also consists of recommendations for future research.

5.2 Conclusion

The present research was designed to determine the performance of materials used as biopolymer electrolytes (SBEs) to be applied in energy storage application and confirms its capability in EDLC. The present work also characterized the electrical and structural properties of the solid biopolymer electrolytes.

As a conclusion, a new system has been discovered and successfully prepared by the solution casting technique that contains CMC-PVA doped with various amounts of NH_4Br based biopolymer electrolytes. Thus, the first objective of the research was successfully achieved. The amorphous nature and interaction between the CMC-PVA polymer blend with NH_4Br were investigated via FTIR spectroscopy analysis and XRD analysis to correlate the ionic conductivity of SBEs. The FTIR analysis revealed that the complexation happened when the NH_4Br was incorporated in the CMC-PVA polymer blend by protonation (H^+), suggesting it has taken place at the carboxylate anion (COO^-) group of the pure CMC via the Grotthus mechanism.

The XRD peak intensity showed a gradual decrease upon the addition of 5 wt. % NH_4Br due to an improvement in the amorphous nature of the SBE, thus proving that the intermolecular H-bonding reduced the degree of crystallinity. The crystallite sizes of all SBEs have been calculated and it was found that the sample with 20 wt.% of NH_4Br (AB20) showed an amorphous phase. TGA results proved that the thermal stability of the CMC-PVA polymer blend was increased by the introduction of NH_4Br . The TGA also

proved that the addition of NH_4Br in the polymer blend increased the decomposition temperature, T_d and decreased the total weight loss, resulting in the enhancement of thermal stability in the SBEs. The lowest glass transition temperature, T_g value given by AB20 is another proof that it is highly amorphous compared to other amounts of added NH_4Br .

The incorporation of different amounts of NH_4Br which acts as ionic dopant in the CMC-PVA polymer blend improved the ionic conductivity in the biopolymer electrolytes. The present work has revealed the highest ionic conductivity is $3.21 \pm 0.005 \times 10^{-4} \text{ S cm}^{-1}$ for the sample containing 20 wt. % of NH_4Br at room temperature. The temperature dependence of all SBE systems follows an Arrhenius behaviour and is thermally activated. The highest conducting electrolyte showed the lowest activation energy of $0.08 \pm 0.002 \text{ eV}$, suggesting for ions to move freely, they require less energy to hop from one site to another site in the polymer backbone. The frequency dependence of both dielectric moduli was found to be of the non-Debye type. Studies on transport properties was carried out via the Fitting method from Nyquist plots. It revealed that the number of ionic mobility and diffusion coefficient influenced the ionic conductivity behaviour. In addition, TNM results showed that the cationic transference number, t_{H^+} is 0.31 for the most conducting electrolyte. The findings based on the present research have fulfilled the objective to optimize the structural, thermal and ionic conduction properties of CMC-PVA- NH_4Br solid biopolymer electrolytes system. Thus, the second objective was achieved.

The stability of electrochemical windows was investigated via LSV and it was observed that the voltage breakdown occurred at 1.55 V. The EDLC cell containing CMC-PVA doped 20 wt. % NH_4Br exhibits the specific capacitance value of 17.47 F g^{-1} which obtained from CV analysis at a scan rate of 2 mV s^{-1} . The charge discharge performance of EDLC further was characterized via GCD analysis and was found to be stable up to 1600 cycles. The specific capacitance obtained from the GCD curve was $\sim 11 \text{ F g}^{-1}$. The higher ionic conductivity is believed to influence the increment of specific capacitance value in the present work. The abrupt jump in voltage at the discharge process was elucidated to be caused by ohmic loss. The power density and energy density has been calculated and recorded to be $\sim 31.36 \text{ W kg}^{-1}$ and $\sim 1.19 \text{ Wh kg}^{-1}$, respectively. The present finding provides evidence that the SBE based CMC-PVA polymer blend doped NH_4Br is a potential candidate for fabrication into EDLCs which fulfilled the third

objective to evaluate the electrochemical performance of SBE. Therefore, the third objective was successfully achieved.

5.3 Recommendations

For future work, a few significant steps must be improved in order to enhance the electrolyte in terms of electrical, mechanical, thermal strength and physical characteristics of the CMC-PVA-NH₄Br biopolymer electrolytes. The following are some suggestions and opinions based on the research findings that can be investigated for a better system in the future:

- Further study using tensile strength can be carried out to investigate the mechanical strength of the electrolytes.
- Enhancement of the ionic conductivity by adding plasticizers. Plasticisers can be function to dissociate the ionic dopant, thus helping to increase the ability of the polymer electrolytes (Osman et al., 2001).
- Further studies can use Field Emission Scanning Electron Microscopy (FESEM) and Density Functional Theory (DFT) characterization in order to obtain detailed characterization of the surface structure of SBEs and to confirm the homogeneity of the system. The DFT analysis can provide information on the molecular structure of the polymer which can be correlated with the FTIR analysis.
- The appropriate method to fabricate EDLC coin cell is recommended to enhance the interfacial contact between electrode/electrolyte.

Although the fabrication of EDLC carried out in present research is suitable to be used in low power applications, a stable performance and environmentally friendly type of device is needed for long term usage. Thus, further improvements are required. Therefore, the present results and recommendations given can hopefully be a reference for other researchers in the related fields.

REFERENCES

- Abbas, Q., Mirzaeian, M., Ogwu, A. A., Mazur, M., & Gibson, D. (2018). Effect of physical activation/surface functional groups on wettability and electrochemical performance of carbon/activated carbon aerogels based electrode materials for electrochemical capacitors. *International Journal of Hydrogen Energy*, 45(25), 13586-13595.
- Abd El-Kader, F. H., Shehap, A. M., Abo-Ellil, M. S., & Mahmoud, K. H. (2005). Relaxation phenomenon of poly (vinyl alcohol)/sodium carboxy methyl cellulose blend by thermally stimulated depolarization currents and thermal sample technique. *Journal of Applied Polymer Science*, 95(6), 1342-1353.
- Abdelgawad, A. M., Hudson, S. M., & Rojas, O. J. (2014). Antimicrobial wound dressing nanofiber mats from multicomponent (chitosan/silver-NPs/polyvinyl alcohol) systems. *Carbohydrate Polymers*, 100, 166-178.
- Agrawal, I. L., & Awadhia, A. (2004). DSC and conductivity studies on PVA based proton conducting gel electrolytes. *Bulletin of Materials Science*, 27(6), 523-527.
- Ahmad, A., Isa, K. B. M., & Osman, Z. (2011). Conductivity and structural studies of plasticized polyacrylonitrile (PAN)-lithium triflate polymer electrolyte films. *Sains Malaysiana*, 40(7), 691-694.
- Ahmad, N., & Isa, M. (2016). Characterization of un-plasticized and propylene carbonate plasticized carboxymethyl cellulose doped ammonium chloride solid biopolymer electrolytes. *Carbohydrate polymers*, 137, 426-432.
- Ahmad, N. H., & Isa, M. I. N. (2015a). Conduction mechanism of solid biopolymer electrolytes system based on carboxymethyl cellulose--ammonium chloride. *American-Eurasian Journal of Sustainable Agriculture*, 9, 1-7.
- Ahmad, N. H., & Isa, M. I. N. (2015). Proton conducting solid polymer electrolytes based carboxymethyl cellulose doped ammonium chloride: ionic conductivity and transport studies. *International Journal of Plastics Technology*, 19(1), 47-55.
- Ahmad, N. H., & Isa, M. I. N. (2015b). Structural and Ionic Conductivity Studies of CMC Based Polymerelectrolyte Doped with NH_4Cl . Paper presented at the Advanced Materials Research.
- Ahmad, N. H., & Isa, M. I. N. (2016). Characterization of un-plasticized and propylene carbonate plasticized carboxymethyl cellulose doped ammonium chloride solid biopolymer electrolytes. *Carbohydrate Polymers*, 137, 426-432.
- Ahmad, N. H., & Isa, M. I. N. M. (2015). Conduction mechanism of solid biopolymer electrolytes system based on carboxymethyl cellulose--ammonium chloride. *American-Eurasian Journal of Sustainable Agriculture*, 1-8.

- Ahmad, N. H. B., & Isa, M. I. N. B. M. (2015). Proton conducting solid polymer electrolytes based carboxymethyl cellulose doped ammonium chloride: ionic conductivity and transport studies. *International Journal of Plastics Technology*, 19(1), 47-55.
- Ahmad, Z., & Isa, M. I. N. (2012). Ionics conduction via correlated barrier hopping mechanism in CMC-SA solid biopolymer electrolytes. *International Journal of Latest Research in Science and Technology* 1(2), 2278-5299.
- Aishova, A., Mentbayeva, A., Isakhov, B., Batyrbekuly, D., Zhang, Y., & Bakenov, Z. (2018). Gel polymer electrolytes for lithium-sulfur batteries. *Materials Today: Proceedings*, 5(11), 22882-22888.
- Albdiry, M., & Yousif, B. (2013). Morphological structures and tribological performance of unsaturated polyester based untreated/silane-treated halloysite nanotubes. *Materials & Design*.
- Alexandre, S. A., Silva, G. G., Santamaría, R., Trigueiro, J. P. C., & Lavall, R. L. (2019). A highly adhesive PIL/IL gel polymer electrolyte for use in flexible solid state supercapacitors. *Electrochimica Acta*, 299, 789-799.
- Alves, R., Sentanin, F., Sabadini, R. C., Pawlicka, A., & Silva, M. M. (2017). Innovative electrolytes based on chitosan and thulium for solid state applications: synthesis, structural, and thermal characterization. *Journal of Electroanalytical Chemistry*, 788, 156-164.
- Ambika, C., Karuppasamy, K., Vikraman, D., Lee, J. Y., Regu, T., Raj, T. A. B., . . . Kim, H.-S. (2018). Effect of dimethyl carbonate (DMC) on the electrochemical and cycling properties of solid polymer electrolytes (PVP-MSA) and its application for proton batteries. *Solid State Ionics*, 321, 106-114.
- Anjali, T. (2012). Modification of carboxymethyl cellulose through oxidation. *Carbohydrate Polymers*, 87(1), 457-460.
- Appetecchi, G., Croce, F., Gerace, F., Panero, S., Passerini, S., Spila, E., & Scrosati, B. (1994). New concepts in primary and rechargeable solid state lithium polymer batteries. *MRS Online Proceedings Library Archive*, 369.
- Appetecchi, G. B., Croce, F., Persi, L., Ronci, F., & Scrosati, B. (2000). Transport and interfacial properties of composite polymer electrolytes. *Electrochimica Acta*, 45(8-9), 1481-1490.
- Armand, M., Endres, F., MacFarlane, D. R., Ohno, H., & Scrosati, B. (2011). Ionic-liquid materials for the electrochemical challenges of the future. In *Materials For Sustainable Energy: A Collection of Peer-Reviewed Research and Review Articles from Nature Publishing Group* (pp. 129-137): World Scientific.
- Armstrong, R. D., Dickinson, T., & Willis, P. M. (1974). The AC impedance of powdered and sintered solid ionic conductors. *Journal of electroanalytical Chemistry and interfacial electrochemistry*, 53(3), 389-405.

- Arof, A., Amirudin, S., Yusof, S., & Noor, I. (2014). A method based on impedance spectroscopy to determine transport properties of polymer electrolytes. *Physical Chemistry Chemical Physics*, 16(5), 1856-1867.
- Arof, A. K., Amirudin, S., Yusof, S. Z., & Noor, I. M. (2014). A method based on impedance spectroscopy to determine transport properties of polymer electrolytes. *Physical Chemistry Chemical Physics*, 16(5), 1856-1867.
- Arof, A. K., Kufian, M. Z., Syukur, M. F., Aziz, M. F., Abdelrahman, A. E., & Majid, S. R. (2012). Electrical double layer capacitor using poly (methyl methacrylate)–C₄BO₈Li gel polymer electrolyte and carbonaceous material from shells of mata kucing (*Dimocarpus longan*) fruit. *Electrochimica Acta*, 74, 39-45.
- Arora, N., Singh, S., Kumar, R., Kumar, R., & Kumari, A. (2018). Ionic conductivity, SEM, TGA and rheological studies of Nano-dispersed silica based polymer gel electrolytes containing LiBF₄. *Solid State Ionics*, 317, 175-182.
- Aziz, N. A. N., Idris, N. K., & Isa, M. I. N. (2010). Proton conducting polymer electrolytes of methylcellulose doped ammonium fluoride: Conductivity and ionic transport studies. *International Journal of Physical Sciences*, 5(6), 748-752.
- Aziz, S. B., Abidin, Z. H. Z., & Arof, A. K. (2010). Effect of silver nanoparticles on the DC conductivity in chitosan–silver triflate polymer electrolyte. *Physica B: Condensed Matter*, 405(21), 4429-4433.
- Aziz, S. B., Abidin, Z. H. Z., & Arof, A. K. (2010). Influence of silver ion reduction on electrical modulus parameters of solid polymer electrolyte based on chitosan-silver triflate electrolyte membrane. *Express Polym. Lett*, 5, 300-310.
- Aziz, S. B., Hamsan, M. H., Abdullah, R. M., & Kadir, M. F. Z. (2019). A Promising Polymer Blend Electrolytes Based on Chitosan: Methyl Cellulose for EDLC Application with High Specific Capacitance and Energy Density. *Molecules*, 24(13), 2503.
- Aziz, S. B., Hamsan, M. H., Kadir, M. F. Z., Karim, W. O., & Abdullah, R. M. (2019). Development of polymer blend electrolyte membranes based on chitosan: dextran with high ion transport properties for EDLC application. *International journal of molecular sciences*, 20(13), 3369.
- Azlan, A. L., & Isa, M. I. N. (2011). Proton conducting biopolymer electrolytes based on tapioca starch-NH₄NO₃. *Solid State Science and Technology Letters*, 18(1), 124-129.
- Badr, S., Sheha, E., Bayomi, R. M., & El-Shaarawy, M. G. (2010). Structural and electrical properties of pure and H₂SO₄ doped (PVA) 0.7 (NaI) 0.3 solid polymer electrolyte. *Ionics*, 16(3), 269-275.
- Bakar, N. Y. A., Muhamaruesa, N. H. M., Aniskari, N. A. B., & Isa, M. I. N. M. (2015). Electrical studies of carboxy methylcellulose-chitosan blend biopolymer doped dodecyltrimethyl ammonium bromide solid electrolytes. *American Journal of Applied Sciences*, 12(1), 40.

- Bandara, T. M. W. J., Dissanayake, M. A. K. L., Albinsson, I., & Mellander, B.-E. (2011). Mobile charge carrier concentration and mobility of a polymer electrolyte containing PEO and $\text{Pr}_4\text{N}^+ \text{I}^-$ using electrical and dielectric measurements. *Solid State Ionics*, 189(1), 63-68.
- Bao, J., Qu, X., Qi, G., Huang, Q., Wu, S., Tao, C., . . . Chen, C. (2018). Solid electrolyte based on waterborne polyurethane and poly (ethylene oxide) blend polymer for all-solid-state lithium ion batteries. *Solid State Ionics*, 320, 55-63.
- Barsoukov, E., & Macdonald, J. R. (2018). *Impedance spectroscopy: theory, experiment, and applications*: John Wiley & Sons.
- Baskaran, R., Selvasekarapandian, S., Hirankumar, G., & Bhuvaneshwari, M. S. (2004). Vibrational, ac impedance and dielectric spectroscopic studies of poly (vinylacetate)-N, N-dimethylformamide-LiClO₄ polymer gel electrolytes. *Journal of Power sources*, 134(2), 235-240.
- Baskaran, R., Selvasekarapandian, S., Kuwata, N., Kawamura, J., & Hattori, T. (2006). Conductivity and thermal studies of blend polymer electrolytes based on PVAc-PMMA. *Solid State Ionics*, 177(26-32), 2679-2682.
- Beck, F., Dolata, M., Grivei, E., & Probst, N. (2001). Electrochemical supercapacitors based on industrial carbon blacks in aqueous H₂SO₄. *Journal of Applied Electrochemistry*, 31(8), 845-853.
- Bertuzzi, M. A., Vidaurre, E. F. C., Armada, M., & Gottifredi, J. C. (2007). Water vapor permeability of edible starch based films. *Journal of Food Engineering*, 80(3), 972-978.
- Bhargav, P. B., Mohan, V. M., Sharma, A. K., & Rao, V. V. R. N. (2009). Investigations on electrical properties of (PVA: NaF) polymer electrolytes for electrochemical cell applications. *Current Applied Physics*, 9(1), 165-171.
- Bhide, A., & Hariharan, K. (2007). Ionic transport studies on (PEO)₆: NaPO₃ polymer electrolyte plasticized with PEG400. *European Polymer Journal*, 43(10), 4253-4270.
- Biswal, D., & Singh, R. (2004). Characterisation of carboxymethyl cellulose and polyacrylamide graft copolymer. *Carbohydrate polymers*, 57(4), 379-387.
- Böckenfeld, N., Jeong, S. S., Winter, M., Passerini, S., & Balducci, A. (2013). Natural, cheap and environmentally friendly binder for supercapacitors. *Journal of Power Sources*, 221, 14-20.
- Brandt, A., & Balducci, A. (2014). Theoretical and practical energy limitations of organic and ionic liquid-based electrolytes for high voltage electrochemical double layer capacitors. *Journal of Power Sources*, 250, 343-351.
- Brown, M. E. (2001). *Introduction to thermal analysis: techniques and applications (Vol. 1)*: Springer Science & Business Media.

- Brownson, D. A., Kampouris, D. K., & Banks, C. E. (2012). Graphene electrochemistry: fundamental concepts through to prominent applications. *Chemical Society Reviews*, 41(21), 6944-6976.
- Brownson, D. A. C., Kampouris, D. K., & Banks, C. E. (2011). An overview of graphene in energy production and storage applications. *Journal of Power Sources*, 196(11), 4873-4885.
- Buraidah, M., & Arof, A. (2011). Characterization of chitosan/PVA blended electrolyte doped with NH₄I. *Journal of Non-Crystalline Solids*, 357(16), 3261-3266.
- Buraidah, M. H., & Arof, A. K. (2011). Characterization of chitosan/PVA blended electrolyte doped with NH₄I. *Journal of Non-Crystalline Solids*, 357(16-17), 3261-3266.
- Buraidah, M. H., Teo, L. P., Majid, S. R., & Arof, A. K. (2009). Ionic conductivity by correlated barrier hopping in NH₄I doped chitosan solid electrolyte. *Physica B: Condensed Matter*, 404(8-11), 1373-1379.
- Burke, A. (2000). Ultracapacitors: why, how, and where is the technology. *Journal of power sources*, 91(1), 37-50.
- Chai, M. N., & Isa, M. I. N. (2011). Carboxyl methylcellulose solid polymer electrolytes: Ionic conductivity and dielectric study. *J. Curr. Eng. Res*, 1(2), 23-27.
- Chai, M. N., & Isa, M. I. N. (2012). Investigation on the conduction mechanism of carboxyl methylcellulose-oleic acid natural solid polymer electrolyte. *International Journal of Advanced Technology & Engineering Research*, 2(6), 36-39.
- Chai, M. N., & Isa, M. I. N. (2013a). Electrical characterization and ionic transport properties of carboxyl methylcellulose-oleic acid solid polymer electrolytes. *International Journal of Polymer Analysis and Characterization*, 18(4), 280-286.
- Chai, M. N., & Isa, M. I. N. (2013b). The oleic acid composition effect on the carboxymethyl cellulose based biopolymer electrolyte. *Journal of Crystallization Process and Technology*, 3(01), 1.
- Chai, M. N., & Isa, M. I. N. (2016). Novel proton conducting solid bio-polymer electrolytes based on carboxymethyl cellulose doped with oleic acid and plasticized with glycerol. *Scientific reports*, 6, 27328.
- Chen, J., Asano, M., Maekawa, Y., & Yoshida, M. (2008). Fuel cell performance of polyetheretherketone-based polymer electrolyte membranes prepared by a two-step grafting method. *Journal of Membrane Science*, 319(1-2), 1-4.
- Chen, W., Beidaghi, M., Penmatsa, V., Bechtold, K., Kumari, L., Li, W., & Wang, C. (2010). Integration of carbon nanotubes to C-MEMS for on-chip supercapacitors. *IEEE Transactions on Nanotechnology*, 9(6), 734-740.

- Chen, W., Fan, Z., Gu, L., Bao, X., & Wang, C. (2010). Enhanced capacitance of manganese oxide via confinement inside carbon nanotubes. *Chemical Communications*, 46(22), 3905-3907.
- Chew, K. W., Ng, T. C., & How, Z. H. (2013). Conductivity and microstructure study of PLA-based polymer electrolyte salted with lithium perchlorate, LiClO₄. *Int J Electrochem Sci*, 8(5).
- Chilikov, D., & Protophristov, C. (2008). Electrochemical properties of the Kazichene treasure. Paper presented at the Proceedings of the International Conference.
- Choudhary, S., & Sengwa, R. J. (2013). Effects of preparation methods on structure, ionic conductivity and dielectric relaxation of solid polymeric electrolytes. *Materials Chemistry and Physics*, 142(1), 172-181.
- Choudhury, N. A., Sampath, S., & Shukla, A. K. (2009). Hydrogel-polymer electrolytes for electrochemical capacitors: an overview. *Energy & Environmental Science*, 2(1), 55-67.
- Chowdari, B. V. R., & Gopalakrishnan, R. (1987). AC conductivity analysis of glassy silver iodomolybdate system. *Solid State Ionics*, 23(3), 225-233.
- Coats, A. W., & Redfern, J. P. (1963). Thermogravimetric analysis. A review. *Analyst*, 88(1053), 906-924.
- Connes, P. (1984). Early history of Fourier transform spectroscopy. *Infrared Physics*, 24(2-3), 69-93.
- Croce, F., Persi, L., Scrosati, B., Serraino-Fiory, F., Plichta, E., & Hendrickson, M. A. (2001). Role of the ceramic fillers in enhancing the transport properties of composite polymer electrolytes. *Electrochimica Acta*, 46(16), 2457-2461.
- Cuba-Chiem, L. T., Huynh, L., Ralston, J., & Beattie, D. A. (2008). In situ particle film ATR-FTIR studies of CMC adsorption on talc: The effect of ionic strength and multivalent metal ions. *Minerals Engineering*, 21(12-14), 1013-1019.
- Das, S. K., Mandal, S. S., & Bhattacharyya, A. J. (2011). Ionic conductivity, mechanical strength and Li-ion battery performance of mono-functional and bi-functional ("Janus") "soggy sand" electrolytes. *Energy & Environmental Science*, 4(4), 1391-1399.
- Debeaufort, F., Voilley, A., & Meares, P. (1994). Water vapor permeability and diffusivity through methylcellulose edible films. *Journal of Membrane Science*, 91(1-2), 125-133.
- Deka, M., & Kumar, A. (2011). Electrical and electrochemical studies of poly (vinylidene fluoride)-clay nanocomposite gel polymer electrolytes for Li-ion batteries. *Journal of Power Sources*, 196(3), 1358-1364.
- DeMerlis, C. C., & Schoneker, D. R. (2003). Review of the oral toxicity of polyvinyl alcohol (PVA). *Food and Chemical Toxicology*, 41(3), 319-326.

- Deraman, S. K., Mohamed, N. S., & Subban, R. H. Y. (2014). Ionic liquid incorporated PVC based polymer electrolytes: electrical and dielectric properties. *Sains Malaysiana*, 43(6), 877-883.
- Deraman, S. K., Subban, R. H. Y., & Nor Sabirin, M. (2012). Ionic conductivity of PVC-NH₄I-EC proton conducting polymer electrolytes. Paper presented at the Advanced Materials Research.
- Du, F., Fischer, J. E., & Winey, K. I. (2003). Coagulation method for preparing single-walled carbon nanotube/poly (methyl methacrylate) composites and their modulus, electrical conductivity, and thermal stability. *Journal of Polymer Science Part B: Polymer Physics*, 41(24), 3333-3338.
- Du, J. F., Bai, Y., Chu, W. Y., & Qiao, L. J. (2010). Synthesis and performance of proton conducting chitosan/NH₄Cl electrolyte. *Journal of Polymer Science Part B: Polymer Physics*, 48(3), 260-266.
- Du, J. F., Bai, Y., Pan, D. A., Chu, W. Y., & Qiao, L. J. (2009). Characteristics of proton conducting polymer electrolyte based on chitosan acetate complexed with CH₃COONH₄. *Journal of Polymer Science Part B: Polymer Physics*, 47(6), 549-554.
- El-Gamal, S., El Sayed, A. M., & Abdel-Hady, E. E. (2017). Effect of Cobalt Oxide Nanoparticles on the Nano-scale Free Volume and Optical Properties of Biodegradable CMC/PVA Films. *Journal of Polymers and the Environment*, 26(6), 2536-2545.
- El-Kader, F. H. A., Gaafar, S. A., Mahmoud, K. H., Bannan, S. I., & El-Kader, M. F. H. A. (2008). Effects of the Composition Ratio, Eosin Addition, and γ Irradiation on the Dielectric Properties of Poly (vinyl Alcohol)/Glycogen Blends. *Journal of Applied Polymer Science*, 110(3), 1281-1288.
- El-Sawy, N. M., El-Arnaouty, M. B., & Ghaffar, A. M. A. (2010). γ -Irradiation effect on the non-cross-linked and cross-linked polyvinyl alcohol films. *Polymer-Plastics Technology and Engineering*, 49(2), 169-177.
- El-Sayed, S., Mahmoud, K. H., Fatah, A. A., & Hassen, A. D. S. C. (2011). DSC, TGA and dielectric properties of carboxymethyl cellulose/polyvinyl alcohol blends. *Physica B: Condensed Matter*, 406(21), 4068-4076.
- Evans, J., Vincent, C. A., & Bruce, P. G. (1987). Electrochemical measurement of transference numbers in polymer electrolytes. *Polymer*, 28(13), 2324-2328.
- Fadzallah, I., Noor, I., Careem, M., & Arof, A. (2016). Investigation of transport properties of chitosan-based electrolytes utilizing impedance spectroscopy. *Ionics*, 22(9), 1635-1645.
- Faraji, M., & Abedini, A. (2019). Fabrication of electrochemically interconnected MoO₃/GO/MWCNTs/graphite sheets for high performance all-solid-state symmetric supercapacitor. *International Journal of Hydrogen Energy*, 44(5), 2741-2751.

- Fenton, D. E. (1973). Complexes of alkali metal ions with poly (ethylene oxide). *Polymer*, 14, 589.
- Fergus, J. W. (2010). Ceramic and polymeric solid electrolytes for lithium-ion batteries. *Journal of Power Sources*, 195(15), 4554-4569.
- Feuillade, G., & Perche, P. h. (1975). Ion-conductive macromolecular gels and membranes for solid lithium cells. *Journal of Applied Electrochemistry*, 5(1), 63-69.
- Fonseca, C. P., Rosa, D. S., Gaboardi, F., & Neves, S. (2006). Development of a biodegradable polymer electrolyte for rechargeable batteries. *Journal of power sources*, 155(2), 381-384.
- Gaaz, T., Sulong, A., Akhtar, M., Kadhun, A., Mohamad, A., & Al-Amiery, A. (2015). Properties and applications of polyvinyl alcohol, halloysite nanotubes and their nanocomposites. *Molecules*, 20(12), 22833-22847.
- Gale, E., Wirawan, R. H., Silveira, R. L., Pereira, C. S., Johns, M. A., Skaf, M. S., & Scott, J. L. (2016). Directed discovery of greener cosolvents: New cosolvents for use in ionic liquid based organic electrolyte solutions for cellulose dissolution. *ACS Sustainable Chemistry & Engineering*, 4(11), 6200-6207.
- Geiculescu, O. E., Rajagopal, R., Creager, S. E., DesMarteau, D. D., Zhang, X., & Fedkiw, P. (2006). Transport properties of solid polymer electrolytes prepared from oligomeric fluorosulfonimide lithium salts dissolved in high molecular weight poly (ethylene oxide). *The Journal of Physical Chemistry B*, 110(46), 23130-23135.
- Genova, F. K. M., Selvasekarapandian, S., Karthikeyan, S., Vijaya, N., Pradeepa, R., & Sivadevi, S. (2015). Study on blend polymer (PVA-PAN) doped with lithium bromide. *Polymer Science Series A*, 57(6), 851-862.
- Greatbatch, W., & Holmes, C. F. (1991). History of implantable devices. *IEEE Engineering in Medicine and Biology Magazine*, 10(3), 38-41.
- Gu, H.-B., Kim, J.-U., Song, H.-W., Park, G.-C., & Park, B.-K. (2000). Electrochemical properties of carbon composite electrode with polymer electrolyte for electric double-layer capacitor. *Electrochimica Acta*, 45(8-9), 1533-1536.
- Guirguis, O. W., & Moselhey, M. T. (2012a). Thermal and structural studies of poly (vinyl alcohol) and hydroxypropyl cellulose blends. *Natural Science*, 4(1), 57.
- Guirguis, O. W., & Moselhey, M. T. H. (2012b). Thermal and structural studies of poly (vinyl alcohol) and hydroxypropyl cellulose blends. *Natural Science*, 4(1), 57.
- Guo, F., Gupta, N., & Teng, X. (2018). Enhancing Pseudocapacitive Process for Energy Storage Devices: Analyzing the Charge Transport Using Electro-kinetic Study and Numerical Modeling. *Supercapacitors: Theoretical and Practical Solutions*, 87.

- Hafiza, M. N., Bashirah, A. N. A., Bakar, N. Y., & Isa, M. I. N. (2014). Electrical properties of carboxyl methylcellulose/chitosan dual-blend green polymer doped with ammonium bromide. *International Journal of Polymer Analysis and Characterization*, 19(2), 151-158.
- Hafiza, M. N., & Isa, M. I. N. (2014). Ionic conductivity and conduction mechanism studies of CMC/chitosan biopolymer blend electrolytes. *Research Journal of Recent Sciences* 2277, 2502.
- Hafiza, M. N., Muhamaruesa, M. R., & Isa, M. I. N. (2017). Transport studies of carboxymethyl cellulose/chitosan-ammonium bromide biopolymer blend electrolytes as an ionic conductor. *Journal of Sustainability Science and Management Special Issue Number 2: Fundamental Interdisciplinary Pathways To Future Sustainability*, 2, 58-64.
- Hamsan, M. H., Shukur, M. F., & Kadir, M. F. Z. (2017a). The effect of NH_4NO_3 towards the conductivity enhancement and electrical behavior in methyl cellulose-starch blend based ionic conductors. *Ionics*, 23(5), 1137-1154.
- Hamsan, M. H., Shukur, M. F., & Kadir, M. F. Z. (2017b). NH_4NO_3 as charge carrier contributor in glycerolized potato starch-methyl cellulose blend-based polymer electrolyte and the application in electrochemical double-layer capacitor. *Ionics*, 23(12), 3429-3453.
- Han, D. G., & Choi, G. M. (1998). Computer simulation of the electrical conductivity of composites: the effect of geometrical arrangement. *Solid State Ionics*, 106(1-2), 71-87.
- Hashmi, S. A., Kumar, A., Maurya, K. K., & Chandra, S. (1990). Proton-conducting polymer electrolyte. I. The polyethylene oxide+ NH_4ClO_4 system. *Journal of Physics D: Applied Physics*, 23(10), 1307.
- Hashmi, S. A., Kumar, A., & Tripathi, S. K. (2007). Experimental studies on poly methyl methacrylate based gel polymer electrolytes for application in electrical double layer capacitors. *Journal of Physics D: Applied Physics*, 40(21), 6527.
- Hashmi, S. A., Latham, R. J., Linford, R. G., & Schlindwein, W. S. (1997). Studies on all solid state electric double layer capacitors using proton and lithium ion conducting polymer electrolytes. *Journal of the Chemical Society, Faraday Transactions*, 93(23), 4177-4182.
- Hatta, F. F., Kudin, T. I. T., Subban, R. H. Y., Ali, A. M. M., Harun, M. K., & Yahya, M. Z. A. (2009). Plasticized PVA/PVP-KOH alkaline solid polymer blend electrolyte for electrochemical cells. *Functional Materials Letters*, 2(03), 121-125.
- Hema, M., Selvasekarapandian, S., Arunkumar, D., Sakunthala, A., & Nithya, H. F. T. I. R. (2009). FTIR, XRD and ac impedance spectroscopic study on PVA based polymer electrolyte doped with NH_4X (X= Cl, Br, I). *Journal of Non-Crystalline Solids*, 355(2), 84-90.

- Hema, M., Selvasekarapandian, S., Nithya, H., Sakunthala, A., & Arunkumar, D. (2009). Structural and ionic conductivity studies on proton conducting polymer electrolyte based on polyvinyl alcohol. *Ionics*, 15(4), 487-491.
- Hema, M., Selvasekerapandian, S., & Hirankumar, G. (2007). Vibrational and impedance spectroscopic analysis of poly (vinyl alcohol)-based solid polymer electrolytes. *Ionics*, 13(6), 483-487.
- Hema, M., Selvasekerapandian, S., Hirankumar, G., Sakunthala, A., Arunkumar, D., & Nithya, H. (2009). Structural and thermal studies of PVA: NH₄I. *Journal of Physics and Chemistry of Solids*, 70(7), 1098-1103.
- Hema, M., Selvasekerapandian, S., Sakunthala, A., Arunkumar, D., & Nithya, H. (2008). Structural, vibrational and electrical characterization of PVA–NH₄Br polymer electrolyte system. *Physica B: Condensed Matter*, 403(17), 2740-2747.
- Hirankumar, G., Selvasekarapandian, S., Kuwata, N., Kawamura, J., & Hattori, T. (2005). Thermal, electrical and optical studies on the poly (vinyl alcohol) based polymer electrolytes. *Journal of Power Sources*, 144(1), 262-267.
- Hodge, R. M., Edward, G. H., & Simon, G. P. (1996). Water absorption and states of water in semicrystalline poly (vinyl alcohol) films. *Polymer*, 37(8), 1371-1376.
- Holbrook, D., Cohen, W. M., Hounshell, D. A., & Klepper, S. (2000). The nature, sources, and consequences of firm differences in the early history of the semiconductor industry. *Strategic Management Journal*, 21(10-11), 1017-1041.
- Hu, X., Muchakayala, R., Song, S., Wang, J., Chen, J., & Tan, M. (2018). Synthesis and optimization of new polymeric ionic liquid poly (diallyldimethylammonium) bis (trifluoromethane sulfonyl) imide based gel electrolyte films. *International Journal of Hydrogen Energy*, 43(7), 3741-3749.
- Huang, X., Qi, X., Boey, F., & Zhang, H. (2012). Graphene-based composites. *Chemical Society Reviews*, 41(2), 666-686.
- Huang, Y., Huang, Y., Liu, B., Cao, H., Zhao, L., Song, A., . . . Zhang, Z. (2018). Gel polymer electrolyte based on p (acrylonitrile-maleic anhydride) for lithium ion battery. *Electrochimica Acta*, 286, 242-251.
- Hwang, B. J., Santhanam, R., & Liu, D. G. (2001). Effect of various synthetic parameters on purity of LiMn₂O₄ spinel synthesized by a sol–gel method at low temperature. *Journal of Power Sources*, 101(1), 86-89.
- Ibrahim, A. A., Adel, A. M., El–Wahab, Z. H. A., & Al–Shemy, M. T. (2011). Utilization of carboxymethyl cellulose based on bean hulls as chelating agent. Synthesis, characterization and biological activity. *Carbohydrate Polymers*, 83(1), 94-115.
- Idris, N. K., Aziz, N. A. N., Zambri, M. S. M., Zakaria, N. A., & Isa, M. I. N. (2009). Ionic conductivity studies of chitosan-based polymer electrolytes doped with adipic acid. *Ionics*, 15(5), 643-646.

- Islam, S. M. M., Reza, M. A. R., & Kiber, M. A. (2013). Development of multi-frequency electrical impedance spectroscopy (EIS) system for early detection of breast cancer. *Int. J. Electron. Inform*, 2(1), 26-32.
- Iwamoto, R., Miya, M., & Mima, S. (1979). Determination of crystallinity of swollen poly (vinyl alcohol) by laser Raman spectroscopy. *Journal of Polymer Science: Polymer Physics Edition*, 17(9), 1507-1515.
- Jinisha, B., Femy, A. F., Ashima, M. S., & Jayalekshmi, S. (2018). Polyethylene oxide (PEO)/polyvinyl alcohol (PVA) complexed with lithium perchlorate (LiClO₄) as a prospective material for making solid polymer electrolyte films. *Materials Today: Proceedings*, 5(10), 21189-21194.
- Johan, M. R., & Ibrahim, S. (2012). Optimization of neural network for ionic conductivity of nanocomposite solid polymer electrolyte system (PEO–LiPF₆–EC–CNT). *Communications in Nonlinear Science and Numerical Simulation*, 17(1), 329-340.
- Johari, N. A., Kudin, T. I. T., Ali, A. M. M., Winie, T., & Yahya, M. Z. A. (2009). Studies on cellulose acetate-based gel polymer electrolytes for proton batteries. *Materials Research Innovations*, 13(3), 232-234.
- Kadir, M., Majid, S., & Arof, A. (2010). Plasticized chitosan–PVA blend polymer electrolyte based proton battery. *Electrochimica Acta*, 55(4), 1475-1482.
- Kadir, M. F. Z., & Arof, A. K. (2011). Application of PVA–chitosan blend polymer electrolyte membrane in electrical double layer capacitor. *Materials Research Innovations*, 15(sup2), 217-220.
- Kadir, M. F. Z., Aspanut, Z., Majid, S. R., & Arof, A. K. (2011). FTIR studies of plasticized poly (vinyl alcohol)–chitosan blend doped with NH₄NO₃ polymer electrolyte membrane. *Spectrochimica Acta Part A: Molecular and Biomolecular Spectroscopy*, 78(3), 1068-1074.
- Kadir, M. F. Z., Majid, S. R., & Arof, A. K. (2010). Plasticized chitosan–PVA blend polymer electrolyte based proton battery. *Electrochimica Acta*, 55(4), 1475-1482.
- Kadir, M. F. Z., Salleh, N. S., Hamsan, M. H., Aspanut, Z., Majid, N. A., & Shukur, M. F. (2018). Biopolymeric electrolyte based on glycerolized methyl cellulose with NH₄Br as proton source and potential application in EDLC. *Ionics*, 24(6), 1651-1662.
- Kamarudin, K. H., & Isa, M. I. N. (2013). Structural and DC Ionic conductivity studies of carboxy methylcellulose doped with ammonium nitrate as solid polymer electrolytes. *International Journal of Physical Sciences*, 8(31), 1581-1587.
- Khanmirzaei, M. H., Ramesh, S., & Ramesh, K. (2015). Polymer electrolyte based dye-sensitized solar cell with rice starch and 1-methyl-3-propylimidazolium iodide ionic liquid. *Materials & Design*, 85, 833-837.
- Khiar, A. S. A., & Arof, A. K. (2010). Conductivity studies of starch-based polymer electrolytes. *Ionics*, 16(2), 123-129.

- Khiar, A. S. A., & Arof, A. K. (2011). Electrical properties of starch/chitosan-NH₄NO₃ polymer electrolyte. *WASET*, 59, 23-27.
- Khiar, A. S. A., Puteh, R., & Arof, A. K. (2006). Conductivity studies of a chitosan-based polymer electrolyte. *Physica B: Condensed Matter*, 373(1), 23-27.
- Kibi, Y., Saito, T., Kurata, M., Tabuchi, J., & Ochi, A. (1996). Fabrication of high-power electric double-layer capacitors. *Journal of Power Sources*, 60(2), 219-224.
- Kim, H.-S., Kum, K.-S., Cho, W.-I., Cho, B.-W., & Rhee, H.-W. (2003). Electrochemical and physical properties of composite polymer electrolyte of poly (methyl methacrylate) and poly (ethylene glycol diacrylate). *Journal of Power Sources*, 124(1), 221-224.
- Kim, J.-K., Cheruvally, G., Li, X., Ahn, J.-H., Kim, K.-W., & Ahn, H.-J. (2008). Preparation and electrochemical characterization of electrospun, microporous membrane-based composite polymer electrolytes for lithium batteries. *Journal of Power Sources*, 178(2), 815-820.
- Klug, H. P., & Alexander, L. E. (1974). X-ray diffraction procedures: for polycrystalline and amorphous materials. *X-Ray Diffraction Procedures: For Polycrystalline and Amorphous Materials*, 2nd Edition, by Harold P. Klug, Leroy E. Alexander, pp. 992. ISBN 0-471-49369-4. Wiley-VCH, May 1974., 992.
- Koduru, H. K., Marinov, Y. G., Hadjichristov, G. B., & Scaramuzza, N. (2019). Characterization of polymer/liquid crystal composite based electrolyte membranes for sodium ion battery applications. *Solid State Ionics*, 335, 86-96.
- Koh, M. H. (2013). Preparation and characterization of carboxymethyl cellulose from sugarcane bagasse. UTAR,
- Koksbang, R., & Skou, E. (1995). Transference number measurements on a hybrid polymer electrolyte. *Electrochimica Acta*, 40(11), 1701-1706.
- Kopitzke, R. W., Linkous, C. A., Anderson, H. R., & Nelson, G. L. (2000). Conductivity and water uptake of aromatic-based proton exchange membrane electrolytes. *Journal of the Electrochemical Society*, 147(5), 1677-1681.
- Krimm, S., Liang, C., & Sutherland, G. (1956). Infrared spectra of high polymers. V. Polyvinyl alcohol. *Journal of Polymer Science Part A: Polymer Chemistry*, 22(101), 227-247.
- Kumar, M., Tiwari, T., & Srivastava, N. (2012). Electrical transport behaviour of bio-polymer electrolyte system: Potato starch+ ammonium iodide. *Carbohydrate Polymers*, 88(1), 54-60.
- Kumar, P. S., Sakunthala, A., Reddy, M. V., & Prabu, M. (2018). Structural, morphological, electrical and electrochemical study on plasticized PVdF-HFP/PEMA blended polymer electrolyte for lithium polymer battery application. *Solid State Ionics*, 319, 256-265.

- Kumar, R., Sharma, S., Pathak, D., Dhiman, N., & Arora, N. (2017). Ionic conductivity, FTIR and thermal studies of nano-composite plasticized proton conducting polymer electrolytes. *Solid State Ionics*, 305, 57-62.
- Kumar, Y., Hashmi, S. A., & Pandey, G. P. (2011). Ionic liquid mediated magnesium ion conduction in poly (ethylene oxide) based polymer electrolyte. *Electrochimica Acta*, 56(11), 3864-3873.
- Kuppu, S. V., Jeyaraman, A. R., Guruviah, P. K., & Thambusamy, S. (2018). Preparation and characterizations of PMMA-PVDF based polymer composite electrolyte materials for dye sensitized solar cell. *Current Applied Physics*, 18(6), 619-625.
- Kuutti, L., Haavisto, S., Hyvarinen, S., Mikkonen, H., Koski, R., Peltonen, S., . . . Kyllönen, H. (2011). Properties and flocculation efficiency of cationized biopolymers and their applicability in papermaking and in conditioning of pulp and paper sludge. *BioResources*, 6(3), 2836-2850.
- Lakshmi, N., & Chandra, S. (2002). Rechargeable solid-state battery using a proton-conducting composite as electrolyte. *Journal of power sources*, 108(1-2), 256-260.
- Lee, S. S., Lim, Y. J., Kim, H. W., Kim, J.-K., Jung, Y.-G., & Kim, Y. (2016). Electrochemical properties of a ceramic-polymer-composite-solid electrolyte for Li-ion batteries. *Solid State Ionics*, 284, 20-24.
- Lewandowska, K. (2009). Miscibility and thermal stability of poly (vinyl alcohol)/chitosan mixtures. *Thermochimica Acta*, 493(1-2), 42-48.
- Liew, C.-W., & Ramesh, S. (2015). Electrical, structural, thermal and electrochemical properties of corn starch-based biopolymer electrolytes. *Carbohydrate Polymers*, 124, 222-228.
- Liew, C.-W., Ramesh, S., & Arof, A. K. (2014a). Good prospect of ionic liquid based-poly (vinyl alcohol) polymer electrolytes for supercapacitors with excellent electrical, electrochemical and thermal properties. *International Journal of Hydrogen Energy*, 39(6), 2953-2963.
- Liew, C.-W., Ramesh, S., & Arof, A. K. (2014b). Investigation of ionic liquid-based poly (vinyl alcohol) proton conductor for electrochemical double-layer capacitor. *High Performance Polymers*, 26(6), 632-636.
- Liew, C.-W., Ramesh, S., & Arof, A. K. (2014c). A novel approach on ionic liquid-based poly (vinyl alcohol) proton conductive polymer electrolytes for fuel cell applications. *International Journal of Hydrogen Energy*, 39(6), 2917-2928.
- Liew, C.-W., Ramesh, S., & Arof, A. K. (2015). Characterization of ionic liquid added poly (vinyl alcohol)-based proton conducting polymer electrolytes and electrochemical studies on the supercapacitors. *International Journal of Hydrogen Energy*, 40(1), 852-862.

- Liew, C.-W., Ramesh, S., & Arof, A. K. (2016a). Enhanced capacitance of EDLCs (electrical double layer capacitors) based on ionic liquid-added polymer electrolytes. *Energy*, 109, 546-556.
- Liew, C.-W., Ramesh, S., & Arof, A. K. (2016b). Investigation of ionic liquid-doped ion conducting polymer electrolytes for carbon-based electric double layer capacitors (EDLCs). *Materials & Design*, 92, 829-835.
- Lim, C.-S., Teoh, K. H., Liew, C.-W., & Ramesh, S. (2014a). Capacitive behavior studies on electrical double layer capacitor using poly (vinyl alcohol)–lithium perchlorate based polymer electrolyte incorporated with TiO₂. *Materials Chemistry and Physics*, 143(2), 661-667.
- Lim, C.-S., Teoh, K. H., Liew, C.-W., & Ramesh, S. (2014b). Electric double layer capacitor based on activated carbon electrode and biodegradable composite polymer electrolyte. *Ionics*, 20(2), 251-258.
- Linford, R. G. (1988). *Materials for solid state batteries*. Edited by BVR Chowdari and S. Radhakrishna, World Scientific Press, Singapore (under the auspices of COSTED: Committee on Science and Technology in Developing Countries), 1986. pp. xiii+ 502, price£ 47.70. ISBN 9971-50-149-X. *Journal of Chemical Technology & Biotechnology*, 42(2), 159-160.
- Liu, J., Wu, X., He, J., Li, J., & Lai, Y. (2017). Preparation and performance of a novel gel polymer electrolyte based on poly (vinylidene fluoride)/graphene separator for lithium ion battery. *Electrochimica Acta*, 235.
- Liu, S., Imanishi, N., Zhang, T., Hirano, A., Takeda, Y., Yamamoto, O., & Yang, J. (2010). Effect of nano-silica filler in polymer electrolyte on Li dendrite formation in Li/poly (ethylene oxide)–Li (CF₃SO₂)₂N/Li. *Journal of Power Sources*, 195(19), 6847-6853.
- Liu, S., Tao, D., Bai, H., & Liu, X. (2012). Cellulose-nanowhisker-templated synthesis of titanium dioxide/cellulose nanomaterials with promising photocatalytic abilities. *Journal of Applied Polymer Science*, 126(S1), 282-290.
- Long, L., Wang, S., Xiao, M., & Meng, Y. (2016). Polymer electrolytes for lithium polymer batteries. *Journal of Materials Chemistry A*, 4(26), 10038-10069.
- Ma, X.-H., Xu, Z.-L., Liu, Y., & Sun, D. (2010). Preparation and characterization of PFSA–PVA–SiO₂/PVA/PAN difunctional hollow fiber composite membranes. *Journal of Membrane Science*, 360(1-2), 315-322.
- Ma, X., Chang, P. R., & Yu, J. (2008). Properties of biodegradable thermoplastic pea starch/carboxymethyl cellulose and pea starch/microcrystalline cellulose composites. *Carbohydrate Polymers*, 72(3), 369-375.
- Mahakul, P. C., Sa, K., Das, B., & Mahanandia, P. (2017). Structural investigation of the enhanced electrical, optical and electrochemical properties of MWCNT incorporated Poly [3-hexylthiophene-2, 5-diyl] composites. *Materials Chemistry and Physics*, 199, 477-484.

- Majid, S. R. (2007). High Molecular Weight Chitosan as Polymer Electrolyte for Electrochemical Devices. Jabatan Fizik, Fakulti Sains, Universiti Malaya,
- Majid, S. R., & Arof, A. K. (2005). Proton-conducting polymer electrolyte films based on chitosan acetate complexed with NH_4NO_3 salt. *Physica B: Condensed Matter*, 355(1-4), 78-82.
- Majid, S. R., & Arof, A. K. (2009). Conductivity studies and performance of chitosan based polymer electrolytes in H_2 /air fuel cell. *Polymers for Advanced Technologies*, 20(6), 524-528.
- Manjuladevi, R., Thamilselvan, M., Selvasekarapandian, S., Mangalam, R., Premalatha, M., & Monisha, S. (2017). Mg-ion conducting blend polymer electrolyte based on poly (vinyl alcohol)-poly (acrylonitrile) with magnesium perchlorate. *Solid State Ionics*, 308, 90-100.
- Matos, B. R., Santiago, E. I., Muccillo, R., Velasco-Davalos, I. A., Ruediger, A., Tavares, A. C., & Fonseca, F. C. (2015). Interplay between α -relaxation and morphology transition of perfluorosulfonate ionomer membranes. *Journal of Power Sources*, 293, 859-867.
- Mazuki, N., Rasali, N., Saadiah, M., & Samsudin, A. (2018). Irregularities trend in electrical conductivity of CMC/PVA- NH_4Cl based solid biopolymer electrolytes. Paper presented at the AIP Conference Proceedings.
- Mazuki, N. f., Nagao, Y., & Samsudin, A. S. (2019). Immittance Response on Carboxymethyl Cellulose Blend with Polyvinyl Alcohol-Doped Ammonium Bromide-Based Biopolymer Electrolyte. *Makara Journal Of Technology*, 22(3), 167-170.
- Mazuki, N. F., Rasali, N. M. J., Saadiah, M. A., & Samsudin, A. S. (2018). Irregularities trend in electrical conductivity of CMC/PVA- NH_4Cl based solid biopolymer electrolytes. Paper presented at the ICAMET.
- Mejenom, A. A., Hafiza, M. N., & Mohamad Isa, M. I. N. (2018). X-Ray diffraction and infrared spectroscopic analysis of solid biopolymer electrolytes based on dual blend carboxymethyl cellulose-chitosan doped with ammonium bromide. *ASM Sci. J. Special Issue*, 11, 37-46.
- Misenan, M., Isa, M., & Khiar, A. (2018). Electrical and structural studies of polymer electrolyte based on chitosan/methyl cellulose blend doped with BMIMTFSI. *Materials Research Express*, 5(5), 055304.
- Mishra, R., & Rao, K. (1998). Electrical conductivity studies of poly (ethyleneoxide)-poly (vinylalcohol) blends. *Solid State Ionics*, 106(1-2), 113-127.
- Mitra, S., Shukla, A. K., & Sampath, S. (2001). Electrochemical capacitors with plasticized gel-polymer electrolytes. *Journal of Power Sources*, 101(2), 213-218.
- Mizuno, A., Mitsuiki, M., & Motoki, M. (1998). Effect of crystallinity on the glass transition temperature of starch. *Journal of Agricultural and Food Chemistry*, 46(1), 98-103.

- Mobarak, N., Ahmad, A., Abdullah, M. P., Ramli, N., & Rahman, M. Y. A. (2013). Conductivity enhancement via chemical modification of chitosan based green polymer electrolyte. *Electrochimica Acta*, 92, 161-167.
- Mobarak, N. N., Ramli, N., Ahmad, A., & Rahman, M. Y. A. (2012). Chemical interaction and conductivity of carboxymethyl κ -carrageenan based green polymer electrolyte. *Solid State Ionics*, 224, 51-57.
- Mohamad, A. A., & Arof, A. K. (2007). Plasticized alkaline solid polymer electrolyte system. *Materials Letters*, 61(14-15), 3096-3099.
- Mohamad, A. A., Mohamed, N. S., Yahya, M. Z. A., Othman, R., Ramesh, S., Alias, Y., & Arof, A. K. (2003). Ionic conductivity studies of poly (vinyl alcohol) alkaline solid polymer electrolyte and its use in nickel–zinc cells. *Solid State Ionics*, 156(1-2), 171-177.
- Mokhtar, M., Herianto, E., Talib, M. Z. M., Ahmad, A., Tasirin, S. M., & Daud, W. (2016). A short review on alkaline solid polymer electrolyte based on polyvinyl alcohol (PVA) as polymer electrolyte for electrochemical devices applications. *International Journal of Applied Engineering Research*, 11(19), 10009-10015.
- Molak, A., Ksepko, E., Gruszka, I., Ratuszna, A., Paluch, M., & Ujma, Z. (2005). Electric permittivity and conductivity of $(\text{Na}_{0.5}\text{Pb}_{0.5})(\text{Mn}_{0.5}\text{Nb}_{0.5})\text{O}_3$ ceramics. *Solid State Ionics*, 176(15-16), 1439-1447.
- Moniha, V., Alagar, M., Selvasekarapandian, S., Sundaresan, B., & Boopathi, G. (2018). Conductive bio-polymer electrolyte iota-carrageenan with ammonium nitrate for application in electrochemical devices. *Journal of Non-Crystalline Solids*, 481, 424-434.
- Moon, R. J., Martini, A., Nairn, J., Simonsen, J., & Youngblood, J. (2011). Cellulose nanomaterials review: structure, properties and nanocomposites. *Chemical Society Reviews*, 40(7), 3941-3994.
- Na, R., Wang, X., Lu, N., Huo, G., Lin, H., & Wang, G. (2018). Novel egg white gel polymer electrolyte and a green solid-state supercapacitor derived from the egg and rice waste. *Electrochimica Acta*, 274, 316-325.
- Nadiah, N. S., Omar, F. S., Numan, A., Mahipal, Y. K., Ramesh, S., & Ramesh, K. (2017). Influence of acrylic acid on ethylene carbonate/dimethyl carbonate based liquid electrolyte and its supercapacitor application. *International Journal of Hydrogen Energy*, 42(52), 30683-30690.
- Nawaz, H., Casarano, R., & El Seoud, O. A. (2012). First report on the kinetics of the uncatalyzed esterification of cellulose under homogeneous reaction conditions: a rationale for the effect of carboxylic acid anhydride chain-length on the degree of biopolymer substitution. *Cellulose*, 19(1), 199-207.
- Ng, L. S., & Mohamad, A. A. (2006). Protonic battery based on a plasticized chitosan- NH_4NO_3 solid polymer electrolyte. *Journal of Power Sources*, 163(1), 382-385.

- Ng, L. S., & Mohamad, A. A. (2008). Effect of temperature on the performance of proton batteries based on chitosan–NH₄NO₃–EC membrane. *Journal of Membrane Science*, 325(2), 653-657.
- Nik Aziz, N. A., Idris, N. K., & Isa, M. I. N. (2010). Solid polymer electrolytes based on methylcellulose: FT-IR and ionic conductivity studies. *International Journal of Polymer Analysis and Characterization*, 15(5), 319-327.
- Ning, W., Xingxiang, Z., Haihui, L., & Benqiao, H. (2009). 1-Allyl-3-methylimidazolium chloride plasticized-corn starch as solid biopolymer electrolytes. *Carbohydrate Polymers*, 76(3), 482-484.
- Noor, I. M. (2016). Characterization and transport properties of pva–libob based polymer electrolytes with application in dye sensitized solar cells. University of Malaya,
- Noor, N. A. M., & Isa, M. I. N. (2015). Ionic conductivity and dielectric properties of CMC doped NH₄SCN solid biopolymer electrolytes. *Advanced Materials Research*, 1107, 230.
- Noor, N. A. M., & Isa, M. I. N. (2019). Investigation on transport and thermal studies of solid polymer electrolyte based on carboxymethyl cellulose doped ammonium thiocyanate for potential application in electrochemical devices. *International Journal of Hydrogen Energy*, 44, 8298-8306.
- Nordström, J., Matic, A., Sun, J., Forsyth, M., & MacFarlane, D. R. (2010). Aggregation, ageing and transport properties of surface modified fumed silica dispersions. *Soft Matter*, 6(10), 2293-2299.
- Numan, A., Duraisamy, N., Omar, F. S., Mahipal, Y. K., Ramesh, K., & Ramesh, S. (2016). Enhanced electrochemical performance of cobalt oxide nanocube intercalated reduced graphene oxide for supercapacitor application. *RSC Advances*, 6(41), 34894-34902.
- Omar, F. S., Numan, A., Duraisamy, N., Bashir, S., Ramesh, K., & Ramesh, S. J. R. A. (2016). Ultrahigh capacitance of amorphous nickel phosphate for asymmetric supercapacitor applications. *RSC Advances*, 6(80), 76298-76306.
- Osińska-Broniarz, M., Pokora, M., Walkowiak, M., & Martyła, A. (2015). Composite polymer electrolytes with modified mesoporous silica filler for Li-ion batteries. *Composites Theory and Practice*, 15(3), 124--129.
- Osińska, M., Walkowiak, M., Zalewska, A., & Jesionowski, T. (2009). Study of the role of ceramic filler in composite gel electrolytes based on microporous polymer membranes. *Journal of Membrane Science*, 326(2), 582-588.
- Osman, Z., Ibrahim, Z. A., & Arof, A. K. (2001). Conductivity enhancement due to ion dissociation in plasticized chitosan based polymer electrolytes. *Carbohydrate Polymers*, 44(2), 167-173.
- Padmasree, K. P., Kanchan, D. K., & Kulkarni, A. R. (2006). Impedance and modulus studies of the solid electrolyte system 20CdI₂–80 [xAg₂O–y (0.7 V₂O₅–0.3B₂O₃)], where 1 ≤ x/y ≤ 3. *Solid State Ionics*, 177(5-6), 475-482.

- Pandey, G. P., Kumar, Y., & Hashmi, S. A. (2010). Ionic liquid incorporated polymer electrolytes for supercapacitor application. *Indian Journal of Chemistry*, 49A, 743-751.
- Pandey, G. P., Kumar, Y., & Hashmi, S. A. (2011). Ionic liquid incorporated PEO based polymer electrolyte for electrical double layer capacitors: a comparative study with lithium and magnesium systems. *Solid State Ionics*, 190(1), 93-98.
- Pandey, G. P., & Rastogi, A. C. (2012). Graphene-based all-solid-state supercapacitor with ionic liquid gel polymer electrolyte. *MRS Online Proceedings Library Archive*, 1440.
- Pandey, K., Dwivedi, M. M., Singh, M., & Agrawal, S. L. (2010). Studies of dielectric relaxation and ac conductivity in [(100-x) PEO+ xNH₄SCN]: Al-Zn ferrite nano composite polymer electrolyte. *Journal of Polymer Research*, 17(1), 127.
- Park, C.-H., Park, M., Yoo, S.-I., & Joo, S.-K. (2006). A spin-coated solid polymer electrolyte for all-solid-state rechargeable thin-film lithium polymer batteries. *Journal of power sources*, 158(2), 1442-1446.
- Park, J.-C., Ito, T., Kim, K.-O., Kim, K.-W., Kim, B.-S., Khil, M.-S., . . . Kim, I.-S. (2010). Electrospun poly (vinyl alcohol) nanofibers: effects of degree of hydrolysis and enhanced water stability. *Polymer Journal*, 42(3), 273.
- Parker, S. P. (1983). McGraw-Hill encyclopedia of physics.
- Polu, A. R., Kumar, R., & Kumar, K. V. (2012). Ionic conductivity and electrochemical cell studies of new Mg₂⁺ ion conducting PVA/PEG based polymer blend electrolytes. *Advanced Materials Letters*, 3(5), 406-409.
- Pratap, R., Singh, B., & Chandra, S. (2006). Polymeric rechargeable solid-state proton battery. *Journal of power sources*, 161(1), 702-706.
- Priya, S. S., Karthika, M., Selvasekarapandian, S., & Manjuladevi, R. (2018). Preparation and characterization of polymer electrolyte based on biopolymer I-Carrageenan with magnesium nitrate. *Solid State Ionics*, 327, 136-149.
- Qian, X., Gu, N., Cheng, Z., Yang, X., Wang, E., & Dong, S. (2001). Impedance study of (PEO)₁₀LiClO₄-Al₂O₃ composite polymer electrolyte with blocking electrodes. *Electrochimica Acta*, 46(12), 1829-1836.
- Quartarone, E., & Mustarelli, P. (2011). Electrolytes for solid-state lithium rechargeable batteries: recent advances and perspectives. *Chemical Society Reviews*, 40(5), 2525-2540.
- Radha, K. P., Selvasekarapandian, S., Karthikeyan, S., Hema, M., & Sanjeeviraja, C. (2013). Synthesis and impedance analysis of proton-conducting polymer electrolyte PVA: NH₄F. *Ionics*, 19(10), 1437-1447.
- Rajantharan, S. (2011). Investigation on the effect of ionic liquid and ionic mixture in biodegradable polymer electrolytes under. UTAR,

- Rajendran, S., Kesavan, K., Nithya, R., & Ulaganathan, M. (2012). Transport, structural and thermal studies on nanocomposite polymer blend electrolytes for Li-ion battery applications. *Current Applied Physics*, 12(3), 789-793.
- Rajendran, S., Mahendran, O., & Kannan, R. (2002). Ionic conductivity studies in composite solid polymer electrolytes based on methylmethacrylate. *Journal of Physics and Chemistry of Solids*, 63(2), 303-307.
- Rajendran, S., Sivakumar, M., & Subadevi, R. (2003). Effect of salt concentration in poly (vinyl alcohol)-based solid polymer electrolytes. *Journal of Power Sources*, 124(1), 225-230.
- Rajendran, S., Sivakumar, M., & Subadevi, R. (2004). Investigations on the effect of various plasticizers in PVA-PMMA solid polymer blend electrolytes. *Materials Letters*, 58(5), 641-649.
- Rajendran, S., Sivakumar, M., Subadevi, R., & Nirmala, M. (2004). Characterization of PVA-PVdF based solid polymer blend electrolytes. *Physica B: Condensed Matter*, 348(1-4), 73-78.
- Rajeswari, N., Selvasekarapandian, S., Karthikeyan, S., Prabu, M., Hirankumar, G., Nithya, H., & Sanjeeviraja, C. (2011). Conductivity and dielectric properties of polyvinyl alcohol-polyvinylpyrrolidone poly blend film using non-aqueous medium. *Journal of Non-Crystalline Solids*, 357(22-23), 3751-3756.
- Rajeswari, N., Selvasekarapandian, S., Sanjeeviraja, C., Kawamura, J., & Bahadur, S. A. (2014). A study on polymer blend electrolyte based on PVA/PVP with proton salt. *Polymer Bulletin*, 71(5), 1061-1080.
- Ramesh, S., Leen, K. H., Kumutha, K., & Arof, A. (2007). FTIR studies of PVC/PMMA blend based polymer electrolytes. *Spectrochimica Acta Part A: Molecular and Biomolecular Spectroscopy*, 66(4-5), 1237-1242.
- Ramesh, S., Liew, C.-W., Morris, E., & Durairaj, R. (2010). Effect of PVC on ionic conductivity, crystallographic structural, morphological and thermal characterizations in PMMA-PVC blend-based polymer electrolytes. *Thermochimica Acta*, 511(1-2), 140-146.
- Ramesh, S., Liew, C.-W., & Ramesh, K. (2011). Evaluation and investigation on the effect of ionic liquid onto PMMA-PVC gel polymer blend electrolytes. *Journal of Non-Crystalline Solids*, 357(10), 2132-2138.
- Ramesh, S., & Lu, S. (2012). Enhancement of ionic conductivity and structural properties by BMIMTf ionic liquid in P (VdF-HFP)-based polymer electrolytes. *Journal of Applied Polymer Science*, 126, 484-492.
- Ramesh, S., & Wen, L. C. (2010). Investigation on the effects of addition of SiO₂ nanoparticles on ionic conductivity, FTIR, and thermal properties of nanocomposite PMMA-LiCF₃SO₃-SiO₂. *Ionics*, 16(3), 255-262.
- Ramesh, S., Yahaya, A. H., & Arof, A. K. (2002). Dielectric behaviour of PVC-based polymer electrolytes. *Solid State Ionics*, 152, 291-294.

- Ramlli, M., Kamarudin, K., & Isa, M. (2015). Ionic conductivity and structural analysis of carboxymethyl cellulose doped with ammonium fluoride as solid biopolymer electrolytes. *American-Eurasian Journal of Sustainable Agriculture*, 46-52.
- Ramlli, M. A., Chai, M. N., & Isa, M. I. N. (2013). Influence of propylene carbonate as a plasticizer in CMC-OA based biopolymer electrolytes: conductivity and electrical study. Paper presented at the Advanced Materials Research.
- Ramlli, M. A., & Isa, M. I. N. (2015). Solid Biopolymer Electrolytes Based Carboxymethyl Cellulose Doped With Ammonium Fluoride: Ionic Transport and Conduction Mechanism. *Polymers from Renewable Resources*, 6(2), 55.
- Ramlli, M. A., & Isa, M. I. N. (2016). Structural and ionic transport properties of protonic conducting solid biopolymer electrolytes based on Carboxymethyl cellulose doped with ammonium fluoride. *The Journal of Physical Chemistry B*, 120(44), 11567-11573.
- Ramlli, M. A., Kamarudin, K. H., & Isa, M. I. N. (2015). Ionic conductivity and structural analysis of carboxymethyl cellulose doped with ammonium fluoride as solid biopolymer electrolytes. *American-Eurasian Journal of Sustainable Agriculture*, 46-52.
- Ramly, K., Isa, M. I. N., & Khair, A. S. A. (2011). Conductivity and dielectric behaviour studies of starch/PEO+ x wt-% NH₄NO₃ polymer electrolyte. *Materials Research Innovations*, 15, 82-85.
- Ramya, C. S., Selvasekarapandian, S., Hirankumar, G., Savitha, T., & Angelo, P. C. (2008). Investigation on dielectric relaxations of PVP-NH₄SCN polymer electrolyte. *Journal of Non-Crystalline Solids*, 354(14), 1494-1502.
- Ramya, C. S., Selvasekarapandian, S., Savitha, T., Hirankumar, G., & Angelo, P. C. (2007). Vibrational and impedance spectroscopic study on PVP-NH₄SCN based polymer electrolytes. *Physica B: Condensed Matter*, 393(1-2), 11-17.
- Ramya, C. S., Selvasekarapandian, S., Savitha, T., Hirankumar, G., Baskaran, R., Bhuvaneshwari, M. S., & Angelo, P. C. (2006). Conductivity and thermal behavior of proton conducting polymer electrolyte based on poly (N-vinyl pyrrolidone). *European Polymer Journal*, 42(10), 2672-2677.
- Rani, M. S. A., Dzulkurnain, N. A., Ahmad, A., & Mohamed, N. S. (2015). Conductivity and dielectric behavior studies of carboxymethyl cellulose from kenaf bast fiber incorporated with ammonium acetate-BMATFSI biopolymer electrolytes. *International Journal of Polymer Analysis and Characterization*, 20(3), 250-260.
- Rani, M. S. A., Hassan, N. H., Ahmad, A., Kaddami, H., & Mohamed, N. S. (2016). Investigation of biosourced carboxymethyl cellulose-ionic liquid polymer electrolytes for potential application in electrochemical devices. *Ionics*, 22(10), 1855-1864.
- Rani, M. S. A., Rudhziah, S., Ahmad, A., & Mohamed, N. S. (2014). Biopolymer electrolyte based on derivatives of cellulose from kenaf bast fiber. *Polymers*, 6(9), 2371-2385.

- Rao, M. C., Rao, C. S., & Srikumar, T. (2018). Structural and ionic conductivity studies of PVA/PVP: KNO₃ composite polymer electrolyte films. *Materials Today: Proceedings*, 5(13), 26365-26371.
- Rao, R. V., Ashokan, P. V., & Shridhar, M. H. (2000). Study of cellulose acetate hydrogen phthalate (CAP)-poly methyl methacrylate (PMMA) blends by thermogravimetric analysis. *Polymer Degradation and Stability*, 70(1), 11-16.
- Rasali, N., Nagao, Y., & Samsudin, A. (2018). Enhancement on amorphous phase in solid biopolymer electrolyte based alginate doped NH₄NO₃. *Ionics*.
- Rasali, N., & Samsudin, A. (2017). Ionic transport properties of protonic conducting solid biopolymer electrolytes based on enhanced carboxymethyl cellulose-NH₄Br with glycerol. *Ionics*, 1-12.
- Rauh, R. D. (1999). Electrochromic windows: an overview. *Electrochimica Acta*, 44(18), 3165-3176.
- Ravi, M., Pavani, Y., Kumar, K. K., Bhavani, S., Sharma, A. K., & Rao, V. V. R. N. (2011). Studies on electrical and dielectric properties of PVP: KBrO₄ complexed polymer electrolyte films. *Materials Chemistry and Physics*, 130(1-2), 442-448.
- Razzak, M. T., & Darwis, D. (2001). Irradiation of polyvinyl alcohol and polyvinyl pyrrolidone blended hydrogel for wound dressing. *Radiation Physics and Chemistry*, 62(1), 107-113.
- Reddeppa, N., Sharma, A. K., Rao, V. V. R. N., & Chen, W. (2014). AC conduction mechanism and battery discharge characteristics of (PVC/PEO) polyblend films complexed with potassium chloride. *Measurement*, 47, 33-41.
- Reed, J. W., & Williams, Q. (2006). An infrared spectroscopic study of NH₄Br—ammonium bromide to 55 GPa. *Solid State Communications*, 140(3-4), 202-207.
- Rice, M. J., & Roth, W. L. (1972). Ionic transport in super ionic conductors: a theoretical model. *Journal of Solid State Chemistry*, 4(2), 294-310.
- Rudhziah, S., Ahmad, A., Ahmad, I., & Mohamed, N. (2015a). Biopolymer electrolytes based on blend of kappa-carrageenan and cellulose derivatives for potential application in dye sensitized solar cell. *Electrochimica acta*, 175, 162-168.
- Rudhziah, S., Ahmad, A., Ahmad, I., & Mohamed, N. S. (2015b). Biopolymer electrolytes based on blend of kappa-carrageenan and cellulose derivatives for potential application in dye sensitized solar cell. *Electrochimica Acta*, 175, 162-168.
- Saadiah, M., & Samsudin, A. (2018). Electrical study on Carboxymethyl Cellulose-Polyvinyl alcohol based bio-polymer blend electrolytes. Paper presented at the IOP Conference Series: Materials Science and Engineering.
- Saadiah, M. A., & Samsudin, A. S. (2018). Electrical study on Carboxymethyl Cellulose-Polyvinyl alcohol based bio-polymer blend electrolytes. Paper presented at the IOP Conference Series: Materials Science and Engineering.

- Saadiah, M. A., Zhang, D., Nagao, Y., Muzakir, S. K., & Samsudin, A. S. (2019). Reducing crystallinity on thin film based CMC/PVA hybrid polymer for application as a host in polymer electrolytes. *Journal of Non-Crystalline Solids*, 511, 201-211.
- Saha, S., & Sinha, T. P. (2006). Dielectric relaxation in $\text{SrFe}_{1/2}\text{Nb}_{1/2}\text{O}_3$. *Journal of Applied Physics*, 99(1), 014109.
- Samad, Y. A., Asghar, A., & Hashaikeh, R. (2013). Electrospun cellulose/PEO fiber mats as a solid polymer electrolytes for Li ion batteries. *Renewable Energy*, 56, 90-95.
- Samir, M. A., Chazeau, L., Alloin, F., Cavaillé, J.-Y., Dufresne, A., & Sanchez, J.-Y. (2005). POE-based nanocomposite polymer electrolytes reinforced with cellulose whiskers. *Electrochimica Acta*, 50(19), 3897-3903.
- Samsudin, A., Lai, H., & Isa, M. (2014). Biopolymer materials based carboxymethyl cellulose as a proton conducting biopolymer electrolyte for application in rechargeable proton battery. *Electrochimica Acta*, 129, 1-13.
- Samsudin, A. S. (2014). Development of carboxymethyl cellulose based proton conducting biopolymer electrolytes and its application in solid-state proton battery. Terengganu: Universiti Malaysia Terengganu,
- Samsudin, A. S., & Isa, M. I. N. (2012). Structural and ionic transport study on CMC doped NH_4Br : A new types of biopolymer electrolytes. *J. Appl. Sci*, 12(2), 174-179.
- Samsudin, A. S., & Isa, M. I. N. (2014). Conductivity and transport properties study of plasticized carboxymethyl cellulose (CMC) based solid biopolymer electrolytes (SBE). Paper presented at the Advanced Materials Research.
- Samsudin, A. S., & Isa, M. I. N. (2015). Conductivity study on plasticized solid bio-electrolytes CMC- NH_4Br and application in solid-state proton batteries *Jurnal Teknologi*, 78(6-5), 43-48.
- Samsudin, A. S., Isa, M. I. N., & Mohamad, N. (2011). New types of biopolymer electrolytes: Ionic conductivity study on CMC doped with NH_4Br . *Journal of current engineering research*, 1(1), 7-11.
- Samsudin, A. S., Khairul, W. M., & Isa, M. I. N. (2012). Characterization on the potential of carboxy methylcellulose for application as proton conducting biopolymer electrolytes. *Journal of Non-Crystalline Solids*, 358(8), 1104-1112.
- Samsudin, A. S., Kuan, E. C. H., & Isa, M. I. N. (2011). Investigation of the potential of proton-conducting biopolymer electrolytes based methyl cellulose-glycolic acid. *International Journal of Polymer Analysis and Characterization*, 16(7), 477-485.
- Samsudin, A. S., Lai, H. M., & Isa, M. I. N. (2014). Biopolymer materials based carboxymethyl cellulose as a proton conducting biopolymer electrolyte for application in rechargeable proton battery. *Electrochimica Acta*, 129, 1-13.

- Saroj, A. L., & Singh, R. K. (2012). Thermal, dielectric and conductivity studies on PVA/Ionic liquid [EMIM][EtSO₄] based polymer electrolytes. *Journal of Physics and Chemistry of Solids*, 73(2), 162-168.
- Schantz, S., & Torell, L. (1993). Evidence of dissolved ions and ion pairs in dilute poly (propylene oxide)-salt solutions. *Solid State Ionics*, 60(1-3), 47-53.
- Schütter, C., Ramirez-Castro, C., Oljaca, M., Passerini, S., Winter, M., & Balducci, A. (2015). Activated carbon, carbon blacks and graphene based nanoplatelets as active materials for electrochemical double layer capacitors: a comparative study. *Journal of the Electrochemical Society*, 162(1), A44-A51.
- Selvasekarapandian, S., Hema, M., Kawamura, J., Kamishima, O., & Baskaran, R. (2010). Characterization of PVA–NH₄NO₃ polymer electrolyte and its application in rechargeable proton battery. *Journal of the Physical Society of Japan*, 79(Suppl. A), 163-168.
- Selvasekarapandian, S., Hirankumar, G., Kawamura, J., Kuwata, N., & Hattori, T. (2005). ¹H solid state NMR studies on the proton conducting polymer electrolytes. *Materials Letters*, 59(22), 2741-2745.
- Shaffie, A. H., & Khair, A. S. A. (2018). Characterization of chitosan-starch blend based biopolymer electrolyte doped with ammonium nitrate. Paper presented at the AIP Conference Proceedings.
- Sharma, P., Kanchan, D., Gondaliya, N., Pant, M., & Jayswal, M. S. (2013). Conductivity relaxation in Ag⁺ ion conducting PEO–PMMA–PEG polymer blends. *Ionics*, 19(2), 301-307.
- Shin, J.-H., & Passerini, S. (2004). Effect of fillers on the electrochemical and interfacial properties of PEO–LiN(SO₂CF₂CF₃)₂ polymer electrolytes. *Electrochimica Acta*, 49(9-10), 1605-1612.
- Shuhaimi, N., Teo, L., Woo, H., Majid, S., & Arof, A. K. (2012). Electrical double-layer capacitors with plasticized polymer electrolyte based on methyl cellulose. *Polymer bulletin*, 69(7), 807-826.
- Shuhaimi, N. E. A., Majid, S. R., & Arof, A. K. (2009). On complexation between methyl cellulose and ammonium nitrate. *Materials Research Innovations*, 13(3), 239-242.
- Shuhaimi, N. E. A., Teo, L. P., Woo, H. J., Majid, S. R., & Arof, A. K. (2012). Electrical double-layer capacitors with plasticized polymer electrolyte based on methyl cellulose. *Polymer Bulletin*, 69(7), 807-826.
- Shukur, M., Ithnin, R., & Kadir, M. (2014). Electrical properties of proton conducting solid biopolymer electrolytes based on starch–chitosan blend. *Ionics*, 20(7), 977-999.
- Shukur, M., & Kadir, M. (2015). Hydrogen ion conducting starch-chitosan blend based electrolyte for application in electrochemical devices. *Electrochimica Acta*, 158, 152-165.

- Shukur, M. F., Ithnin, R., Illias, H. A., & Kadir, M. F. Z. (2013). Proton conducting polymer electrolyte based on plasticized chitosan–PEO blend and application in electrochemical devices. *Optical Materials*, 35(10), 1834-1841.
- Shukur, M. F., Ithnin, R., & Kadir, M. F. Z. (2014a). Electrical characterization of corn starch-LiOAc electrolytes and application in electrochemical double layer capacitor. *Electrochimica Acta*, 136, 204-216.
- Shukur, M. F., Ithnin, R., & Kadir, M. F. Z. (2014b). Electrical properties of proton conducting solid biopolymer electrolytes based on starch–chitosan blend. *Ionics*, 20(7), 977-999.
- Shukur, M. F., Ithnin, R., & Kadir, M. F. Z. (2014c). Protonic transport analysis of starch-chitosan blend based electrolytes and application in electrochemical device. *Molecular Crystals and Liquid Crystals*, 603(1), 52-65.
- Shukur, M. F., & Kadir, M. F. Z. (2015). Hydrogen ion conducting starch-chitosan blend based electrolyte for application in electrochemical devices. *Electrochimica Acta*, 158, 152-165.
- Sikkanthar, S., Karthikeyan, S., Selvasekarapandian, S., Pandi, D. V., Nithya, S., & Sanjeeviraja, C. (2015). Electrical conductivity characterization of polyacrylonitrile-ammonium bromide polymer electrolyte system. *Journal of Solid State Electrochemistry*, 19(4), 987-999.
- Singh, R. K., & Singh, A. K. (2013). Optimization of reaction conditions for preparing carboxymethyl cellulose from corn cobic agricultural waste. *Waste and Biomass Valorization*, 4(1), 129-137.
- Sit, Y. K., Samsudin, A. S., & Isa, M. I. N. (2012). Ionic conductivity study on hydroxyethyl cellulose (HEC) doped with NH_4Br based biopolymer electrolytes. *Research Journal of Recent Sciences*, 2277, 2502.
- Sivadevi, S., Selvasekarapandian, S., Karthikeyan, S., Sanjeeviraja, C., Nithya, H., Iwai, Y., & Kawamura, J. (2015). Proton-conducting polymer electrolyte based on PVA-PAN blend doped with ammonium thiocyanate. *Ionics*, 21(4), 1017-1029.
- Siyal, S. H., Li, M., Li, H., Lan, J.-L., Yu, Y., & Yang, X. (2019). Ultraviolet irradiated PEO/LATP composite gel polymer electrolytes for lithium-metallic batteries (LMBs). *Applied Surface Science*.
- Soldano, C., Mahmood, A., & Dujardin, E. (2010). Production, properties and potential of graphene. *carbon*, 48(8), 2127-2150.
- Srivastava, N., & Chandra, S. (2000). Studies on a new proton conducting polymer system: poly (ethylene succinate)+ NH_4ClO_4 . *European Polymer Journal*, 36(2), 421-433.
- Stainer, M., Hardy, L. C., Whitmore, D. H., & Shriver, D. F. (1984). Stoichiometry of formation and conductivity response of amorphous and crystalline complexes formed between poly (ethylene oxide) and ammonium salts: $\text{PEO}_x \cdot \text{NH}_4\text{SCN}$ and $\text{PEO}_x \cdot \text{NH}_4\text{SO}_3 \text{CF}_3$. *Journal of the Electrochemical Society*, 131(4), 784-790.

- Stephan, A. M., & Nahm, K. S. (2006). Review on composite polymer electrolytes for lithium batteries. *Polymer*, 47(16), 5952-5964.
- Su, J.-F., Huang, Z., Yuan, X.-Y., Wang, X.-Y., & Li, M. (2010). Structure and properties of carboxymethyl cellulose/soy protein isolate blend edible films crosslinked by Maillard reactions. *Carbohydrate Polymers*, 79(1), 145-153.
- Sudhakar, Y. N., Kumar, S., & Bhat, d. k. (2018). An introduction of Biopolymer Electrolytes. In (pp. 1-34).
- Sudhakar, Y. N., & Selvakumar, M. (2013). Ionic conductivity studies and dielectric studies of poly (styrene sulphonic acid)/starch blend polymer electrolyte containing LiClO₄. *Journal of Applied Electrochemistry*, 43(1), 21-29.
- Sudhamani, S. R., Prasad, M. S., & Sankar, K. U. (2003). DSC and FTIR studies on gellan and polyvinyl alcohol (PVA) blend films. *Food Hydrocolloids*, 17(3), 245-250.
- Sukeshini, A. M., Nishimoto, A., & Watanabe, M. (1996). Transport and electrochemical characterization of plasticized poly (vinyl chloride) solid electrolytes. *Solid State Ionics*, 86, 385-393.
- Sun, J., Bayley, P., Macfarlane, D. R., & Forsyth, M. (2007). Gel electrolytes based on lithium modified silica nano-particles. *Electrochimica Acta*, 52(24), 7083-7090.
- Sun, Y., Wu, Q., & Shi, G. (2011). Graphene based new energy materials. *Energy & Environmental Science*, 4(4), 1113-1132.
- Sundaramahalingam, K., Nallamuthu, N., Manikandan, A., Vanitha, D., & Muthuvinayagam, M. (2018). Studies on sodium nitrate based polyethylene oxide/polyvinyl pyrrolidone polymer blend electrolytes. *Physica B: Condensed Matter*, 547, 55-63.
- Teo, L., Buraidah, M., Nor, A., & Majid, S. (2012). Conductivity and dielectric studies of Li₂SnO₃. *Ionics*, 18(7), 655-665.
- Teoh, K. H., Lim, C.-S., Liew, C.-W., & Ramesh, S. (2015). Electric double-layer capacitors with corn starch-based biopolymer electrolytes incorporating silica as filler. *Ionics*, 21(7), 2061-2068.
- Thomson, G. (1968). The early history of electron diffraction. *Contemporary Physics*, 9(1), 1-15.
- Tuhania, P., Singh, P. K., Bhattacharya, B., Dhapola, P. S., Yadav, S., Shukla, P. K., & Gupta, M. (2018). PVDF-HFP and 1-ethyl-3-methylimidazolium thiocyanate-doped polymer electrolyte for efficient supercapacitors. *High Performance Polymers*, 30(8), 911-917.
- Ulaganathan, M., Pethaiah, S. S., & Rajendran, S. (2011). Li-ion conduction in PVAc based polymer blend electrolytes for lithium battery applications. *Materials Chemistry and Physics*, 129(1-2), 471-476.

- Varnell, D. F., & Coleman, M. M. (1981). FT ir studies of polymer blends: V. Further observations on polyester-poly (vinyl chloride) blends. *Polymer*, 22(10), 1324-1328.
- Varnell, D. F., Runt, J. P., & Coleman, M. M. (1983). FT ir and thermal analysis studies of blends of poly (ϵ -caprolactone) with homo-and copolymers of poly (vinylidene chloride). *Polymer*, 24(1), 37-42.
- Varzi, A., & Passerini, S. (2015). Enabling high areal capacitance in electrochemical double layer capacitors by means of the environmentally friendly starch binder. *Journal of Power Sources*, 300, 216-222.
- Vashishta, P., Mundy, J. N., & Shenoy, G. (1979). Fast ion transport in solids: electrodes and electrolytes.
- Vijaya, N., Selvasekarapandian, S., Malathi, J., Iwai, Y., Nithya, H., & Kawamura, J. (2013). ¹HNMR study on PVP-NH₄Cl based-proton conducting polymer electrolyte. *Indian J. Appl. Res*, 3, 506.
- Vöge, A., Deimede, V., Paloukis, F., Neophytides, S. G., & Kallitsis, J. K. (2014). Synthesis and properties of aromatic polyethers containing poly (ethylene oxide) side chains as polymer electrolytes for lithium ion batteries. *Materials Chemistry and Physics*, 148(1-2), 57-66.
- Walker, C. W., & Salomon, M. (1993). Improvement of ionic conductivity in plasticized PEO-based solid polymer electrolytes. *Journal of the Electrochemical Society*, 140(12), 3409-3412.
- Wang, J., Song, S., Muchakayala, R., Hu, X., & Liu, R. (2017). Structural, electrical, and electrochemical properties of PVA-based biodegradable gel polymer electrolyte membranes for Mg-ion battery applications. *Ionics*, 23(7), 1759-1769.
- Wang, K., Zhang, X., Li, C., Sun, X., Meng, Q., Ma, Y., & Wei, Z. (2015). Chemically crosslinked hydrogel film leads to integrated flexible supercapacitors with superior performance. *Advanced Materials*, 27(45), 7451-7457.
- Wang, X., Hao, X., Xia, Y., Liang, Y., Xia, X., & Tu, J. (2019). A polyacrylonitrile (PAN)-based double-layer multifunctional gel polymer electrolyte for lithium-sulfur batteries. *Journal of Membrane Science*, 582, 37-47.
- Wang, X., Yao, C., Wang, F., & Li, Z. (2017). Cellulose-based nanomaterials for energy applications. *Small*, 13(42), 1702240.
- Watanabe, M., & Nishimoto, A. (1995). Effects of network structures and incorporated salt species on electrochemical properties of polyether-based polymer electrolytes. *Solid State Ionics*, 79, 306-312.
- Watson, E. S., O'Neill, M. J., Justin, J., & Brenner, N. (1964). A Differential Scanning Calorimeter for Quantitative Differential Thermal Analysis. *Analytical Chemistry*, 36(7), 1233-1238.

- Wei, Q.-B., Fu, F., Zhang, Y.-Q., Wang, Q., & Ren, Y.-X. (2014). pH-responsive CMC/PAM/PVP semi-IPN hydrogels for theophylline drug release. *Journal of Polymer Research*, 21(6), 453.
- Wiers, B. M. (2015). *Charge Transport In Metal-Organic Frameworks*. UC Berkeley,
- Woo, H. J., Majid, S. R., & Arof, A. K. (2011). Transference number and structural analysis of proton conducting polymer electrolyte based on poly (ϵ -caprolactone). *Materials Research Innovations*, 15(sup2), 49-54.
- Wright, P. V. (1975). Electrical conductivity in ionic complexes of poly (ethylene oxide). *Polymer International*, 7(5), 319-327.
- Wüthrich, R., & Mandin, P. (2009). Electrochemical discharges—Discovery and early applications. *Electrochimica Acta*, 54(16), 4031-4035.
- Xie, Z., Wu, Z., An, X., Yoshida, A., Wang, Z., Hao, X., . . . Guan, G. (2019). Bifunctional ionic liquid and conducting ceramic co-assisted solid polymer electrolyte membrane for quasi-solid-state lithium metal batteries. *Journal of Membrane Science*, 586, 122-129.
- Yahya, M. Z. A., Harun, M. K., Ali, A. M. M., Mohammat, M. F., Hanafiah, M. A. K. M., Ibrahim, S. C., . . . Latif, F. (2006). XRD and surface morphology studies on chitosan-based film electrolytes. *Journal of applied sciences*, 6(15), 3510-3154.
- Yang, C.-C., Hsu, S.-T., & Chien, W.-C. (2005). All solid-state electric double-layer capacitors based on alkaline polyvinyl alcohol polymer electrolytes. *Journal of power sources*, 152, 303-310.
- Yang, H., Liu, Y., Kong, L., Kang, L., & Ran, F. (2019). Biopolymer-based carboxylated chitosan hydrogel film crosslinked by HCl as gel polymer electrolyte for all-solid-state supercapacitors. *Journal of Power Sources*, 426, 47-54.
- Yang, J.-M., & Wang, S.-A. (2015). Preparation of graphene-based poly (vinyl alcohol)/chitosan nanocomposites membrane for alkaline solid electrolytes membrane. *Journal of Membrane Science*, 477, 49-57.
- Yang, J. M., Chiang, C. Y., Wang, H. Z., & Yang, C. C. (2009). Two step modification of poly (vinyl alcohol) by UV radiation with 2-hydroxy ethyl methacrylate and sol-gel process for the application of polymer electrolyte membrane. *Journal of Membrane Science*, 341(1-2), 186-194.
- Yong, H., Park, H., Jung, J., & Jung, C. (2019). A fundamental approach to design of injectable high-content gel polymer electrolyte for activated carbon electrode supercapacitors. *Journal of Industrial and Engineering Chemistry*, 76, 429-436.
- Yu, A., Chabot, V., & Zhang, J. (2013). *Electrochemical supercapacitors for energy storage and delivery: fundamentals and applications*. New York: CRC press.
- Yue, Z., McEwen, I. J., & Cowie, J. M. G. (2003). Novel gel polymer electrolytes based on a cellulose ester with PEO side chains. *Solid State Ionics*, 156(1-2), 155-162.

- Yuhanees, M. Y. (2017). Characteristics of corn starch/chitosan blend green polymer electrolytes complexed with ammonium iodide and its application in energy devices/Yuhanees Mohamed Yusof. University of Malaya,
- Yusof, Y., Illias, H., & Kadir, M. (2014). Incorporation of NH₄Br in PVA-chitosan blend-based polymer electrolyte and its effect on the conductivity and other electrical properties. *Ionics*, 20(9), 1235-1245.
- Yusof, Y. M., Illias, H. A., & Kadir, M. F. Z. (2014). Incorporation of NH₄Br in PVA-chitosan blend-based polymer electrolyte and its effect on the conductivity and other electrical properties. *Ionics*, 20(9), 1235-1245.
- Zainuddin, N. K., Saadiah, M. A., Abdul Majeed, A. P. P., & Samsudin, A. S. (2018). Characterization on conduction properties of carboxymethyl cellulose/kappa carrageenan blend-based polymer electrolyte system. *International Journal of Polymer Analysis and Characterization*, 23(4), 321-330.
- Zainuddin, N. K., & Samsudin, A. S. (2018). Investigation on the Effect of NH₄Br at Transport Properties in K-Carrageenan Based Biopolymer Electrolytes via Structural and Electrical Analysis. *Materials Today Communications*, 14, 199-209.
- Zakaria, N. A., Yahya, S. Y. S., Isa, M. I. N., Nor Sabirin, M., & Subban, R. H. Y. (2010). Conductivity and dynamic mechanical studies of PVC/PEMA blend polymer electrolytes (Vol. 93): Trans Tech Publ.
- Zeng, J., Li, R., Liu, S., & Zhang, L. (2011). Fiber-like TiO₂ nanomaterials with different crystallinity phases fabricated via a green pathway. *ACS applied materials & interfaces*, 3(6), 2074-2079.
- Zhang, P., Yang, L. C., Li, L. L., Ding, M. L., Wu, Y. P., & Holze, R. (2011). Enhanced electrochemical and mechanical properties of P(VDF-HFP)-based composite polymer electrolytes with SiO₂ nanowires. *Journal of Membrane Science*, 379(1-2), 80-85.
- Zhang, S. S. (2013). Liquid electrolyte lithium/sulfur battery: fundamental chemistry, problems, and solutions. *Journal of Power Sources*, 231, 153-162.
- Zhu, M., Wu, J., Wang, Y., Song, M., Long, L., Siyal, S. H., . . . Sui, G. (2018). Recent advances in gel polymer electrolyte for high-performance lithium batteries. *Journal of Energy Chemistry*.
- Zubieta, L., & Bonert, R. (2000). Characterization of double-layer capacitors for power electronics applications. *IEEE Transactions on industry applications*, 36(1), 199-205.

APPENDIX A

The required weight of NH_4Br was determine via following relation:

$$\frac{x}{x+y} \times 100\% = z\% \quad 5.1$$

$$100x = zx + zy \quad 5.2$$

$$(100 - z)x = zy \quad 5.3$$

$$x = \frac{zy}{(100 - z)} \quad 5.4$$

where, x is weight of NH_4Br in gram, y is weight of CMC-PVA polymer blend in gram and z is weight percentage, wt. % of NH_4Br .

1) Fourier Transform Infrared Spectroscopy (FTIR)



اونیورسیتی ملیسیا قهغ
UNIVERSITI MALAYSIA PAHANG

2) X-ray Diffraction



3) Thergravimetric analysis (TGA)



اونیورسیتی ملیسیا قهغ
UNIVERSITI MALAYSIA PAHANG

4) Differential scanning calorimeter



5) Electrical impedance spectroscopy with oven used to measure the ionic conductivity of biopolymer electrolytes.



اونيفورسيتي مليسيا قهق
UNIVERSITI MALAYSIA PAHANG

6) Transference number measurement (TNM)



7) Model Autolab used for cyclic voltammetry and linear sweep voltammetry characterization



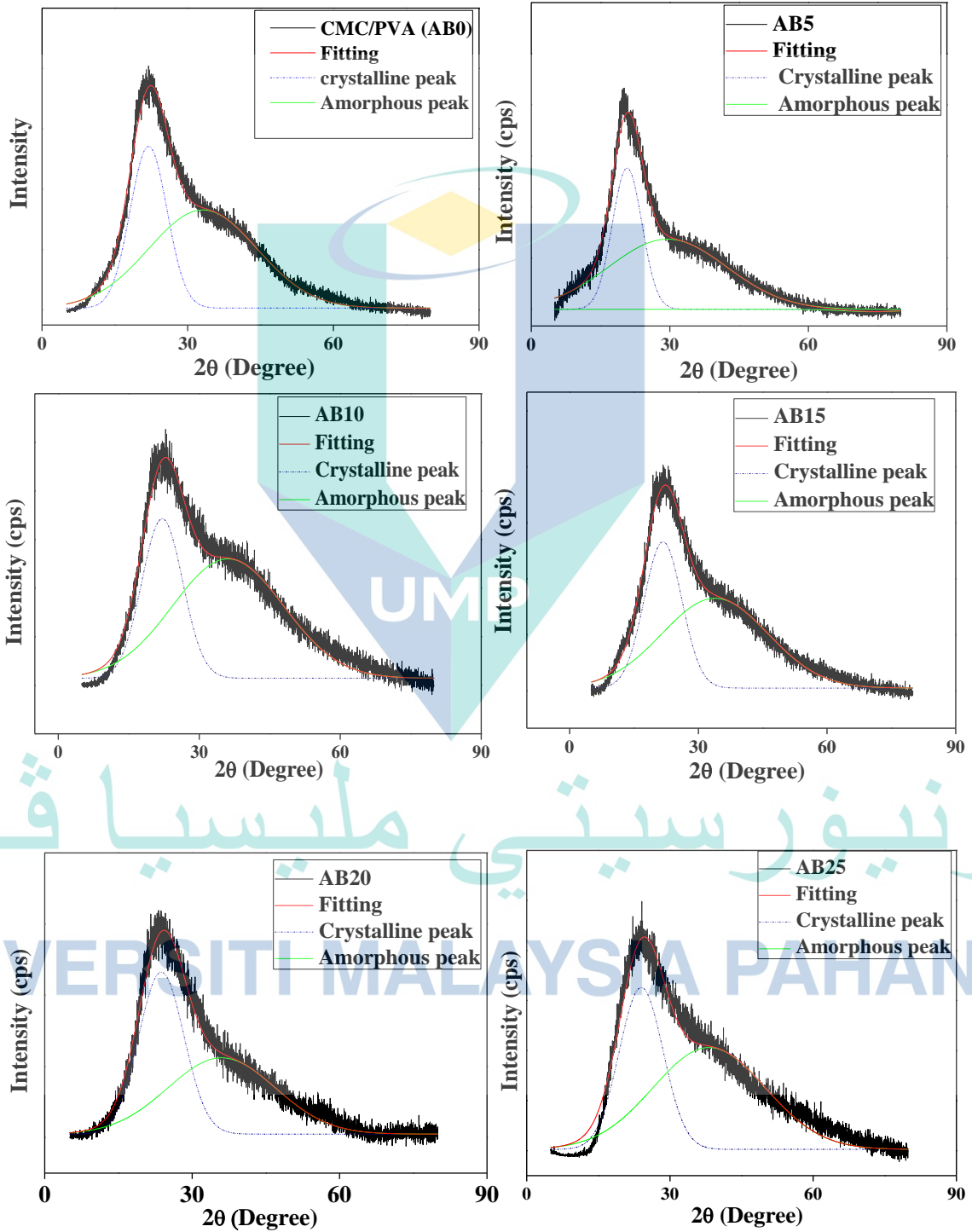
8) Battery testing system connected to a computer.

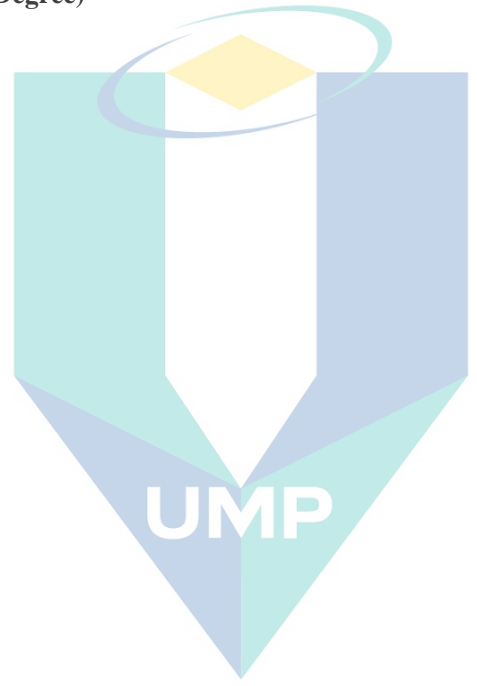
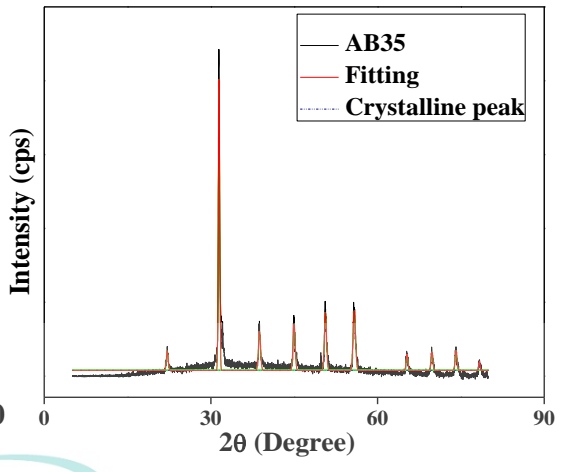
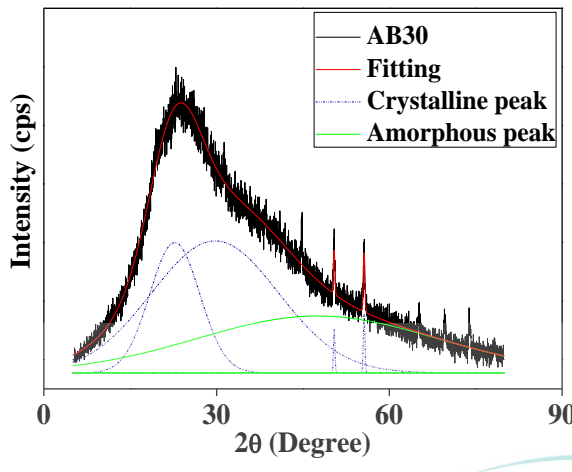


اونیورسیتی ملیسیا قهغ
UNIVERSITI MALAYSIA PAHANG

APPENDIX B

- 1) XRD deconvolution of CMC-PVA polymer blend incorporated with different NH₄Br from 5 to 35 wt.% based SBEs.





اونيورسيتي ملايسيا قهغ
 UNIVERSITI MALAYSIA PAHANG

LISTS OF JOURNAL PUBLICATION AND CONFERENCE PROCEEDING

1. N.F. Mazuki, A.P.P. Abdul Majeed, Y. Nagao, A.S. Samsudin (2020). "Studies on ionic conduction properties of amorphous materials based CMC-PVA polymer blend electrolytes via impedance approach". *Journal of Polymer Testing*, 81, 106234. <https://doi.org/10.1016/j.polymertesting.2019.106234>.
2. A. Zulkifli, M.A. Saadiah, N.F. Mazuki and A.S. Samsudin (2020). Characterization of an amorphous materials hybrid polymer electrolyte based on a LiNO₃-doped, CMC-PVA blend for application in an electrical double layer capacitor. *Materials Chemistry and Physics*, 123312. <https://doi.org/10.1016/j.matchemphys.2020.123312>.
3. N. K. Zainuddin, N. M. J. Rasali, N. F. Mazuki, M. A. Saadiah, A. S. Samsudin, (2020). Investigation on favourable ionic conduction based on CMC-K carrageenan proton conducting hybrid solid bio-polymer electrolytes for applications in EDLC. *International Journal of Hydrogen Energy*. <https://doi.org/10.1016/j.ijhydene.2020.01.038>.
4. N.F. Mazuki, A.P.P. Abdul Majeed and A.S. Samsudin (2020). "Study on the electrochemical properties performance of CMC-PVA doped NH₄Br based solid polymer electrolytes as application for EDLC". *Journal of Polymer Research*, 27, 1-13. <https://doi.org/10.1007/s10965-020-02078-5>.
5. N.F. Mazuki, A.F. Fuzlin, M.A. Saadiah, A.S. Samsudin (2019). "An investigation on the abnormal trend of the conductivity properties of CMC/PVA-doped NH₄Cl-based solid biopolymer electrolyte system". *Ionics* 25, 2657-2667. <https://doi.org/10.1007/s11581-018-2734-9>.
6. N.F. Mazuki, N.M.J. Rasali, M.A. Saadiah, A.S. Samsudin (2018). "Irregularities trend in electrical conductivity of CMC/PVA-NH₄Cl based solid biopolymer electrolytes". *AIP Conference Proceedings* 2030, 020221. <https://doi.org/10.1063/1.5066862>.
7. N.F. Mazuki, Y. Nagao, A.S. Samsudin (2019). "Immittance Response on Carboxymethyl Cellulose Blend with Polyvinyl Alcohol-Doped Ammonium Bromide-Based Biopolymer Electrolyte". *Makara Journal Technology* 22, 167-170. doi: 10.7454/mst.v22i3.3638.
8. N.F. Mazuki, N.M.J Rasali, B. Sahraoui and A.S. Samsudin (2019). "Ionic conduction and electrochemical properties of Alginate-NH₄NO₃ based biopolymer electrolytes as an application in EDLC". *Makara Journal Technology* 24, 7-12. 10.7454/mst.v24i1.3832.

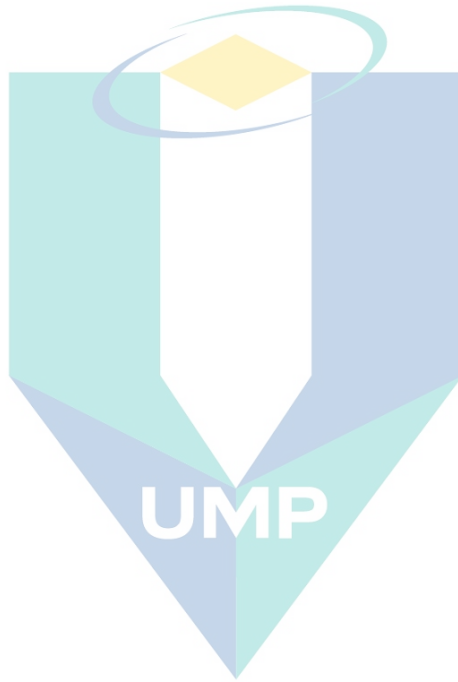
BIODATA OF THE AUTHOR



The author was born on 05 May 1995 in Dungun, Terengganu, Malaysia. She received her primary education at Sekolah Kebangsaan Tanjung Pati, Terengganu. She continued his secondary education at Sekolah Menengah Kebangsaan Balai Besar until form 3 and transfer to Sekolah Menengah Tengku Intan Zaharah, Terengganu until she finished her study in secondary education. Then, she get offer from Pahang Matriculation College for her one year study before she take her first degree at Universiti Malaysia Terengganu in Physics, Electronic and Instrumentation. She then further her study in Master degree at Universiti Malaysia Pahang. The author can be contacted via her phone number and email address of +6013-9415049 and fatihmazuii@gmail.com., respectively.

اونيورسيتي ملايسيا قهغ

UNIVERSITI MALAYSIA PAHANG



اونيورسيتي ملايسيا قهغ

UNIVERSITI MALAYSIA PAHANG